CONTRIBUTION TO THE CHARACTERIZATION OF HUMAN KINETOCHORE PROTEINS CENP-C AND hMis12 *IN VITRO* AND *IN VIVO*

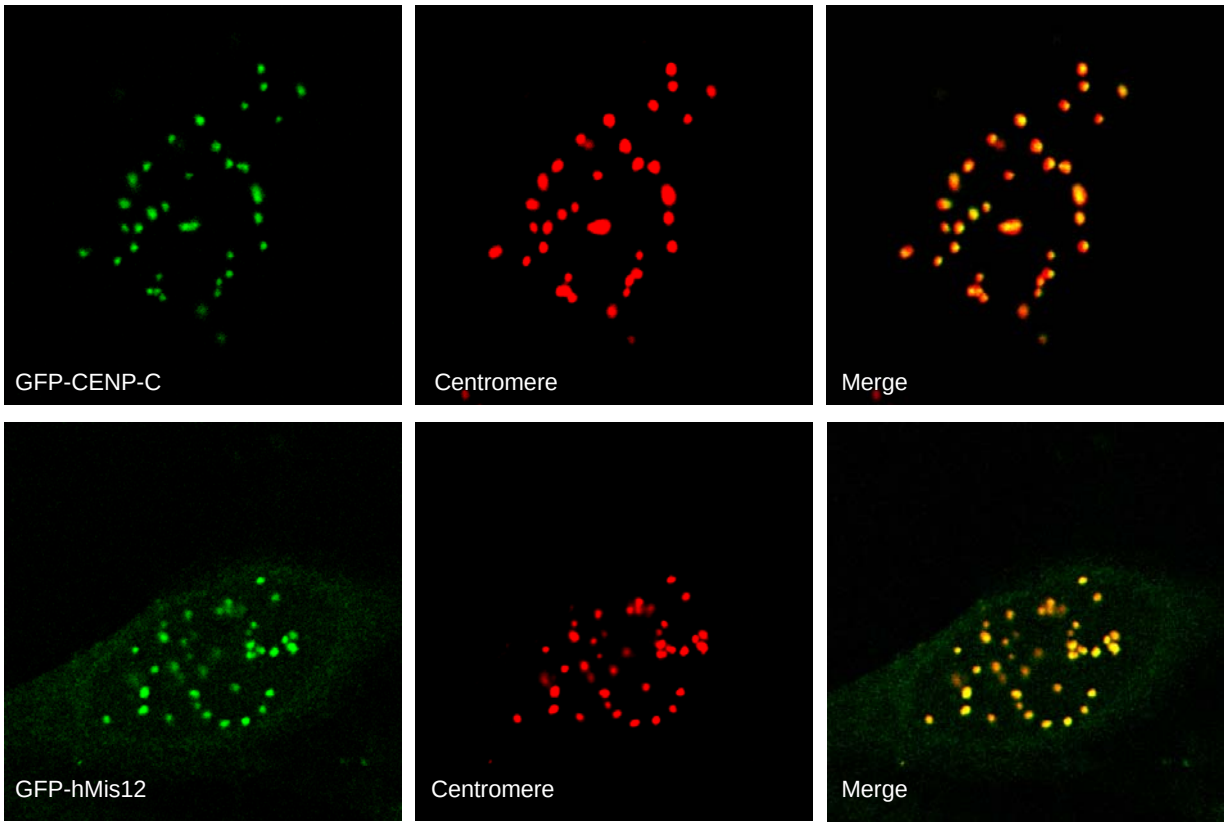

Indri Erliandri MSc.

Biologisch-Parmazeutischen Fakultät
Friedrich Schiller Universität Jena
2007

CONTRIBUTION TO THE CHARACTERIZATION OF HUMAN KINETOCHORE PROTEINS CENP-C AND hMis12 *IN VITRO* AND *IN VIVO*

DISSERTATION

zur Erlangung des akademischen Grades
Doctor rerum naturalium (Dr. rer. nat.)

vorgelegt dem
Rat der Biologisch-Parmazeutischen Fakultät
der Friedrich Schiller Universität Jena

von Fr. Indri Erliandri Msc
geboren am 13. Februar 1970, Cianjur/Indonesia

Gutachter :

Prof. Dr. Stephan Diekmann
Institute of Age Research – Fritz Lipmann Institute
Friedrich-Schiller University – Jena

PD Dr. Hans Jürgen Agricola
Institut für Allgemeine Zoologie und Tierphysiologie
Friedrich-Schiller University – Jena

Prof. Dr. Jörg Langowsky
German Cancer Research Center (DKFZ)
Ruprecht-Karls University - Heidelberg

Tag der Öffentlichen Verteidigung: October 8th, 2007

CONTENT

CONTENT		**i**
ABBREVIATIONS		**iv**
SUMMARY		**vii**
ZUSSAMENFASSUNG		**ix**
1 .	**INTRODUCTION**	**1**
1.1.	The human centromere/kinetochore	2
1.2.	The Foundation Inner Centromere/Kinetochore Protein complex	4
1.2.1.	CENP-C	5
1.2.2.	hMis12	8
1.2.3.	Further member of the inner kinetochore complex	9
1.3	Linker proteins for human outer kinetochore proteins	10
1.4.	Models of centromere/kinetochore complex	11
1.5.	The centromere/kinetochore during mitosis	14
1.6.	Aims	15
2.	**MATERIAL AND METHODS**	**17**
2.1.	Material	17
2.1.1.	Chemicals	17
2.1.2.	Standards and kits	17
2.1.3.	Bacterial strains and cell lines	17
2.1.4.	DNA templates	18
2.1.5.	Plasmid vectors	18
2.1.6.	Oligonucleotide primers	18
2.1.6.1.	CENP-C primers	18
2.1.6.2.	hMis12 primers	19
2.1.6.3.	SETDB1 primers	19
2.1.6.4.	PSMB10 primers	20
2.1.7.	Antibodies	20

2.1.8.	Software	20
2.2.	Methods	21
2.2.1.	PCR process	21
2.2.1.1.	Generation of *CENP-C* full length and *CENP-C* fragments	21
2.2.1.2.	Generation of *hMis12*	22
2.2.1.3.	Generation of *SETDB1*and *PSMB10*	22
2.2.2.	GST-CENP-C and GST-hMis12 protein expression	23
2.2.3.	GST-CENP-C and GST-hMis12 protein purification	24
2.2.4.	Strep tag-hMis12 protein expression	24
2.2.5.	Strep tag-hMis12 protein purification	25
2.2.6.	Immunoblotting	26
2.2.6.1.	Immunoblotting Method A	26
2.2.6.2.	Immunoblotting Method B	26
2.2.7.	Factor Xa digestion	27
2.2.8.	Centromere chromatin complex isolation	27
2.2.9.	GST pull-down assay	29
2.2.9.1.	Bait protein preparation	29
2.2.9.2.	Bait-Prey elution and analysis	29
2.2.10.	Yeast two hybrid analysis	29
2.2.10.1.	Auto-activation test	29
2.2.10.2.	Interaction mating	30
2.2.11.	Cell culture	30
2.2.12.	Transfection and cell harvesting for Western blot analysis	30
2.2.13.	Transfection for immunofluorescence	31
2.2.14.	Immunofluorescence	31
2.2.15.	Dynamic analysis by FCS and FRAP	32
2.2.15.1.	FCS	32
2.2.15.2.	FRAP	33
3.	**RESULTS**	**35**
3.1.	*In vitro* and heterologous interaction studies	35
3.1.1.	Affinity chromatography interaction studies	36
3.1.2.	Yeast two hybrid interaction (Y2H) assay	42
3.2.	Analysis of Y2H identified interacting protein	47

3.3.	Localization analysis of CENP-C and hMis12	53
3.3.1.	Localization analysis of CENP-C and CENP-C truncated proteins	54
3.3.2.	Localization analysis of hMis12	61
3.4.	Dynamic behavior measurements of CENP-C and hMis12	63
3.4.1.	Fluorescence Correlation Sprectroscopy (FCS)	63
3.4.2.	Fluorescent recovery after photobleaching (FRAP)	68
4.	**DISCUSSION**	**74**
4.1.	CENP-C and hMis12 failed to show the direct interaction with identified foundation kinetocore proteins	75
4.2.	False positive and false negative Yeast two-hybrid result	77
4.3.	SETDB1 interact with CENP-C	79
4.4.	Molecular dissection of CENP-C demonstrates the binding ability and functional domain of truncated CENP-C	81
4.5.	hMis12 might bridge the inner and outer kinetochore	82
4.6.	Consequences to the inner kinetochore complex architecture	83
5.	**REFERENCES**	**86**

APPENDIX

Appendix 1 CENP-C gene (2832 bp)
Appendix 2 hMis12 gene (618 bp)
Appendix 3 SETDB1 gene (1194 bp)
Appendix 4 PSMB10 gene (822 bp)

ACKNOWLEDGMENT

PUBLICATION AND SCIENTIFIC POSTER

SELBSTÄNDIGKEITERKLÄRUNG

CURRICULUM VITAE

ABBREVIATIONS

ACA	Anti centromere antibody
APC/C	Anaphase promoting complex or cyclosome
BUB	Budding uninhibited by benomyl
CAD	CENP-A Nucleosome Distal
Cdc20	Cell division cycle 20
CEN	Centromere
CENP	Centromere protein
CENP-A	Centromere protein A
CENP-B	Centromere protein B
CENP-C	Centromere protein C
CENP-E	Centromere protein E
CENP-F	Centromere protein F
CENP-G	Centromere protein G
CENP-H	Centromere protein H
CFP	Cyan fluorescent protein
ChIP	Chromatin immunoprecipitation
CLAPS	CLIP associating proteins
CLIPS	Cytoplasmic linker proteins
Co-IP	Co-immunoprecipitation
CREST	Calcinosis, Raynaud's phenomenon, esophageal dysmotility, sclerodactyly and telangiectasia
CRMP1	Collapsing response mediator protein 1
DNA	Deoxyribonucleic acid
DNMT3	DNA methyltransferase
ECFP	Enhanced cyan fluorescent protein
EPB47	Erythrocyte protein band 49
Esp1	Separin (separation) 1 protein
FCS	Fluorescence correlation spectroscopy
EYFP	Enhanced red-shifted yellow fluorescent protein

FISH	Fluorescence in situ hybridization
FRET	Fluorescence resonance energy transfer
FRAP	Fluorescence recovery after photobleaching
G-phase	Gap phase in eukaryotic cell cycle
GFP	Green fluorescent protein
GST	Glutathione *S-transferase*
GTP	Guanosine 5'-triphosphate
H3K4	histone H3 Methylate Lysine-4
H3K9	histone H3 Methylate Lysine-9
HDAC1	histone deacetylase 1
HDaxx protein	human Daxx protein
Hec1	Highly enhanced in cancer cells 1
hMis12	Human mini-chromosome instability 12
HP 1	Heterochromatin protein 1
ICIS	Inner centromere KinI stimulator protein
IgG	Immunoglubulin G
INCENP	Inner centromere protein
IP	Immunoprecipitation
IPTG	Isopropyl β-D thiogalactoside
KIAA1377	Kazusa Institute AA1377
MAD	Mitotic arrest defective
MCAK	Mitotic centromere-associated kinesin
MCS	Multiple cloning sites
MGC	Mammalian Gene Collection
MRPL20	Mitochondria ribosomal protein Large subunit 20
NAC	Nucleosome Associated Complex
ND10	Discrete nuclear substructure 10 protein
Ndc80	Nuclear division cycle 80
NES	Nuclear Export signal
NLS	Nuclear localization signal
NOR90	Nucleolus organizer region 90 protein

OD	Optical density
PCP	Purkinje Cell Protein
PCR	Polymerase chain reaction
PLK	Polo-like kinase
PML	Promyeolocytic leukemia
PSMB10	proteasome β subunit 10
QARS	Glutaminyl-tRNA synthetase
RNA pol	Ribonucleic acid polymerase
rRNA	ribosomal ribonucleic acid
RNAi	Ribonucleic acid interference
SET domain	Su(var)3-9, E(5), trithorax domain
S-phase	Synthesized DNA phase in eukaryotic cell cycle
Scc1	Spindle chromosome complex 1 protein
Scc3	Spindle chromosome complex 3 protein
SDII	synthetic minimal dextrose medium II
SDIV	synthetic minimal dextrose medium IV
SETDB1	SET Domain Bifurcated protein 1
SFC	Splicing factor compartment
Sgo1	Shugoshin protein 1
Smc1	Structural Maintenance of chromosomes 1
Smc3	Structural Maintenance of chromosomes 3
SPG7	Spastic paraplegia 7
SUMO-1	Small ubiquitin-like modifier 1 protein
Su(var)	Suppressor of variegation
TBP	TATA binding protein
UBF	Upstream Binding Factor
UBR1	Ubiquitine-protein ligase E3 component N-recognin 1
UV	Ultraviolet
YFP	Yellow fluorescent protein
YDP	Yeast extract, peptone, dextrose medium

SUMMARY

The centromere is the genetic ("CEN"-) locus required for the precise and accurate chromosome segregation. It is composed of i) the kinetochore, ii) the central DNA centromere domain and iii) the pairing domain. The assembly of the kinetochore and the interaction between kinetochore proteins is still vague.

Two foundation inner kinetochore proteins were studied in this thesis: CENP-C and hMis12. CENP-C is a 110 kDa protein that is composed of several functional domains. hMis12 is a much smaller protein of 25 kDa. Binding strength, location and orientation of these two kinetochore proteins and the determination of their binding partners are of central importance for the understanding of the inner kinetochore complex formation. CENP-C and its subdomains as well as hMis12 were cloned and characterized in this work *in vitro* and *in vivo*.

The *in vitro* affinity chromatography experiments could not detect any direct interaction between hMis12 and the three CENP-C subdomains with either CENP-A, CENP-B or CENP-C. The *in vivo* analysis with the Yeast two-hybrid system suggested that the CENP-C C-terminus interacts with SETDB1, a histone H3K9 methylase activity, and PSMB10, a 26S proteasome family member. These two proteins were cloned and studied in this thesis. SETDB1 showed only partial localization at the centromeres. The PSMB10 did not localize at the centromeres but accumulated in the spindle poles. Thus, PSMB10 seems not to be involved in kinetochore function. Instead, its colocalization with Cajal bodies indicated the involvement in transcription and processing of RNAs in the nucleus.

The dynamic behaviour of full length CENP-C demonstrated the stable binding of CENP-C to the inner kinetochore during the whole cell cycle. The CENP-C subfragments cloned in this thesis were still able to localize to the centromeres, however, with different binding behavior: they were found to be freely mobile. FCS and FRAP data indicated that CENP-C 315-635 is less mobile than CENP-C 1-315 and CENP-C 635-943. hMis12, as CENP-C, binds completely to the centromeres during mitosis. However, during interphase hMis12 binds to the centromeres less tightly: hMis12 was found to be mobile in interphase. hMis12 thus has a cell cycle induced shift in function. During interphase,

hMis12 might bind at the surface of the inner kinetochore, and might have a molecular function to establish a bridge between the inner and outer kinetochore during mitosis.

The data obtained here suggest that the inner kinetochore is a stable protein complex. The binding stability of CENP-C is not determined by the binding strength of CENP-C subdomains to their binding sites but instead by additional elements. Such an element might be the CENP-C di-/oligomerization at the centromere. In contrast, hMis12 exchanges very fast at the centromere suggesting that during interphase it is not a member of the stably binding inner kinetochore proteins but probably belongs to the 'mid zone' kinetochore proteins.

The repetitive α-satellite DNA might provide an ideal spacing in the chromatin structure for inner kinetochore proteins to di-/oligomerize and by this process forming a stable complex. The dynamic data obtained here indicate that the inner kinetochore proteins do not form a precomplex in the nucleoplasm but instead bind to the centromere/kinetochore as single proteins.

ZUSAMMENFASSUNG

Das Centromer ist der genetische („CEN“-) Lokus, der für die genaue und sorgfältige Chromosomensegregation benötigt wird. Die Centromere höherer Eukaryoten bestehen aus (i) der zentralen ´Centromer´-Domäne, (ii) der Kinetochor-Domäne und (iii) der Paarungs-Domäne. Die Wechselwirkung zwischen den Proteinen des Kinetochors ist noch unklar.

Zwei der Basisproteine des inneren Kinetochors wurden in der vorliegende Arbeit studiert: CENP-C und hMis12. CENP-C, ein 110 kDa Protein, ist ein inneres Kinetochor-Protein, welches sich aus mehreren funktionellen Domänen zusammensetzt. hMis12 ist ein wesentlich kleineres 25 kDa Protein. Die Bindungsstärke, die Lokalisation und die Orientierung von CENP-C und hMis12 sowie die Identifizierung ihrer Bindungspartner sind von zentraler Bedeutung für das Verständnis des inneren Kinetochor-Komplexes. CENP-C und dessen Subfragmente sowie hMis12 wurden kloniert und in der vorliegenden Arbeit *in vitro* und *in vivo* untersucht.

Die *in vitro* Affinitätschromatographie-Experimente konnten keine direkte Wechselwirkung zwischen hMis12 und den drei CENP-C-Unterdomänen mit jeweils CENP-A, CENP-B oder CENP-C nachweisen.

Die *in vivo* Untersuchungen mit Hilfe des Hefe-2-Hybridsystems (Y2H) zeigten, dass der C-terminale Bereich von CENP-C mit SETDB1 interagiert, welches Histon H3K9-Methylaseaktivität hat, sowie mit PSMB10, welches zu der 26S Proteasomenfamilie gehört. Diese beiden Proteine wurden in dieser Arbeit kloniert und untersucht. SETDB1 zeigte nur teilweise Lokalisierung mit den Centromeren. PSMB10 lokalisierte nicht an den Centromeren, zeigte aber Akkumulation an den Spindelpolen, welches gegen eine Beteiligung in der Kinetochorfunktion spricht. Dagegen deutet die Kolokalisation von PSMB10 mit Cajal-Kernkörperchen darauf hin, dass es an der RNA-Transkription und -Prozessierung im Nukleus beteiligt ist. Das dynamische Verhalten des Volllängen-CENP-C demonstrierte eine stabile Bindung dieses Proteins am inneren Kinetochor während des ganzen Zellzyklus. Die in dieser Arbeit klonierten CENP-C-Subfragmente waren ebenso in der Lage, sich am Centromer anzureichern, jedoch mit unterschiedlich starker Affinität und freier Beweglichkeit. Die FCS- und FRAP-Ergebnisse zeigten, dass CENP-C 315-

635 weniger beweglich ist als CENP-C 1-315 und CENP-C 635-943. hMis12, wie CENP-C, bindet komplett an den Centromeren während der Mitose. Dagegen ist die Bindung von hMis12 während der Interphase nicht sehr stark: hMis12 ist mobil in der Interphase und nur während der Mitose immobil. Daher könnte hMis12 an der Oberfläche der inneren Kinetochor binden und so während der Mitose die Funktion einer Brücke zwischen dem inneren- und äußeren Kinetochor ausüben.

Die Ergebnisse deuten an, dass das innere Kinetochor ein stabiler Proteinkomplex ist. Die CENP-C-Bindungsstabilität ist nicht durch die Bindungsstärke seiner Subdomänen bestimmt, sondern durch zusätzliche Faktoren. Ein solcher Faktor könnte die Di-/ Oligomerisierung des CENP-C-Proteins am Centromer sein. Im Gegensatz dazu bewegt sich hMis12 sehr schnell im Centromer. Dies weist darauf hin, dass während der Interphase hMis12 kein Element des stabil bindenden inneren Kinetochor-Protein-Komplexes ist, aber möglicherweise zu den ‚mid zone'-Kinetochor-Proteinen gehört.

In der Chromatinstruktur könnte die repetitive α-Satelliten-DNA am Centromer einen günstigen Abstand vorgeben, der eine Dimerisierung von CENP-B (und vielleicht CENP-H) und eine Oligomerisierung von CENP-C ermöglicht. Dieser Prozess führt dann, so unser Modell, zur Stabilität des inneren Kinetochor-Komplexes. Die dynamischen Ergebnisse der vorliegenden Arbeit zeigen, dass die Proteine des inneren Kinetochors einzeln am Centromer/Kinetochor binden und keinen Vorkomplex im Nukleoplasma bilden.

1. INTRODUCTION

The centromere is the genetic ("CEN"-) locus required for precise and accurate chromosome segregation (24). DNA centromere sizes are different for every organism: the DNA centromere of budding yeast *S. cerevisiae* is 125 bp long (36), of fission yeast 40 to 100 kb (155), in *Drosophila* it is 100 to 420 kb long (89, 196, 201, B. Sullivan personal communication), and human centromere DNA consist of AT-rich α-satellite 171 bp long DNA tandemly arranged into higher-order repeats which extend from 200 kb to 4 Mb (175, 67, 220). Centromeres of higher eukaryotes are composed of (i) the pairing domain, (ii) the central DNA "centromere" domain and (iii) the kinetochore multi-protein complex settling at the centromere (162, see Figure 1).

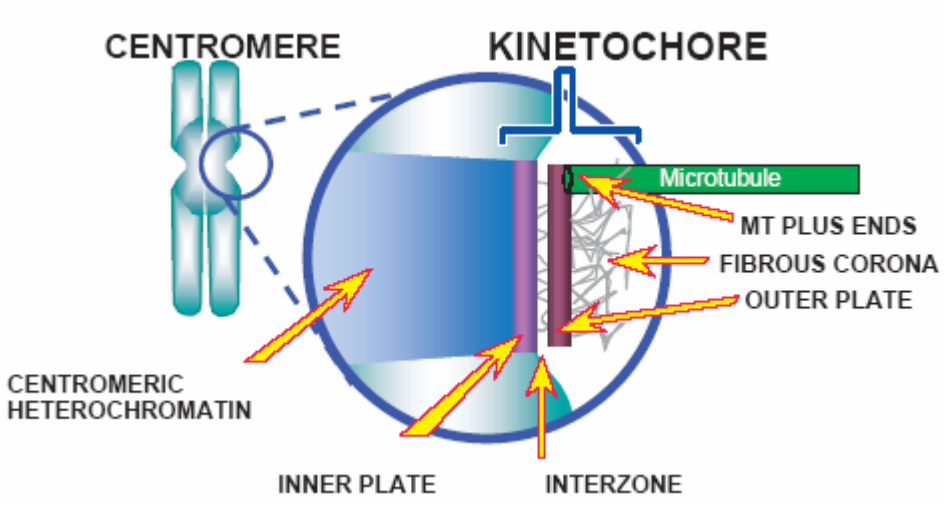

Fig. 1. The organization of mammalian centromere/kinetochore
(according to118)

The central domain is a heterochromatic block that underlies the centromere and the kinetochore protein complex while the pairing domain is the inner centromere region where sister chromatids are in most intimate contact (47, 37). Simultaneous dissolution of cohesion on all chromosomes defines anaphase initiation. The centromere flanking

centromeric heterochromatin consists of heterogeneous repeats including also transposable elements that can insert themselves randomly throughout the genome (225, 61). At the centromere, the kinetochore multi-protein complex assembles granting spindle attachment to the chromosome (197, 24, 4, 81) thus allowing microtubule binding (207, 94), and is involved in chromosome movements and cell cycle surveillance. In electron microscopy, the mitotic kinetochore is visibly formed as a trilaminar disc that consists of an inner plate, the interzone and an outer plate (see Fig. 1; 73, 197).

1.1. The human centromere/kinetochore

The formation of a functional kinetochore onto centromeric chromatin is very complex and in many steps still elusive. Electron microscopy demonstrated that the multi-layered human metaphase kinetochore comprises a distinct protein composition (156). Kinetochore protein organization is discussed in several publications and reviews (for a selection, see 5, 16, 27, 176, 216, 220).

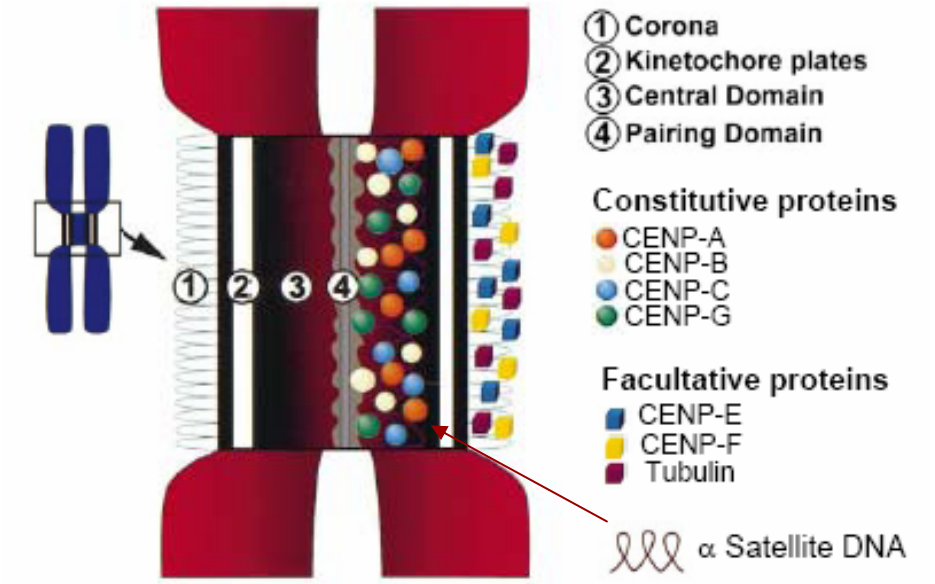

Fig. 2. The mammalian Centromere/Kinetochore complex domain
(according to 216)

Several kinetochore proteins have been defined to localize in the inner plate while others bind the fibrous corona and the outer plate (Fig. 2). The fibrous corona and outer kinetochore plate contain proteins that monitor the integrity of kinetochore attachment (134) such as the proteins of the Hec1 complex (41, 13) as well as CENP-E (232, 119), CENP-F (74) and BubR1 (84). The inner plate comprises the foundation inner centromere proteins, centromeric chromatin and several other complex proteins such as the inner centromere Aurora B complex: Aurora B, INCENP (2), Survivin (23) and Borealin/Dasra (63). The protein composition in the middle zone is not known (27) but several protein complexes are suggested to be positioned there (127, 125). According to a review (216), CENP-A, CENP-B and CENP-C reside in the inner kinetochore region together with CENP-G (Fig. 2). CENP-B binds the 17 bp CENP-B-box DNA sequence that is present in the α-satellite DNA (208). CENP-G is an inner kinetochore protein that associates with α-satellite DNA (72). Recently, 11 new proteins of the inner kinetochore were identified, the proteins of the "CENP-A Associated Nucleosome complex (NAC)" and "CENP-A nucleosome distal complex (CAD)" (54, 146). NAC contains CENP-M, CENP-N, CENP-T, CENP-U(50), CENP-C and CENP-H, while CAD contains CENP-K, CENP-L, CENP-O, CENP-P, CENP-Q, CENP-R and CENP-S (54). The other inner kinetochore proteins were identified and partially analyzed as revealed in the previous studies (6, 83). The kinetochore assembly follows a temporal order according to the hierarchical binding and loading into the kinetochore complex (27, 111). For instance, CENP-F appears at the kinetochore between G2 and prophase (163) while CENP-C binds during the whole cell cycle (95). CENP-F localization not only depends on hBub1 but also on CENP-I, a protein in the inner plate (112). CENP-I is necessary for CENP-C targeting (140).

Centromeric binding of many outer kinetochore proteins are found to depend on the presence of CENP-A; Polo Like Kinase (PLK) (8), ROD (15), Zwint-1 (216), ZW10 (15), the microtubule motor dynein (227), the kinesin motor CENP-E (164), the spindle motor checkpoint proteins (MPS1 (190), BUBR1 (164, 101), MAD1 and MAD2 (112)) and CLASP (3) require CENP-A for targeting to the kinetochore (111; reviewed in 118).

1.2. The foundation inner centromere/kinetochore protein complex

The six foundation inner kinetochore proteins CENP-A, CENP-B, CENP-C, CENP-H, CENP-I and hMis12 were found to have various roles and mutual interactions (5). Their association with centromeric DNA and heterochromatin was supposed to create a structural domain that supports the different functions of the centromere/kinetochore. Very little is known about the newly identified inner kinetochore proteins of the NAC and CAD complexes (146, 54, 6, 83). A model of the complex arrangement is shown in Figure 3. CENP-C targeting depends on CENP-A in humans (77). CENP-C binds α-satellite DNA, however sequence unspecifically (160). Applying a ChIP assay, a previous study confirmed that CENP-A forms a DNA chromatin complex with CENP-B and CENP-C (6, 139). Nevertheless, there is no report demonstrating a direct interaction between CENP-A and CENP-C.

The linear model in Fig. 3 illustrates that in humans the kinetochore assembles on α-I satellite DNA, which contains 17 bp CENP-B boxes (80, 235). The interdependence among foundation kinetochore proteins is indicated in the Fig. 3 (inset): hMis12 interacts with CENP-I and CENP-H directly but independently from CENP-A. The dashed arrows indicate the relation of CENP-B to CENP-A and CENP-C (122). This thesis study investigates the network relationship and behavior of two of these foundation proteins, CENP-C and hMis12, *in vitro* and particularly *in vivo*.

CENP-A is a 17 kDa histone H3 variant protein which replaces H3 in centromeric chromatin (199, 217, 195). It is required but not sufficient for defining active centromeres (149, 200, 111) and has a role in templating centromere replication (77). CENP-A-depleted chicken DT40 cells revealed mis-localisation of inner (CENP-C, CENP-H and CENP-I) and outer (Nuf2, Hec1, Mad2 and CENP-E) kinetochore proteins. Moreover, these cells lack proper chromosome congression on the mitotic spindle, transient delay in prometaphase and chromosome mis-segregation (60). Furthermore, BubR1 mis-localisation demonstrated a specific role of CENP-A in mitotic checkpoint signalling (164). CENP-A knockout cells indicated that CENP-H and -I have a role in targeting newly expressed CENP-A to centromeres (146).

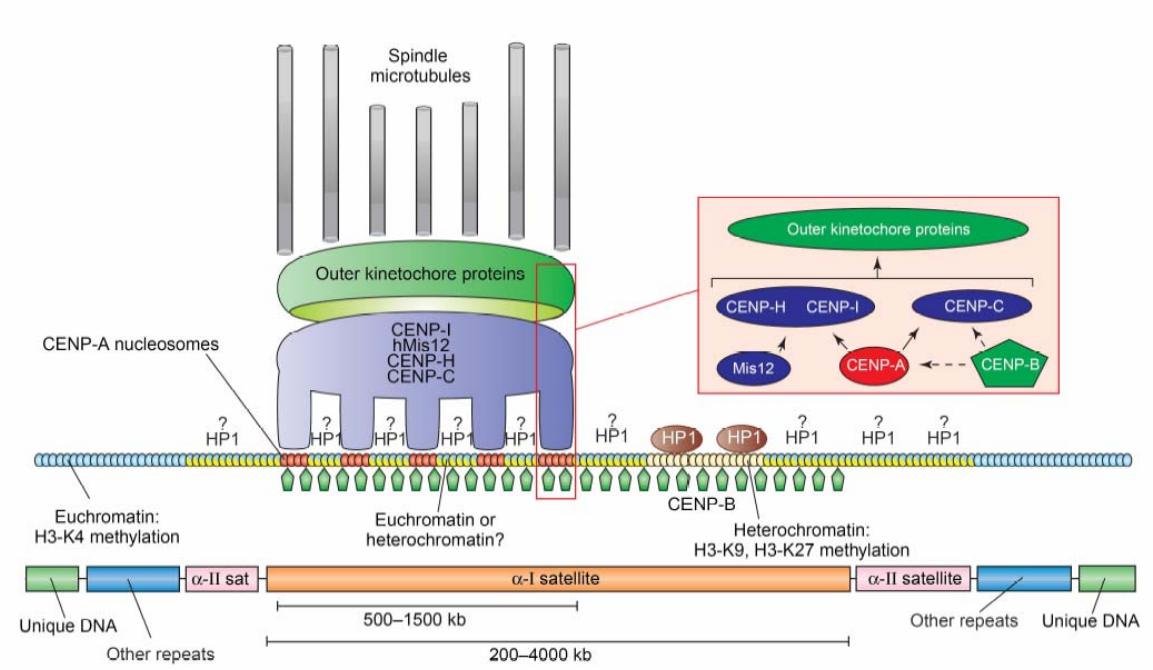

Fig. 3. The foundation inner kinetochore proteins
(according to 5)

CENP-B is an 80 kDa protein that specifically binds to the 17 bp CENP-B box DNA which is repeatedly present in α-satellite DNA (121). CENP-B is the only kinetochore protein with a specific DNA binding site (208). It is observed to colocalize with the centromere throughout the cell cycle and to distribute throughout centromeric heterochromatin (35). This protein binds to the CENP-B boxes in active and inactive centromeres (121). CENP-B knockout mice showed normal viability and localization of other centromere proteins (79, 88, see also 5). Yeast two hybrid analysis revealed a CENP-B interaction with CENP-C (203). CENP-B is able to induce a translational positioning of nucleosomes (208).

1.2.1. CENP-C

CENP-C, a 110 kDa protein consisting of 943 amino acids, is an inner kinetochore protein component (168). CENP-C had been identified as a chromosomal autoantigen in patients with scleroderma spectrum disease, CREST (calcinosis, Raynaud's phenomenon,

esophageal dysmotility, sclerodactyly and telangiectasia) syndrome (133). CENP-C interacts with the nucleolar transcription factor UBF/NOR90 that was independently identified as a nucleolar autoantigen in scleroderma (158). *Arabidopsis thaliana* CENP-C was observed to be present at the centromeres throughout the cell cycle, as its human homolog, indicating evolutionary conserved functions for CENP-C (143). Previous studies reported that CENP-C is composed of several functional domains (see Fig. 4). The centromere targeting domain was identified in a 60 amino acid long region (Fig. 4 green bar) between residues 478 to 537 and in a 310 amino acid long region between residues 634 to 943 (yellow bar; 229, 185). Further analysis revealed that the critical region of centromere targeting domains localize in amino acid region between residues 522 to 533 (185). The region between residues 1 to 323 is the "instability domain" and is assumed to be involved to regulate the temporal destruction of proteins at specific stages of the cell cycle (102). *In vitro* experiments had shown that the N-terminal amino acids 74 to 244 and the C-terminus between amino acids 820 to 943 are oligomerization and dimerization domains (194). *In vitro* studies showed that CENP-C is able to bind DNA nonspecifically (229) although it can bind α-satellite DNA of HeLa cells selectively (160). The CENP-C DNA binding domain is localized between residues 433 to 520 (Fig. 4, pink bar) and the nuclear localization signal (NLS) is found at residue position 484 to 499 (229). Previous study showed that two distinct domains, between amino acids 478 to 537 and 634 to 943, are capable of binding α-satellite DNA and are able to localize at the centromere, indicating that CENP-C may target the centromere by establishing multiple contacts with DNA and protein constituents of the kinetochore (213).

Human chromosome studies demonstrated that CENP-C is present only at active centromeres, indicating that CENP-C has a noteworthy role in centromere function (46, 148). It is supposed to maintain proper kinetochore size and contributes to stabilizing microtubule attachment (212). Anti-CENP-C antibody nuclear microinjection during interphase in HeLa cells resulted in metaphase arrest and reduced the size of kinetochores due to the lack of CENP-C at centromeres (95). The inactivation of the *Cenp-C* gene in HeLa and Chicken DT40 cells resulted in metaphase to anaphase delay and also chromosome missegregation followed by apoptosis (58). Gene disruption in mouse

embryos showed mitotic arrest indicating CENP-C involvement in mitotic progression from metaphase to anaphase (90).

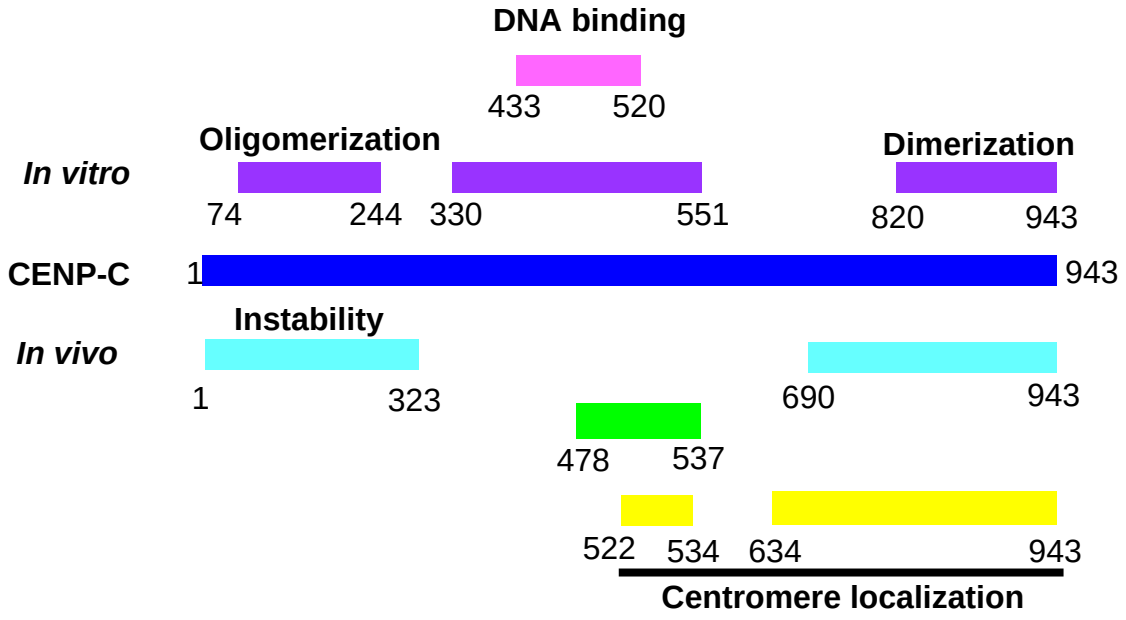

Fig. 4. Summary of CENP-C functional domain dissection
(following 213)

The interaction of CENP-C with the other centromere proteins and molecules is not yet fully revealed, in particular not *in vivo*. Immuno-fluorescence analysis revealed that CENP-A reduction results in loss of discrete CENP-C binding to centromeres, and after CENP-A deletion, CENP-C is unable to precipitate the kinetochore indicating that CENP-A is essential for kinetochore targeting of CENP-C (77). This however, does not prove a direct interaction between CENP-A and CENP-C. Chromatin immunoprecipitation (ChIP) analysis on HeLa cells suggested that CENP-C interacts with CENP-B/CENP-A nucleosome complexes (6). A previous interaction study confirmed the direct interaction between CENP-C and CENP-B in the region between residues 283 – 429 and 727 – 943 by a Yeast two-hybrid assay (203). These CENP-C regions are homologous with Mif2 of *S. cerevisiae* (20, 126). Although CENP-C is able to assemble without CENP-B (203), the interaction may be involved in the correct

assembly of CENP-C on alphoid DNA (145). Overexpression of a truncated CENP-C interaction domain resulted in abnormal duplication of CENP-C and cell cycle arrest (203). Immunocytochemical analysis against chicken CENP-H-depleted cells showed that the CENP-C signal was diffused and there was no CENP-C signal in CENP-I deficient cells, demonstrating that CENP-H and CENP-I are necessary for CENP-C localization (59, 140). CENP-C colocalized with CENP-H and CENP-I throughout the cell cycle (193, 140).

An involvement of CENP-C in apoptosis is supported by a Yeast two-hybrid assay that indicates an interaction between CENP-C and the hDaxx protein: Daxx is present at interphase centromeres (159). Daxx is a component of the ND10 body and is able to modulate Fas-mediated apoptosis (230). CENP-C amino terminal residues 1 to 315 interact directly with the carboxhyl-terminal residues 636 to 740 of hDaxx which are responsible for binding apoptosis signaling proteins (159). SUMO-1 that colocalizes with the ND10 body and centromeres in a cell cycle-dependent manner, is modifying CENP-C, indicating a connection between ND10 and centromere through the SUMO-1 modification pathway (50, 58).

1.2.2. hMis12

The minichromosome instability (mis) centromeric proteins are conserved in budding yeast, filamentous fungi and human (204). Mis12 is one of 12 identified mis proteins (64). Mis12 has a role in regulating the functional centromere during the cell cycle. It is required for correct spindle morphogenesis in metaphase but not for sister chromatid segregation (29). ChIP assays suggest that Mis12 interacts with the inner kinetochore and FISH experiment determined that Mis12 was critical for creating and maintaining the inner kinetochore structure (64).

Arabidopsis thaliana (AtMis12) and human Mis12 (hMis12) are localized at centromeres throughout the cell cycle (29, 171). RNAi treatment showed that reduction of hMis12 induced missalignment of chromosomes in metaphase and lagging chromosomes in anaphase, followed by frequent micronuclei formation in interphase (65). These abnormalities reflect the chromosome missegregation and aneuploidy phenotype of

cancer cells (180). hMis12 is still localized at the centromere after CENP-A RNAi knockdown indicating that in the kinetochore assembly process, hMis12 follows a CENP-A independent pathway (65,111).

Recent immunoprecipitation (IP) and subsequent mass spectrometry studies indicated that hMis12 may interact with nine human proteins (141): Hec1/Kntc2 and Zwint-1 (kinetochore proteins), HP-1α and HP-1γ (heterochromatin components), also KIAA1570, c20orf172, DC8 and PMF1 (human proteins of unknown function). Further investigation in that study confirmed that GFP-tagged c20orf172 and DC-8 are localized to centromeres. c20orf172 is essential for correct chromosome alignment during metaphase and HP-1α and HP-1γ are required for functional kinetochore formation through the interaction with hMis12 (141). These results suggest that HP-1 might provide a platform for hMis12 to anchor and connect to Zwint-1 at the outer kinetochore. This is in agreement with the finding that hMis12 assembles at the kinetochore independently of CENP-A (65, 141). It was shown by affinity chromatography and localization analysis that hMis12 forms a stable complex with three kinetochore proteins: hNnf1 (PMF1), hNsl1 (DC31) and hDsn1 (Q9H410) (29, 93). hMis12 complex depleted human cells displayed chromosome misalignment, mitotic delay and chromosome biorientation defects (93). This complex is required for outer kinetochore recruitment (29). Mis12 may be involved in recruiting the checkpoint components to the spindle (64). Two outer kinetochore proteins, CENP-E and Hec1 that contribute to stable kinetochore formation and bioriented kinetochore microtubule attachment, are reduced in hMis12 complex depleted HeLa cells (93). In human cells, the Hec1 (yeast Ndc80 homolog) complex is comprised of four proteins: Hec1, Nuf2, Spc24 and Spc25 (30, 33, 41).

1.2.3. Further members of the inner kinetochore complex

CENP-H is a 34 kDa protein that contains a coiled-coil structure and localizes at the centromere throughout the cell cycle (192). CENP-H appears at active centromeres and colocalizes with other centromeric proteins such as CENP-A, CENP-B, CENP-C, CENP-E and MCAK (193). CENP-H knockout chicken DT40 cells demonstrated chromosome missegregation and mitotic arrest (59). The interaction between chicken CENP-H with

Hec1 showed that CENP-H enables connections from the inner to the outer kinetochore (128). A previous study revealed that CENP-C requires CENP-H for centromere targeting (59).

CENP-I is an 87 kDa constitutive kinetochore protein (142) that colocalizes with CENP-A, CENP-C and CENP-H throughout the cell cycle (140). CENP-I depleted cells demonstrated cell cycle delays in G2 phase and showed absence of CENP-F and the checkpoint proteins MAD1 and MAD2 (112). Even though CENP-I is not required for CENP-A localization, its association with CENP-H is directing CENP-A deposition to centromeres (140, 146).

1.3. Linker proteins for outer human kinetochore proteins

The hMis12 and the Hec1 complexes serve as binding platforms for outer kinetochore proteins (111, 75). Hec1 binds to hMis12 (29). The role of the CENP-A distal CAD complex is unresolved yet; also this complex might be involved in binding of outer kinetochore proteins. Binding of the outer plate proteins also requires the presence of CENP-F (109). CENP-F is a 400 kDa protein that assembles onto kinetochores during late G2 and is observed at every chromosome by the onset of prophase (163, 18). This protein associates with kinetochores independently of tubulin and its dissociation is dependent on events connected with the onset of anaphase (1). Furthermore, Bub1 and Aurora B allow the binding of checkpoint and further proteins of the mitotic checkpoint. These proteins (BubR1, Bub3, Mad2 and Cdc20) are components of the mitotic checkpoint complex MCC (12) which inhibits the anaphase promoting complex APC until all kinetochores are attached to microtubuli (113). BubR1 is a 120 kDa mitotic checkpoint kinase (107). Its phosphorylation is regulated during the mitotic checkpoint activation (210). BubR1 is activated by CENP-E (26, 119), a high molecular weight kinetochore microtubule motor protein of 312 kDa (233, 110). Chromosomes lacking CENP-E have reduced numbers of microtubules bound to the kinetochore, show wrong checkpoint activation and display chromosome misalignment (232).

1.4. Models of the centromere/kinetochore complex

The complete human genome sequence has not revealed major new insights into the composition of the centromeric DNA structure, in part because these regions are difficult to sequence due to their highly repetitive nature. In contrast to the highly conserved structure and function of many eukaryotic kinetochore proteins, flies, yeast, plant and mammals have different sequences of centromere DNA (206).

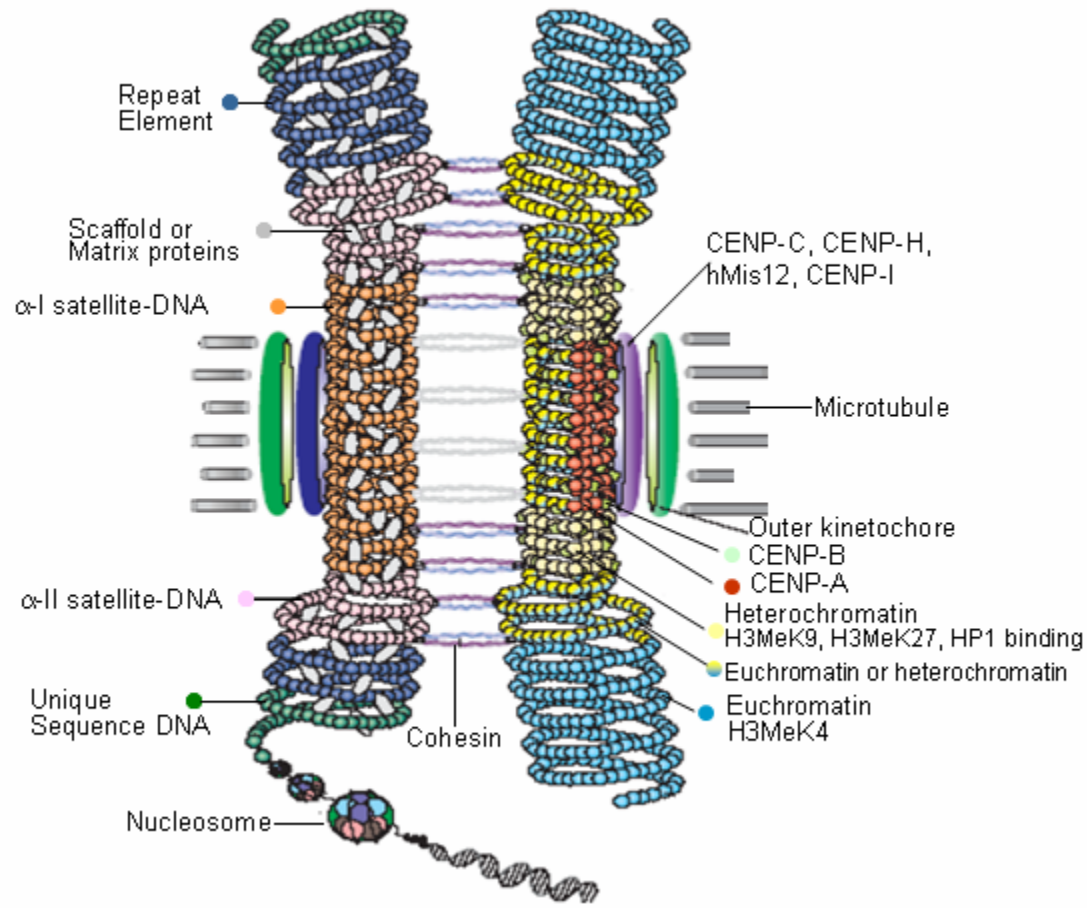

Fig. 5. Model of human centromere organization
(following 5)

The model of organization of the human centromere exhibiting the location of six foundation kinetochore proteins in centromeric heterochromatin and the inner kinetochore is shown in Fig. 5 (for reviews see 5 and 16). A pair of chromatids is

conjoined by cohesin. As the key element of this model, the centromeric chromatin forms a cylinder-shaped spiral. This explains nicely that centromeric chromatin contains regions with two CENP-A molecules per each nucleosome interspersed with regions containing nucleosomes with two H3 histones each (16). In the spiral arrangement, the H3 regions point inwards while the CENP-A regions point outwards and offer a binding surface for the further inner kinetochore proteins CENP-C, -H, -I and hMis12 (violet and blue disc). The presence of scaffold and matrix proteins (left chromatid) and CENP-B as well as epigenetic marks (right chromatid) are indicated. The right chromatid shows CENP-A and CENP-B interspersed in the centromeric heterochromatin. While this model offers a speculation on the structural arrangement of CENP-A and –B, no specific suggestion is made for the other inner kinetochore proteins. The displayed spirals might indicate a 30 nm chromatin fiber structure. The size of the inner kinetochore of approximately 200 nm (9) clearly requires more than one 30 nm fiber at the inner kinetochore layer exhibiting the limitations of this model.

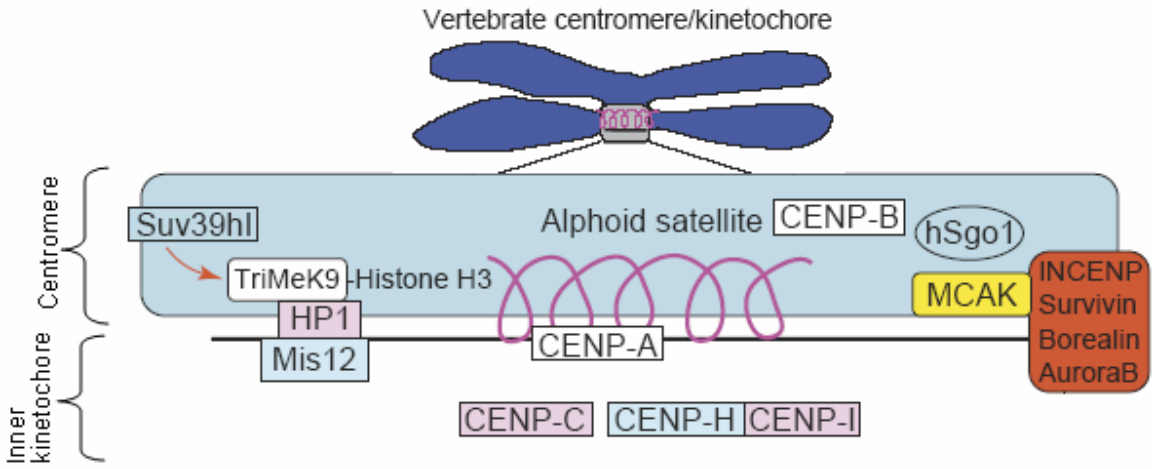

Fig. 6. The schematic model of human centromere protein distribution in human centromere/kinetochore. Proteins are illustrated as the interaction network. The fused shapes indicate direct interaction among proteins. Red arrow indicates enzymatic relationship.
(following 27)

An alternative model of molecular vertebrate kinetochore organization displays the arrangement of these and further inner kinetochore proteins at the centromere (Fig. 6) (27). The model depicts that H3 is trimethylated by Suv39hI at lysine 9. H3triMeK9 binds to HP1 which interacts with hMis12. CENP-A, as CENP-B, binds to alphoid satellite DNA. In agreement with experimental data, CENP-B shows no direct binding to CENP-A. CENP-C and the CENP-H/CENP-I complex localize next to CENP-A with no direct interaction indicated. Aurora B kinase, a chromosomal passenger protein that localizes in the inner centromere (7), forms a complex with INCENP, Survivin and Borealin. The mitotic centromere associated kinesin (MCAK) is fused to this complex. hSgo1, involved in establishing sister centromere cohesion (222), localizes close to this complex, also none interaction was indicated. This model (see review 27) tries to display experimental findings, however, it is even less specific on the structural arrangement of the proteins than the model in Fig. 5 (see review 5): no statements on the stoichiometry or steric situation are made.

These two models are representative for several other models for the inner kinetochore architecture (see for example: Fig. 7) (111). Little is known on the stoichiometry and steric arrangement of the inner kinetochore complex forming the centromeric chromatin. This lack of knowledge is unsatisfying since structural aspects might play a role in kinetochore function. In this thesis, information is gathered on the kinetochore proteins CENP-C and hMis12 in order to help elucidate their involvement in the complex.

Recently, the assembly pathway and interaction network of the kinetochore proteins was studied using RNAi method (111). Their data are summarized in a model shown in Fig. 7. CENP-A is at the top of the hierarchy initiating three different assembly pathways starting with CENP-I, CENP-C and Aurora B. Further kinetochore proteins bind down the assembly lines (as indicated) and interact with one another at nodes (like for example Bub1). Kinetochore complex formation during mitosis is an interactive process allowing precise control at several steps. For example, CENP-F that is regulating the dynein-dynactin complex (231), is depends on CENP-I and BUB1 for centromere localization. CENP-F and the Hec1 complex bind CENP-I. This complex serves as the binding platform for hMPS1, MAD1 and MAD2, in this way connecting the inner and outer

kinetochore. However, also in this model it remains elusive how the kinetochore proteins interact and any information on the stoichiometry and steric situation is missing.

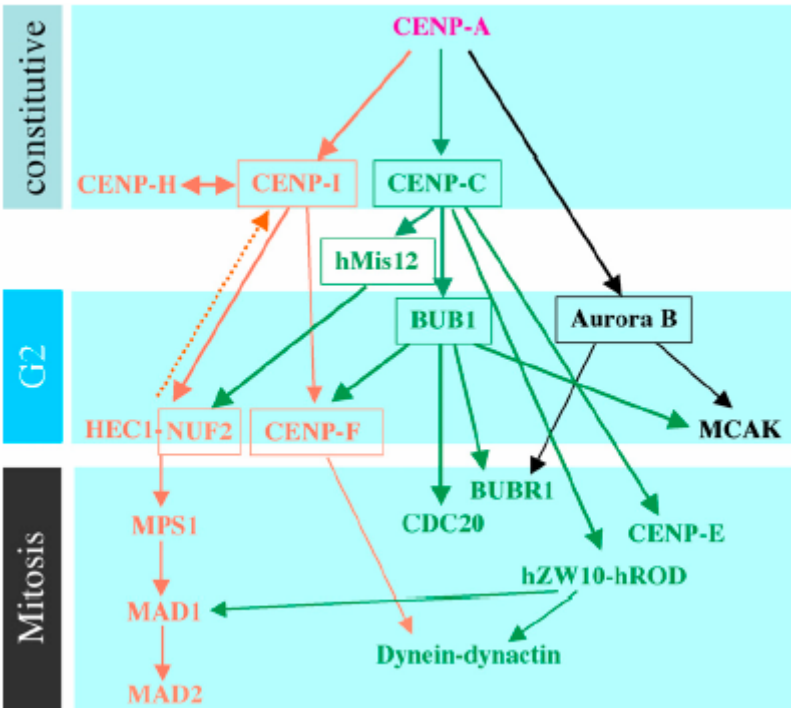

Fig. 7. The overview of kinetochore assembly pathway in human cell (following 111)

1.5. The centromere/kinetochore during mitosis

The inner kinetochore is assumed to define a protein plate (see Figure 1) or cylinder (see Figure 5) (16). This protein layer might represent a specific centromeric chromatin structure containing nucleosomes with at least one specialized histone (H3 variant CENP-A), auxiliary proteins and DNA. It exists as a discrete centromeric heterochromatin domain throughout the cell cycle (157). The inner kinetochore, present during interphase, defines the site of outer kinetochore complex formation beginning in late S-phase (239). The outer kinetochore contains the mitotic cell cycle checkpoint proteins. Further functions of the outer kinetochore include microtubule interaction (197) with about 25

end-on attachment sites for microtubules (118). The precise chromosome segregation requires amphitelic bi-orientation of microtubule attachments for the sister kinetochores. When the chromosomes are segregated unevenly due to attachment to the same spindle pole (synthelic attachment), misorientation occurs and anaphase is delayed (42, 28). This mistake is detected and corrected by Aurora B kinase (100), a chromosomal passenger protein that localizes at the inner centromere from late G2 to metaphase (23). After nuclear envelope breakdown at the onset of pro-metaphase, the spindle microtubules capture the kinetochores and congress them in the equator plate. The microtubules that attach to the kinetochores with opposite orientation, distribute the identical replicated genome copies to their new locations. The process ends with chromosome segregation to the opposite spindle poles (34, 68,173).

1.6. Aims

At centromeres, a histone H3 variant (in humans: CENP-A) replaces H3 in the nucleosomes and serves as the basis of complex formation (149, 183, 14, 223, 111, 200). Further inner kinetochore proteins assemble at this location forming the inner kinetochore that is present at the centromere during the whole cell cycle (80, 193, 140, 236, 160, 54). At least some of these proteins build up a stable complex (223). Surprisingly, no protein interaction could be detected *in vitro* between CENP-A and any other inner kinetochore protein (203). In humans, the centromere consists of multifold repeats of α-satellite DNA. If the centromeric DNA is deleted, a functionally active kinetochore is formed at another "neo"-centromere that might not contain α-satellite DNA (32). Thus, neither CENP-A nor the centromeric DNA offer a specific site for binding of the further inner kinetochore proteins. CENP-A or the centromeric DNA might be epigenetically marked so that they can be identified as specific binding sites. Alternatively (or additionally), the 171 bp repeat length α-satellite DNA with CENP-A loaded nucleosomes might offer a particular chromatin structure which is recognised and fixed by the self-aggregating inner kinetochore proteins CENP-B, -C and -H. Binding strength, location and orientation of CENP-C and the determination of its binding partners are thus of central importance for the understanding of inner kinetochore complex formation and assembly. CENP-C and its subdomains will therefore be cloned and studied in this work.

During interphase, the inner kinetochore proteins form a stable complex. In mitosis, further proteins bind to the structure. Still it is unclear, at which location these proteins bind to the inner kinetochore complex. One potential binding partner would be hMis12, a member of the four protein hMis12 complex. At the surface of the inner kinetochore complex, the hMis12 complex might function as a binding platform for outer kinetochore proteins. Therefore, hMis12 will be cloned and analysed.

To address these points, several experiments will be carried out. For the purpose of the interaction studies, the GST interaction assay and Yeast two-hybrid analysis will be applied. GST fusion proteins allow for affinity chromatography studies, hopefully identifying interaction partners. Yeast two-hybrid analysis is expected to screen the interaction either with known or new human kinetochore proteins from a human cDNA library. Fusions with fluorescent proteins, in particular GFP, are planned to be constructed for *in vivo* localization and dynamic studies. The results of these studies should yield a more detailed picture on the function of these two proteins in the kinetochore complex and should help to understand some aspects of protein binding in the kinetochore assembly pathway.

2. MATERIALS AND METHODS

2.1. MATERIALS

2.1.1. Chemicals

All general chemicals were purchased from Carl Roth GmbH & Co, Merck, Sigma, Serva and AppliChem with high purity grade. Bacterial medium materials were purchased from Gibco and cell line medium materials were purchased from PAA lab GmbH. Restriction enzymes were purchased from New England Biolabs and T4 DNA ligase was purchased from Invitrogen, Liposomes transfection reagents were purchased from Roche, Invitrogen, Biorad and Carl Roth GmbH & Co.

2.1.2. Standards and kits

The following kits and markers were used and obtained from the companies given in brackets:

puRE Taq Ready To Go PCR Beads kit (Amersham), Expand high fidelity plus PCR system kit (Roche), TOPO TA cloning kit (Invitrogen), Zero blunt end TOPO PCR cloning Kit (Invitrogen), pDONR TOPO cloning kit (Invitrogen), BP and LR clonase gateway cloning kit (Invitrogen), 1kb DNA ladder (Fermentas), unstained protein marker (Biorad), unstained protein marker (Fermentas), pre-stained protein marker (Fermentas), PAGEBlue staining solution (Fermentas), Hi-speed plasmid midi kit (Qiagen), Mini-elute gel extraction kit (Qiagen), qiaquick PCR purification kit (Qiagen).

2.1.3. Bacterial strains and cell lines

The following strains were used and obtained from the companies given in brackets:

E. coli XL1-Blue (Stratagene), *E. coli* BL21DE3 (Stratagene), *E. coli* DB3-1 (Stratagene), Yeast L40ccu**a** (*MAT**a** his*3Δ200 *trp1-910leu2-3,112LYS2::(lexAop)$_4$-HIS3ura3::lexAop)$_8$- lacZ ADE2::lexAop$_8$-URA3 GAL4 gal80 can1 cyh2*) (MDC-Berlin), Yeast L40cc**α** (*MAT**α** his*3Δ200 *trp1-910 leu2-3,112 ade2 LYS2::(lexAop)$_4$*

*HIS3ura3::lexAop)$_8$- lacZGAL4 gal80 can1 cyh2***)** (MDC-Berlin), HEp2 cell line (ATCC), U2OS Cell line (ATCC)

2.1.4. DNA templates

The following DNA templates were used:

pTCATG+*Cenp*-C (obtained from Prof. Earnshaw, Edinburg, UK), pOTB7+*hMis*12 (RZPDnoIRAUp969C0611D6), cDNA-derived 2000 human gene fragments in pBTM117 and pGAD426 (MDC-Berlin collection), *SETDB1*(RZPD-IOH14445), *PSMB10* (RZPDo834D015D).

2.1.5. Plasmid vectors

The following plasmids were used and obtained from the sources given in brackets:

pCR2.1 TOPO (Invitrogen), pCR Zero Blunt-TOPO (Invitrogen), pDONR (Invitrogen), pGEX5X2 (Amersham), pGEX5X3 (Amersham), pBTM-117 (MDC-Berlin), pGAD-426 (MDC-Berlin), pACT-4 (MDC-Berlin), pEGFP-C2 (Clontech), pEGFP-C3 (Clontech), pECFP-C2 (Clontech), pECFP-C3 (Clontech), pEYFP-C2 (Clontech), pEYFP-C3 (Clontech), pASK-IBA7 (IBA-Biotechnology), pEGFP-C gateway (FLI-Jena), pEGFP-N gateway (FLI-Jena).

2.1.6. Oligonucleotide primers

CENP-C, hMis12, SETDB1 and PSMB10 primers were synthesized by MWG-Biotech AG (Ebersberg). The primers with the melting temperature (T_m) of 64 – 73 °C were designed using Clone Manager 7 (Scientific & Educational Software, USA). The CENP-C localization domain primers were kindly synthesized by Dr. E. Birch-Hirshfeld (FSU Jena).

2.1.6.1. CENP-C primers

The following primers were used to clone CENP-C and its three subdomains “first (F)” aa 1-315, “middle (M)” aa 315-635, and “last (L)” aa 635-934:

CFF (forward (F)): 5’TTCATCTCGAGTATGGCTGCGTCCGGTCTGGATCA3’

CMF (forward): 5'TTCATCTCGAGTTCTTGGATTACAATACCAAGAAA3'

CLF (forward): 5'TTCATCTCGAGTTCTACAAGAAGCTCAAAGAATGAA3'

CFR (reverse (R)): 5'ACTTACTGCAGCGGCCGCTATCTACTGGCAAAACTTTGATC3'

CMR (reverse): 5'ACTTACTGCAGCGGCCGCTATCTAGAACAATCAAGATTTTTC3'

CLR (reverse): 5'ACTTACTGCAGCGGCCGCTATCATCTTTTTATCTGAGTAAA3'

For cloning of the CENP-C localization domain aa 522-533, the following primers were used:

CpCf (forward):

5'AATTCCTCCCAAAAAGCGGAAAGTGCGAAGAATTTCCAGGCGTCCATCTGATTGGGGGTGGTAAAATAG3'

CpCr (reverse):

5'GATCCTATTTTACCACCCACCAATCAGATGGACGCCTGGAAATTCTTCGCACTTTCCGCTTTTTGGGAGG 3'

2.1.6.2. hMis12 primers

The following primers were used to clone hMis12:

hMis12EcoRI-SalI (forward): 5'GAATTCTGTCGACCATGTCTGTGGATCCAATGA3'

hMis12NotI (reverse): 5'GCGGCCGCTTAAGATATTTTCAGTCGTTTCG3'

hMis12BsaI (forward): 5'GGTCTCAGCGCATGTCTGTGGATCCAATGAC3'

hMis12BsaI (reverse): 5'GGTCTCATATCTTAAGATATTTTCAGTCGTTTCG3'

2.1.6.3. SETDB1 primers

The following primers were used to clone SETDB1 into the Gateway (Invitrogen) entry vector:

fw_attB1SETDB1 (forward)

5'GGGGACAAGTTTGTACAAAAAAGCAGGCTTCGAAAACTTGTATTTTCAGGGCATGTCTTCCCTTCCTGGGTG3'

rev_attB1SETDB1 (reverse)

5'GGGGACCACTTTGTACAAGAAAGCTGGGTAGTTCCCCCCCCACCAACCT3'

2.1.6.4. PSMB10 primers

The following primers were used to clone PSMB10 into the Gateway (Invitrogen) entry vector:

fw_attB1PSMB10 (forward)

5'GGGGACAAGTTTGTACAAAAAAGCAGGCTTCGAAAACCTGTATTTTCAGGGCATGCTGAAGCCAGCCCTGG3'

rev_attB1PSMB10 (reverse)

5'GGGGACCACTTTGTACAAGAAAGCTGGGTATCCACCTCCATAGCCTGA3'

2.1.7. Antibodies

The following antibodies were used, as well as the dilution and the sources are given in brackets.

Human anti centromere antibody (ACA) (1:200; 226), Human anti heterochromatin (EKE Serum) (1: 200, von Mikecz Lab, Düsseldorf Univ.), Human anti PML body MD103122 (1:50, Bad Bramstedt), Human anti PML body MD535 (1:100, Uniklinik Jena), Human anti Cajal body ND 607850 (Uniklinik, Jena), Rabbit anti GST antibody (1:10.000, SIGMA), Mouse anti GFP antibody (1:50, Santa-Cruz), Rhodamin α human (1:200, Dianova), CY3 α Rabbit (1:200, Dianova), CY5 α human (1:200, dianova), Horseradish peroxidase (HRP) anti human (1:4.000, Dianova), HRP anti rabbit (1:4.000, Dianova), HRP anti mouse (1:4.000, Dianova), Strep-tactin alkaline phosphatase conjugate (1:4.000, IBA-Biotechnology).

2.1.8. Software

The following software from the companies given in brackets were used:

Clone manager 6 (Scientific & Educational Software, USA), Clone manager 7 (Scientific & Educational Software, USA), LSM image browser (Zeiss), PSORTII web server, Origin Software (Origin Lab), Excel (Microsoft), LSM confocal software 3.2 (Zeiss).

2.2. METHODS

The following routine molecular biology and cell biology methods were performed according to standard protocols (170, 25):

DNA restriction, DNA ligation, DNA transformation, *E. coli* competent cell preparation, DNA spectrofotometric quatification, DNA gel electrophoresis, DNA-EtBr visualization, protein spectrophotometric quatification, protein gel electrophoresis, bacterial culture and cell line maintenance.

The following molecular biology methods were performed by using commercially available reagents according to the manual:

- PCR reaction mix (puRE Taq Ready To Go PCR Beads kit (Amersham), Expand high fidelity plus PCR system kit (Roche))
- PCR product purification (Qiaquick PCR purification kit, Qiagen)
- Cloning of PCR product (TOPO pCR2.1 TOPO and pCR Zero Blunt-TOPO (Invitrogen)
- Cloning of PCR product into gateway system (Invitrogen)
- Large scale DNA preparation (Hi-speed Qiagen plasmid Midi Kit, Qiagen)
- Protein staining (PAGEBlue staining solution, Fermentas)
- Isolation and purification of DNA from agarose gel (mini elute DNA extraction kit, Qiagen)

The following methods described in detail are those developed or modified during this laboratory work.

2.2.1. PCR process

2.2.1.1. Generation of *CENP-C* full length and *CENP-C* fragments

The PCR process was carried out for 34 cycles that comprised of denaturation at 95 °C for 30 seconds, annealing at 65 °C for 30 seconds and elongation at 72 °C for 2 minutes followed by the stopping process (4 °C). PCR products were purified and cloned into the TOPO cloning system (Invitrogen). DNA recombinants were sequenced (MWG). For

further cloning into expression vectors, *CENP-C* full length and *CENP-C* fragments were isolated from TOPO after digestion with *Xho*I and *Not*I restriction enzymes.

To clone the Cenp-C centromere-targeting domain (aa 522 – 533), a 76 bp DNA fragment was generated by synthesis and hybridization. For hybridization, 20 µl of each DNA forward and reverse primer (synthesis by E. Birch-Hirshfeld, FSU Jena; concentration 1 µg/µl) were mixed. The mixture was heated to 95 °C in order to separate the DNA single strands. The two strands were hybridized by slow overnight cooling down of the DNA mixture to room temperature. The hybridized DNA fragments were analysed in agarose gels. DNA recombinants were sequenced (MWG). The DNA hybridization product was cloned into pEGFP-C3 that was digested with *Eco*RI and *Bam*HI restriction enzymes.

2.2.1.2. Generation of *hMis12*

The PCR process was carried out for 11 cycles that comprised of four steps: 1) a cycle of initial denaturation at 94.2 °C for 1.5 minutes, 2) 5 cycles of second denaturation at 94.2 °C for 25 seconds, annealing at 52 °C for 30 seconds and elongation at 72 °C for 2 minutes, 3) 5 cycles of third denaturation at 94.2 °C for 25 seconds, annealing at 67 °C for 30 seconds and elongation at 72 °C for 2 minutes, 4) a stopping process (4 °C). PCR products were purified and cloned into the TOPO cloning system (Invitrogen). DNA recombinants were sequenced (MWG). For further cloning into expression vectors, *hMis12* was isolated from TOPO after digestion with *Xho*I and *Not*I restriction enzymes and *hMis12str* with *Bsa*I restriction enzyme.

2.2.1.3. Generation of *SETDB1* and *PSMB10*

The PCR process was carried out in five serial processes: 1) a cycle of initial denaturation at 94.2 °C for 1.5 minutes, 2) 5 cycles of second denaturation at 94.2 °C for 25 seconds, annealing at 58 °C for 30 seconds and elongation at 72 °C for 2 minutes, 3) 25 cycles of third denaturation at 94.2 °C for 25 seconds, annealing at 68 °C for 30 seconds and elongation at 72 °C for 2 minutes, 4) an elongation at 72 °C for 10 minutes and 5) a stopping process (4 °C). PCR products were purified and cloned into the pDONR cloning system (Invitrogen). DNA recombinants were sequenced (MWG). *SETDB1* and *PSMB10*

were cloned into the destination vector pEGFP gateway using the Gateway Cloning System kit (Invitrogen).

2.2.2. GST-CENP-C and GST-hMis12 protein expression

GST-CENP-C and GST-hMis12 fusion protein constructs were transformed into *E. coli* BL21DE3. The pilot expression culture was carried out in 2 ml culture. A single colony was picked-up by a toothpick and streaked into LB plus amp agar. Then, a copy was tooth picked and used to inoculated 2 ml LB plus 100 µg/ml amp. A colony on LB agar was incubated at 37 ^{o}C overnight. The 2 ml culture series was incubated in the shaker incubator at 37 °C for 8 hours and induced with 0.1 mM isopropyl-1-thio-β-D-galactopyranoside (IPTG). Each culture was incubated overnight at 37 °C, then 200 µl of the culture was sampled and added to 200 µl 4x Laemmli buffer. Each mixture was heated to 95 ^{o}C for 10 minutes. Samples were split and run in two parallel 12,5 % SDS gels with 1 x SDS running buffer at 50 mA. One of the two gels was blotted and labeled with anti-GST antibody while the other gel was stained with PAGEBlue staining solution. The colony with highest expression signal was used for protein expression. The blotting method was described below in immunoblotting method A.

LB medium:	10 g Bacto peptone, 5 g Yeast Extract, 10 g NaCl
4 x Laemmli buffer:	10 % SDS, Glycerol, Tris pH 6.8, Bromopehnol blue
1 x SDS running buffer:	3.04 g Tris, 14.4 g Glycine, 1 g SDS

The best expressing pilot culture colony was inoculated into 5 ml LB plus ampicilin at 37 °C overnight as inoculum. The inoculum was inoculated into 500 ml LB plus ampicilin and incubated at 37 °C until the optical density was A_{550nm} = 0.7 – 0.8. Protein expressions were carried out by 0.1 mM IPTG induction for 5 hours at 28 ^{o}C. To control the protein expression after IPTG induction, as much as 1 ml culture was sampled at 0 (un-induced), 2 and 5 hours incubation. Culture samples were centrifuged at 14000 rpm for 1 minute, the supernatant was discharged and 100 µl was added for pellet cell suspension. Cells were lysed with 100 µl 4 x Laemmli buffer and heated for 10 minutes at 95 °C. The sample was stored at –20 °C for further analysis. Cultures were harvested by centrifugation at 4500 rpm, 4 °C for 15 minutes. Pellet cells were re-suspended with

TBN 150 buffer containing 1 mM phenylmethylsulfonyl fluoride (PMSF) and 10 mM dithiotreitol (DTT). Cell suspensions were stored at –80 °C.

TBN 150 buffer: 25 mM Tris pH 7.5, 150 mM NaCl, 10 mM β-mercaptoethanol

2.2.3. GST-CENP-C and GST-hMis12 protein purification

Concentrated cells were freeze-thawed three times at –80 °C and 37 °C. Cells were lysed with 1 mg/ml concentrated cell (w/v) lysozyme in 50 µl TBN 150 buffer, mixed gently and incubated for 20 minutes at room temperature. To 50 µl/ml concentrated cells (v/v) 10 % Triton X-100 as the second lysis agent and 8 mM EDTA pH 8.0 was added, mixed gently and incubated for 20 minutes in RT. The lysed-cells were centrifuged by ultracentrifugation at 40000 rpm, 4 ^{o}C for 1 hour. During centrifugation, 100 mg gluthatione beads were swollen in 5 ml TBN 150 buffer for 30 minutes and washed three times with the same buffer. Beads were packed into a column. 10 µl cell lysate was sampled for control, 10 µl 4 x Laemmli buffer was added and heated to 95 °C for 15 minutes. The rest was transferred to the column containing glutathione beads for matrix binding. Beads were washed four times with 20 volumes of EQM buffer. GST-CENP-C and GST-hMis12 proteins were recovered from the beads by elution with elution buffer followed by fractionation. The protein gels were assessed by immunoblotting as described below and stained with PAGEBlue staining solution (Fermentas).

EQM buffer: 50 mM Tris pH 8.0, 100 mM NaCl, 10 mM DTT

Elution buffer: 10 mM glutathione in EQM buffer

2.2.4. Strep tag-hMis12 protein expression

The fusion protein construct was transformed into *E. coli* XL1Blue. A single colony was picked by a toothpick and streaked into LB plus amp agar. Then, a colony was toothpicked and used to inoculate 2 ml LB plus amp, which was incubated at 37 ^{o}C overnight. The 2 ml culture was incubated in the shaker incubator at 37 °C for 8 hours and induced with 2 µl 4 mg/ml anhydrotetracycline (ATC). The culture was incubated overnight. 200 µl culture was added to 200 µl 4 x Laemmli buffer and heated to 95 ^{o}C for 10 minutes. The sample was run in two SDS gels: one gel was blotted and labeled with

anti Strep-tag (immunoblotting Method B), the other was stained with PAGEBlue staining solution (Fermentas). The colony with the strongest expression signal was used for protein expression.

A colony was cultured in 2 ml LB plus ampicilin as inoculum. Inoculum was inoculated into 100 ml LB plus ampicilin and incubated at 37 °C for 2,5 hours until an optical density of A_{550nm} = 0.5 - 0.6 was reached. Protein expressions were carried out by 5µl 4 mg/ml ATC induction for 5 hours, 28 ^{o}C. To control the protein expression after ATC induction, as much as 1 ml culture was sampled at 0 (un-induced), 2 and 5 hours incubation. Culture samples were centrifuged at 14.000 rpm for 1 minute, the supernatant was discharged and 100 µl were added for pellet cell suspension. The cells were lysed with 100 µl 4x Laemmli buffer and heated for 10 minutes at 95 °C. Cells were harvested by centrifugation at 4.500 rpm, 4 °C for 15 minutes. Pellet cells were re-suspended with buffer W. The cell suspensions were stored at –80 °C.

Buffer W: 100 mM Tris HCL, 150 mM NaCl, 1 mM EDTA, pH 8

2.2.5. Strep tag-hMis12 protein purification

Concentrated cells were freeze-thawed three times at –80 °C and 37 °C. Cells were lyzed in a Frech Press lysis machine with 1.000 psrg. The lysed cells were centrifuged by ultracentrifugation at 40.000 rpm, 4^{o}C for 1 hour. 10 µl cell lysate was sampled for control, 10 µl 4x Laemmli buffer was added and heated to 95 °C for 15 minutes. The rest was transferred into a column containing Strep-tactin sepharose beads for matrix binding. Beads were washed four times with 5 volumes of Buffer W. hMis12 proteins were recovered from the beads by elution using Buffer E and gel analysed. The protein gels were assessed by immunoblotting following Method B as described below (2.2.6.2.) and stained with PAGEBlue staining solution (Fermentas).

Buffer E: 100 mM Tris HCL, 150 mM NaCl, 1 mM EDTA, pH 8, desthiobiotin

2.2.6. Immunoblotting

2.2.6.1. Immunoblotting Method A

The protein in the SDS gel was transferred onto a nitrocellulose membrane using wet (transfer buffer) filter paper in a protein transfer apparatus at 25 V, 75 mA for 50 minutes. The membrane was stained with Ponceau Red for 10 minutes in order to visualize the protein bands and rinsed by water until the protein bands were clearly distinct from background. The membrane containing the protein was marked and cut. The protein was blocked with 5 % milk in 1 x PBS-T solution for 1 hour on a shaker at room temperature. The primary antibody was diluted with 5 % milk in 1 x PBS-T prior to the blocking process. The cutting-membranes were laid onto clean parafilm. To each strip of membrane, 50 µl primary antibody solution was added, incubated for 1 hour at room temperature in humidity chamber (kept wet). Membranes were rinsed with 1 x PBS-T three times each side and washed three times with 1 x PBS-T for 10 minutes on a shaker. The secondary antibody was diluted with 5 % milk in 1 x PBS-T during the third washing. Membranes were laid onto clean parafilm and 50 µl secondary antibody was added onto each strip and incubated for 45 minutes at room temperature. Membranes were rinsed three times each side and washed three times with 1 x PBS-T for 10 minutes on a shaker. Chemiluminescent substrate (ECL, Amersham) was prepared during the third washing step. The cut membranes were laid onto clean parafilm. To each strip of membrane, 50 µl chemiluminescent substrate was added and incubated for 2 minutes. The stripped membranes were transfered onto plastic wrap in the developing box. In the dark room, the film was placed onto membranes inside plastic wrap and exposed until a clear signal was detected. The film was developed in the developer machine.

1 x Western blot transfer buffer:	200 ml ethanol, 28,8 g glycine, 6 g Tris
1 x PBS-T:	4.3 mM Na_2HPO_4, 2.7 mM KCl, 1.8 mM KH_2PO_4, 137 mM NaCl, 0.1 % Tween-20

2.2.6.2. Immunoblotting Method B

For immunoblotting using Horseradish peroxidase (HRP) as reporter enzyme, the protein blotting process was the same (see 2.2.6.1). The protein on membrane was blocked with 5

% milk in 1 x TBS-Tween for 1 hour at room temperature. The membrane was washed three times 10 minutes with 1 x TBS-Tween on a shaker at room temperature. Anti-Strep tag antibody was diluted in 1 x TBS-Tween during the third washing step. The membrane was laid onto clean parafilm. Antibody was dropped onto the membrane and incubated for 1 hour at room temperature. Membrane was washed three times for 10 minutes with 1 x TBS-Tween and washed once with 1 x APS buffer for 15 minutes. The chemiluminescent substrate was prepared during APS buffer washing. The membrane was placed into chemiluminescent substrate solution until a clear signal was detected.

1 x TBS-Tween: 150 mM NaCl, 100 mM Tris, pH 7.5, 1 % Tween-20

NBT solution: 7.5 % nitrotetrazolium blue in 70 % dimethylformamide

BCIP solution: 5 % 5-bromo-4chloro-3-indolyl-phosphate in dimethylformamide

1 x APS buffer: 12.1 g Tris, 5.8 g NaCl, 1.02 g $MgCl_2$

Chemiluminescent substrate: 10 ml APS buffer, 10 µl NBT solution, 60 µl BCIP solution

2.2.7. Factor Xa digestion

To remove gluthatione, purified-GST-CENP-C and GST-hMis12 proteins were dialyzed in TBN 150 buffer overnight at 4 °C. The protein was re-bound onto agarose beads and washed with Factor Xa cleavage buffer. Factor Xa protease in Factor Xa cleavage buffer (1 u / 50 µl) was added and incubated at room temperature overnight. Factor Xa digestion mix was centrifuged and the supernatant was transferred into a new sterile tube. P-aminobenza-amidine agarose was added to the solution containing Xa cut protein and incubated for 2 hours at 4 °C. The digested protein was eluted from the beads by centrifugation (1000 rpm) at room temperature for 5 minutes. The supernatant containing pure CENP-C and hMis12 proteins were transferred into new sterile tubes for interaction analysis.

Factor Xa cleavage buffer: 500 mM Tris-HCl pH 8.0, 1 M NaCl, 50 mM $CaCl_2$

2.2.8. Centromere chromatin complex isolation

A HEp2 cell line was propagated under standard conditions, grown in 20 ml DMEM plus 10 % FCS in the 75 cm^3 flask culture overnight at 37 °C and 10 % CO_2. Cells were

harvested, pelleted, washed with 1 x PBS, pH 7.4, resuspended with CIB buffer plus 0.1 % digitonin to a final concentration of 10 µM and incubated on ice for 15 minutes. The suspension was mixed gently every minute. Cells were disrupted with a 1 ml pipette tip by pipetting for 25 to 30 times. The suspension was centrifuged at 700 g for 10 minutes at 4 °C. The pellet was washed with 1 x CIB washing buffer, resuspended with 1 ml 1 x CIB washing buffer, 0.3 M NaCl. The suspension was centrifuged at 700 g for 10 minutes at 4 °C. The pellet was resuspended with 1 ml 1 x CIB washing buffer, 0.3 M NaCl. $CaCl_2$ was added to a final concentration of 3 mM. To the suspension, 40 u MNase for 1 ml sample was added and incubated 5 minutes at 37 °C. The reaction was stopped by adding 0.2 M EGTA (final concentration 5 mM) and chilled on ice for 5 minutes. The suspension was centrifuged at 13000 rpm for 10 minutes at 4 °C. The supernatant was transferred into a new sterilized tube. To the sample, NP-40 was added to a final concentration of 0.1 %. Then, 50 µl of Protein A agarose beads were added which were pre-washed with 1 x CIB washing buffer, 0.3 M NaCl, 0.1 % NP-40. The sample was incubated in the rotation incubator overnight at 4 °C. The sample was centrifuged at 700 g for 5 minutes at 4 °C. The Protein A agarose was saved so that it could be used for negative control experiments. The supernatant was transferred to a new sterilized tube containing 50 µl of ACA-bound protein A agarose beads which were pre-washed with 1 x CIB washing buffer, 0.3 M NaCl, 0.1 % NP-40 and mixed gently on the rotation incubator overnight at 4 °C. The sample was centrifuged at 700 g for 5 minutes at 4 °C and the supernatant was saved to be available for negative controls. Beads containing ACA-bound centromere protein were washed three times with 1 ml ice-cold 1 x CIB washing buffer, 0.3 M NaCl, 0.1 % NP-40. Bound protein was eluted with Tris, pH 3, analyzed on an SDS gel and assayed with the Western blot analysis Method A. The protein was neutralized with 0.1 M NaOH to pH 7.

CIB buffer: 3.75 mM Tris HCl pH 7.4, 20 mM KCl, 0.5 mM EDTA, 0.5 mM DTT, 0.05 mM Spermidine, 0.125 mM spermine, 0.1 M PMSF

2 x CIB washing buffer: 40 mM HEPES-Na pH 8.0, 40 mM KCl, 1 mM EDTA, 1 mM DTT, 0.2 mM PMSF, 0.1 µg/ml pepstatin, 2.0 µg/ml leupeptin

2.2.9. GST pull-down assay

2.2.9.1. Bait protein preparation

Purified GST-CENP-C and GST-hMis12 were dialyzed against TBN 150 buffer to remove glutathione at 4 °C overnight. Proteins were re-bound onto glutathione agarose beads for interaction studies.

2.2.9.2. Bait-Prey elution and analysis

The centromere chromatin complex proteins were added to the protein-bound gluthatione agarose beads (2.2.9.1) and incubated overnight at 4 °C on a rotate incubator. The beads containing this protein mix were centrifuged (1000 g) at room temperature for 1 minute. The supernatant was discarded and the beads were washed with 20 volumes of EQM buffer. Interacted protein was eluted from the beads by 10 mM glutathione in EQM buffer and analyzed on SDS gels. The gels were blotted with the immunoblotting Method A and stained with PAGEBlue staining solution (Fermentas).

2.2.10. Yeast two hybrid analysis

pBTM117+*Cenp-C*s and pBTM117+*hMis12* constructs (as bait) were transformed into yeast L40ccua Mat**a**, while pGAD426+*Cenp*-Cs and pGAD426+*hMis12* (as prey) were transformed into yeast L40ccuα Matα. Protein binding partners for these proteins were proteins from 2000 human cDNA gene fragments (MDC collection) that had been subcloned into a DNA-binding (pBTM117) and an activation domain vector (pGAD426). The Yeast Two Hybrid analysis was carried out in collaboration with U. Stelzl and E. Wanker, MDC, Berlin. The DNA constructs were made as part of this thesis while the yeast analysis was performed in Berlin by U. Stelzl.

2.2.10.1. Auto-activation test

In order to analyze auto-activation, constructs of plasmid encoding baits in yeast L40ccua Mat**a** were grown in YPD medium on 96-well microtiter plates and constructs of plasmid encoding prey in yeast L40ccuα Matα were grown in YPD on 384-well microtiter plates**.** Each independent transformant was plated onto minimal medium lacking tryptophan,

leucine, histidine and uracil (SDIV medium) and incubated at 30 °C for 5 to 10 days. Individual bait and bait-prey mixed clones were picked into microtiter plates and grown overnight in liquid minimal medium lacking tryptophan and leucine (SDII medium). The colonies were spotted onto nylon membranes and placed on SDIV agar plates. Bait that activated the reporter gene in the absence of any interacting partners, was removed.

YPD medium: 10 g Yeast extract, 20 g peptone, 20 g glucose

Minimal medium: 6.7 g Bacto-yeast nitrogen base without amino acids, 20 g glucose

2.2.10.2. Interaction mating

Plasmid constructs encoding baits in L40ccua and preys in L40ccuα were grown in liquid YPD medium. In 384-well matting plates, 5 µl preys in L40ccuα were mixed with 40 µl L40ccua. The mixture was transferred onto YPD agar and incubated 36 hours at 30 °C. Clones were transferred into 384-well matting plates containing SDII liquid medium and incubated 72 hrs at 30 °C. Cultures were spotted onto SDIV agar plates with and without nylon membrane for 5 to 6 days at 30 °C. The nylon membrane was subjected to β galactosidase assay that enabled the simultaneous examination of $(lexAop)_4$-*HIS3*, $(lexAop)_8$-*URA3* and $(lexAop)_8$–*lacZ* reporter.

To confirm the interaction, the baits were mated with positive preys in 96-well mating plate and incubated 36 hours at 30 °C. Clones were transferred into 384-well mating plate containing SDII liquid medium for 4 days at 30 °C. Cultures were spotted onto SDIV agar plates with and without nylon membrane and subjected to β galactosidase assay.

2.2.11. Cell culture

A HEp2 cell line was maintained at 37 °C in an incubator with 10 % CO_2 and 95 % humidity. Cells were grown in DMEM plus 10 % FCS on appropriate sized culture plates and flasks. Cell maintenance followed basic protocols (25).

2.2.12. Transfection and cell harvesting for Western blot analysis

The flask culture with 7 ml DMEM plus 10 % FCS was inoculated with 200 µl cell suspension and incubated at 37 °C and 10 % CO_2 overnight. GFP tagged-DNA was

transfected with liposome transfection agent and incubated for 30 minutes at room temperature. The transfection mix was 10 µg GFP tagged-DNA mixed with 30 µl liposome transfection agent and 500 µl DMEM without 10 % FCS. During transfection mix incubation, the cell in the flask culture was washed twice at room temperature with DMEM without 10 % FCS medium. The cells in DMEM without FCS were added with transfection mix and incubated at 37 °C and 10 % CO_2 for 3 hours. Medium was sucked off and changed with 7 ml DMEM plus 10 % FCS. The incubation was continued at 37 °C, 10 % CO_2 overnight or longer.

The cells were trypsinized, pelleted and then washed twice with ice cold-1 x PBS pH 7.4. The pelleted cells were resuspended with 100 µl ice cold 1 x PBS, pH 7.4. 100 µl Laemmli buffer was added. Cells were heated to 95 °C for 15 minutes. 10 µl were loaded onto an SDS gel. Then, the immunoblotting process Method A was used (see above).

1 x PBS, pH 7.4: 4.3 mM Na_2HPO_4, 2.7 mM KCl, 1.8 mM KH_2PO_4, 137 mM NaCl adjust with 2 M NaOH to pH 7.4

2.2.13. Transfection for immunofluorescence

HEp2 cells were grown in 2 ml DMEM plus 10 % FCS medium on cover slips in 6 well plate culture and incubated at 37 °C and 10 % CO_2 overnight. GFP tagged-DNA transfection into these cells was carried out by the liposome complex method. The transfection mix was 1 µg DNA mixed with 500 µl DMEM without 10 % FCS medium and 5 µl liposome transfection agent. The transfection mix was incubated for 15 minutes at room temperature. The transfection mix was added into cultured cells and incubated at 37 °C at 10 % CO_2 overnight or longer.

2.2.14. Immunofluorescence

Transfected cells on the glass cover slips were washed three times with 1 x PBS, pH 7.4. Cells were fixed onto a cover slip with 4 % formaldehyde in 1 x PBS, pH 7.4, and incubated for 10 minutes at room temperature. Fixed cells were washed three times for 5 minutes with 1 x PBS, pH 7.4. Cells were permeabilized with 0.25 % Triton X-100 in 1 x PBS and incubated 3 minutes at room temperature. The permeabilized cells were washed three times for 5 minutes with 1 x PBS, pH 7.4. The nuclei were labeled with 30 µl

primary antibody and incubated in the dark room for 45 minutes at room temperature. Cells were washed three times for 5 minutes with 1 x PBS, pH 7.4. The nuclei were labeled with the secondary antibody and incubated in the dark room for 45 minutes at room temperature. Cells were washed three times for 5 minutes with 1 x PBS, pH 7.4. DNA was stained with ToPro3 for 10 minutes at room temperature. The mounting agent was dropped onto the object glass. Cells on the cover slip surface stuck on the mounting agent and the cover slip was sealed with nail polish. Cells were observed using the confocal Zeiss 510 Meta microscope with the objective lens 60x Fl/ 1.2 under oil immersions and the argon laser excitation at 488 nm. The images were collected and saved with the LSM image browser (Zeiss).

2.2.15. Dynamic analysis by FCS and FRAP

2.2.15.1. FCS

HEp2 cells were grown in 5 ml DMEM plus 10 % FCS on a 42 mm coverslip in 60 mm plate culture overnight at 37 °C and 10 % CO_2. The transfection mix contained 2 µg pEGFP cloned DNA, 5 µl liposome transfection agent and 200 µl DMEM without FCS. The mix was incubated at room temperature for 15 minutes and transfected into cells. The transfected cells were incubated at 37 °C under 10 % CO_2 overnight or longer. The coverslip was put on the live cell imaging chamber with 1 x PBS, pH 7.4, which then was placed on the microscope.

The dynamic behavior of the GFP-tagged proteins was measured by FCS (Fluorescent correlation spectroscopy). The temperature during the measurement was kept constant at 37 °C. Before the measurement, the three dimensions of the pinhole (x, y, z) were adjusted. The objective lens 40 x Fl/ 1.2 under water immersions and the argon laser excitation at 488 nm was used. The images “pre-“ and “post-measurement” were captured and stored with the LSM format. The fluctuations of the fluorescence particles due to the passage through the focal volume were observed and measured in a confocal volume of 0.25 femtoliter. The random fluctuation was analyzed by the autocorrelation function of the fluctuation signal. Measurements were made for 5 minutes until 30 single measurements were collected. One average was calculated for each 10 data sets. The

detection pinhole had a diameter of 70 µm and emission was recorded through a 505 nm LP-filter. The desired recording positioning was chosen in the LSM imaging mode.

The normalize form of the autocorrelation function is describe as

$G(\tau) = \langle \delta F(t) \cdot \delta F(t+\tau) \rangle / \langle F(t) \rangle^2$

were < > denotes the time averages and $\delta F(t) = F(t) - \langle F(t) \rangle$ the fluctuation around the mean intensity. Autocorrelation curves were fitted to diffusion models in three dimensions with a triplet function. The analytical function for the anomalous diffusion model has the following form

$$G(\tau) = 1 + \frac{1}{N} \cdot \left(1 + \frac{F \cdot e^{-\tau/\tau_F}}{1-F}\right) \cdot \left(\frac{1}{\left(1 + \left(\frac{\tau}{\tau_A}\right)^{\alpha}\right) \cdot \left(1 + \left(\frac{\tau}{\tau_A}\right)^{\alpha} \cdot \frac{1}{S^2}\right)^{1/2}}\right)$$

where *N* represents the total number of particles and *F* the triplet function. The anomalous diffusion times and triplet times are τ_A and τ_F, respectively. α is the temporal coefficient, τ is the correlation time and $S = \omega_z/\omega_{xy}$ is the structural parameter that ω_z and ω_{xy} are representing the half height and radius of the confocal volume that is approximated by a cylinder, respectively. The diffusion coefficient can be calculated according to $D = \omega_{xy}^2/\tau_D$, whereas the transport coefficient is defined as $\Gamma = \omega_{xy}^2/\tau_A$ with $D(\tau) = \Gamma \cdot \tau^{\alpha-1}$.

2.2.15.2. FRAP

The sample preparation was as described above in 2.2.15.1. The image of the whole cell was captured before bleaching. The small bleaching region of interest (ROI) or scan region to be bleached was defined as those where some GFP fused protein colocalized with centromeres in the nucleus. A time series with 5 to 10 scans pre-bleach and 50 to 100 scans post-bleach was performed. The iteration of bleaching was 5 with 100 % laser power. The images were collected using the LSM image browser (Zeiss). The FRAP recovery time of the GFP fusion protein was measured within 5 minutes. The cellular background fluorescence intensity was measured in a region outside the cell and subtracted from these data. For each time point of measurement, the data were corrected by dividing the background-substracted fluorescence by that of a control region of unbleached centromeres. Fluorescence-corrected intensity measurements were

normalized using the mean fluorescence intensities in the ROI and the control region before bleaching:

$$RFI = \frac{(ROI_t\text{-}BG) / (CR_t\text{-}BG)}{(ROI_0\text{-}BG) / (CR_0\text{-}BG)}$$

where RFI is the relative fluorescence intensity, ROI_t and ROI_0 are ROI after bleaching and ROI before bleaching, respectively, BG is background, and control region before bleaching and after bleaching are CR_t and CR_0, respectively.

3. RESULTS

CENP-C is a 107 kDa structural protein that is associated with highly insoluble chromosome scaffold proteins (158). In order to elucidate its centromere function, CENP-C was dissected into several subdomains which were studied independently (for summary see 213). Nevertheless, the definite role of CENP-C remained unclear. hMis12 is a 24 kDa centromere protein that forms a complex with several human nuclear proteins (141). Despite the independent loading pathway of hMis12 into the kinetochore complex, the role of hMis12 in the kinetochore assembly is still elusive. Therefore, both proteins were studied by applying additional, in particular *in vivo* techniques.

In order to elucidate CENP-C function, this gene was dissected into three partial gene fragments, *Cenp-C 1-315*, *Cenp-C 315-635* and *Cenp-C 635-943*. The *Cenp-C* full length, *Cenp-C* fragments and *hMis12* full length genes were cloned into several expression vectors for interaction, localization and dynamic behavior studies. The cloning processes were carried out by recombination of the genes placing them downstream of the tag sequences in the expression vectors.

3.1. *In vitro* and heterologous interaction studies

Expression and production of GST fusion proteins were carried out in *E. coli BL21DE3* as expression host because it is easy to use and offers high growth and production rates. However, expression in *E. coli* is limited for very large foreign proteins (11). The descriptions from previous studies revealed that the percentage of successfully expressed human proteins which could be purified in soluble form is just 18 %; and very hydrophobic proteins generally fail to be expressed successfully in *E. coli*. Therefore, proteins larger than 50 kDa are often truncated (22, 45).

The *Cenp-C* full length, *Cenp-C* fragments and *hMis12* full length genes were amplified by PCR. The PCR products were cloned and multiplied in TOPO vectors (see Fig. 8).

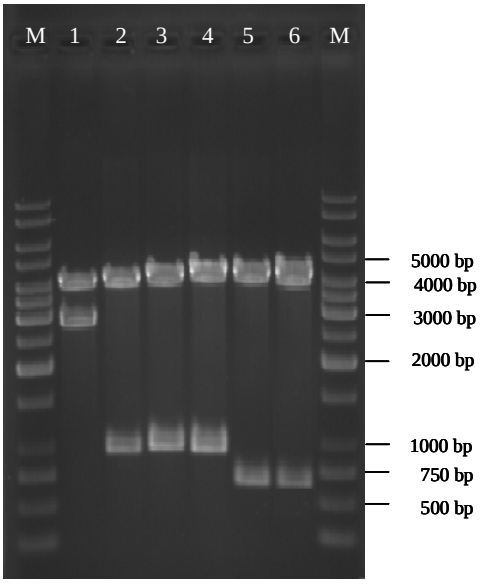

Fig. 8. Constructions of *Cenp-C* and *hMis12* PCR products with TOPO vector.
(1) 2832 bp TOPO-*Cenp-C 1-943*, (2) 945 bp TOPO-*Cenp-C 1-315*, (3) 960 bp TOPO-*Cenp-C 315-635*, (4) 927 bp TOPO-*Cenp-C 635-943*, (5) 618 bp TOPO-*hMis12* and (6) 618 bp TOPO-*hMis12*str. (1-4) *Cenp-C* 1-943 and *Cenp-C* portions were cut with *Xho*I and *Not*I, (5) *hMis12* was cut with *Eco*RI and *Not*I, (6) *hMis12str* was cut with *Bsa*I.

Several methods were applied to identify interactions of target proteins with the cloned recombinant centromere proteins (154). Two common methods used here are:

1. the GST interaction assay, in which an affinity chromatography method provides a way for detecting interacting components and assessing their relative affinities for one another (55, 48) and
2. the Yeast two-hybrid (Y2H) analysis, which provides a way of detecting protein domains that interact with sufficient affinity to generate a transcriptional activator whose activity can be monitored by the expression of reporter constructs *in vivo* (51).

3.1.1. Affinity chromatography interaction studies

Affinity chromatography assays for detecting protein-protein interactions require larger quantities of pure protein. To obtain the required quantities, the proteins were expressed in *E. coli*. Human CENP-C and Mis12 were cloned in fusion with Glutathione S-

transferase (GST) (Fig.9). GST strongly and selectively binds to glutathione agarose. This interaction is used to immobilise the fusion protein to a matrix. The cloning vector contains the *lac*I^q gene expressing a repressor protein that binds to the *tac* promoter operator region, preventing expression of the fusion protein until induction by IPTG and maintaining inserted-gene expression control (136).

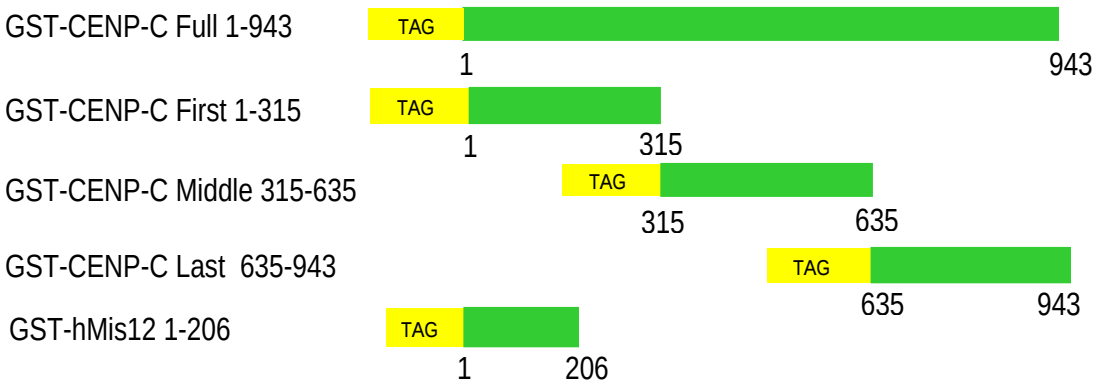

Fig.9. Schematic representation of GST tag CENP-C and hMis12 constructs expressed in *E. coli* BL21DE3. Numbers indicate the amino acid residues of the protein being expressed

In order to provide large amounts of proteins for affinity chromatography, the protein expression was carried out in *E. coli BL21DE3*, a protease-deficient strain. To control the level of protein expression after IPTG induction, the cultures were sampled three times: 0 hour (before IPTG induction), 2 hours and 5 hours. The cells were lysed and the 50 kDa GST-hMis12, 62 kDa GST-CENP-C 1-315, 64 kDa GST-CENP-C 315-635 and 62 kDa GST-CENP-C 635-943 proteins were affinity-purified on glutathione columns (Fig. 10). The coomassie stained gel (Fig. 10B) displayed gel bands of expected size and some additional bands with sizes larger and smaller than the GST-fusion proteins (see below).
Also the Western blot analysis using an anti GST antibody demonstrated that all GST-fusion proteins were expressed (Fig. 10A). Interestingly, GST-CENP-C 315-635 showed three bands with the middle band of expected size for this protein. GST-hMis12 showed two bands, the bigger having the expected size. In order to find out whether the additional bands were GST-fusion proteins, further Western blot analyses using an anti centromere

protein antibody (ACA, antibody mixture against CENP-A, -B and -C) serum was applied. The data confirmed that these additional protein bands were centromere proteins (data not shown).

The larger than expected band size protein might contain additional protein subdomains. The smaller band protein might be a degraded protein or might be a result of premature transcription and/or translation termination.

The 130 kDa GST-CENP-C 1-943 was not expressed well and could not be detected in coomassie gels (data not shown). It was detected, however, in Western blots by the anti GST antibody in the cell lysate as well as the supernatant (Fig. 10C). The low expression level in *E. coli* might be explained by the insolubility of CENP-C (158). Unfortunately, this full length protein failed to bind to glutathione agarose beads (Fig. 10C, AF); hence it could not be purified for further studies.

The pGEX-5X vector expression system contains a Factor Xa protease cleavage site, a site-specific endoprotease that preferentially cleaves the C-terminal peptide bond of the recognition sequence Ile-Glu-Gly-Arg (136). Unfortunately, the effort to cut off the fusion tag and to obtain un-fused CENP-C and hMis12 by digestion with Factor Xa endoproteinase resulted in very low concentrations and poor quality of proteins (data not shown). This preparation was therefore discontinued.

In a second approach to isolate hMis12, this protein was also fused to the Strep-tag using the pASK-IBA-7 vector (also carrying a Xa site). This Strep-tagII consists of eight amino acids, WSHPQFEK, that bind selectively to Strep-tactin, an engineered streptavidin, to allow protein binding to Strep-tactin sepharose beads. This inducible expression vector carries promoter regions from the *tetA* resistance gene that can be blocked by a repressor when its chemical inducer, anhydrotetracycline, is absent. Immunoblotting analysis with Strep-tactin alkaline phosphatase conjugate against Strep-hMis12 pilot cultures revealed a 25 kDa hMis12 band (Fig. 11A). Unfortunately, Strep-hMis12 protein formed inclusion bodies and, when extracted out of *E. coli*, concentrated in the pellet cell fraction, also when the expression process was performed at 23 °C (Fig. 11B). This study thus was discontinued.

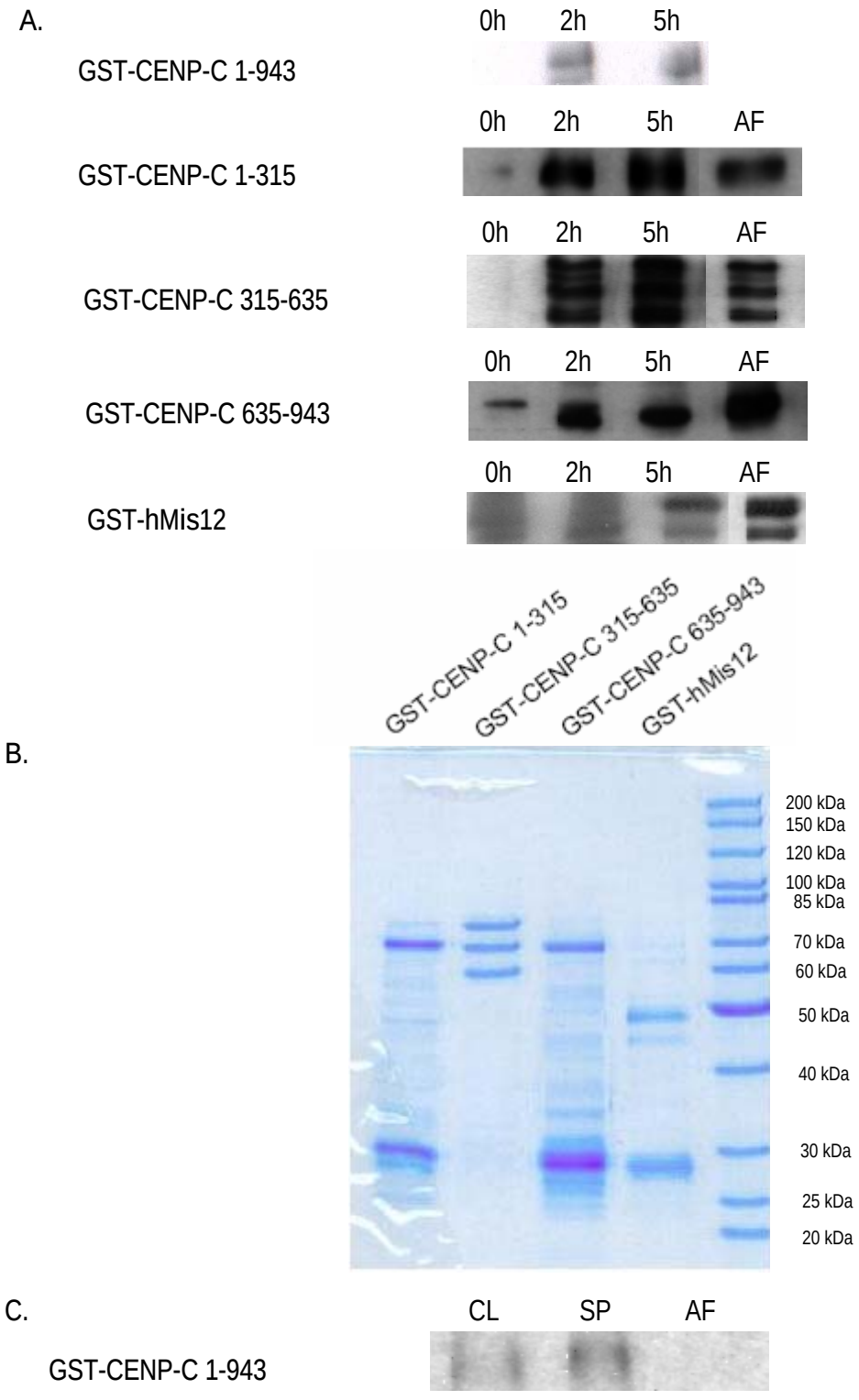

Fig. 10. GST-CENPC and GST-hMis12 fusion proteins. (A). GST fusion protein detected with Western blots using an anti GST antibody. 0 h is before induction, 2 h and 5 h are IPTG induction times, AF is purified fusion protein, (B) Coomassie blue stained lanes of purified soluble GST-CENP-C truncated and GST-hMis12 proteins. (C) Purification step of GST-CENP-C 1-943. CL: cell lysate, SP: ultracentrifuge supernatant, AF: affinity chromatography

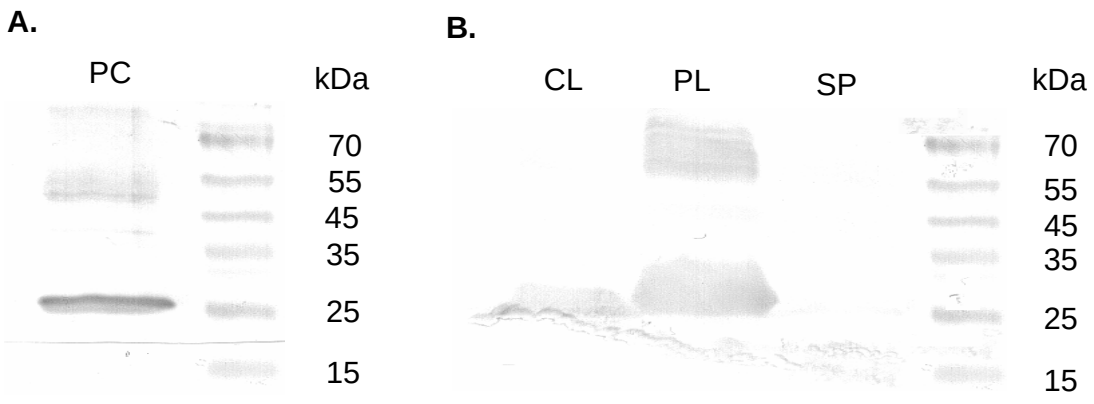

Fig. 11. Strep tag-hMis12 fusion protein on Western blot. (A). 25 kDa Strep-hMis12 in the 2 ml pilot culture. (B). Strep tag-hMis12 protein from scale-up culture 100 ml. PC: Pilot culture, CL: cell lysate, PL: pellet cell, SP: supernatant.

In order to provide potential kinetochore protein binding partners for the purified GST-CENP-C subfragments and GST-hMis12, centromere chromatin complexes were isolated from human HEp2 cells. The isolation method followed a published protocol (234) with slight modifications. After several purification steps as described in Material & Methods, the chromatin complex was collected by centrifugation. Then, chromatin was treated with micrococcal nuclease (MNase) and centromeric chromatin was affinity-purified by chromatography over an agarose matrix with ACA serum antibodies immobilised to the matrix *via* Protein A. The particle contaminants and unbound proteins were washed off and centromere proteins were eluted as described in the Material & Methods (§ 2.2.8). The solubilized chromatin fraction contained, as expected and detected by a Western blot, endogenous full length CENP-A, CENP-B and CENP-C (Fig. 12A) together with additional bands from light and heavy chains of immunoglubulin G (IgG). The assay also detected a 35 kDa unknown human protein (Fig. 12A). The GST-fused proteins immobilized to glutathione agarose beads were incubated with these centromere proteins isolated from HEp2 cells. After the binding process, the beads were washed extensively in order to eliminate false positive binding due to non-specific interactions. Bound protein was eluted and assayed by a Western blot as described in Material & Methods (§ 2.2.9.2).

The Western blot analysis using ACA serum (indicated by white arrows in Fig. 12B) as well as anti GST antibodies (data not shown) showed protein bands corresponding to the

expected protein sizes (truncated GST-CENP-C and GST-hMis12). However, the full length chromatin isolated endogenous proteins CENP-A (17 kDa), CENP-B (80 kDa) and CENP-C (107 kDa) could not be detected (Fig. 12B). *In vivo* studies using the Yeast two-hybrid system had detected the interaction between CENP-B and CENP-C and identified their interacting subdomains (203) so that at least the CENP-C subdomains 315-635 and 635-943 were expected to display CENP-B full length bands. Furthermore, that study could not detect any interaction of CENP-A with CENP-B and CENP-C. Hence, an appearance of CENP-A in these Western blot lanes was not expected. Nevertheless, several strong additional bands of smaller size than full length GST fusion proteins appeared in the lanes indicating that the antibody also recognized shorter GST containing proteins.

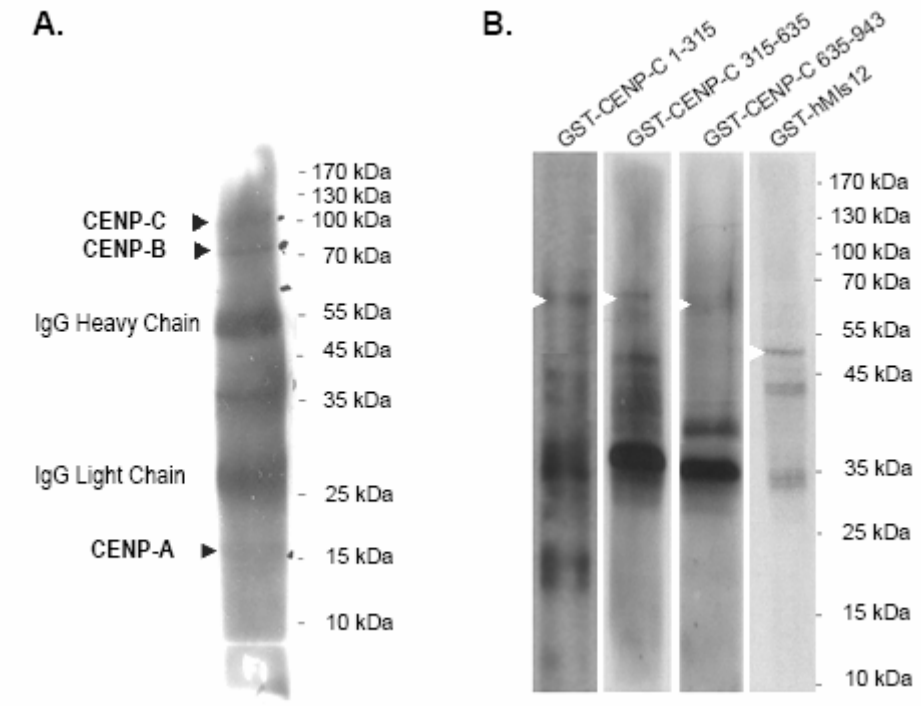

Fig. 12. Affinity chromatography of GST-CENP-C and GST-hMis12 with centromere chromatin protein. A) human endogenous CENP-A, CENP-B and CENP-C proteins isolated from HEp2 cells. B) Western blot analysis of affinity chromatography. White arrows indicated the expected positions of the GST fusion proteins. Western blot A and B were using Anti Centromere Antibody (ACA) serum

Taken together, the *in vitro* affinity chromatography experiments could not detect a direct interaction between the three CENP-C subdomains, hMis12 and either CENP-A, CENP-B or CENP-C.

3.1.2. Yeast two hybrid interaction (Y2H) assay

In order to further analyze the interaction of CENP-C with other identified kinetochore proteins and several candidate proteins from a human cDNA library, the Y2H assay was applied. This method can detect the interactions between two known proteins or search for new interaction partners; it has, however, the limitation of displaying false positive and false negative results. These errors appear with different frequencies at different experimental scales (82, 215, 104). Thus, Y2H suggests that a specific interaction takes place but is not conclusive. Y2H data need to be analyzed further with other independent experimental techniques in order to prove a molecular interaction. For this purpose, this study applies *in vivo* immunofluorescence localization in human cells of those proteins which are detected by Y2H to interact with CENP-C subfragments.

Kinetochore protein genes were cloned into pBTM117, a LexA DNA binding domain vector with TRP1 marker as a bait, and pGAD426, a GAL4 activation domain vector with LEU2 marker as a prey. The interaction mating was carried out in two different haploid yeast strains of opposite mating type, yeast MATa for the DNA-binding construct and yeast MATα for the activation domain construct. The strains were mated to determine if the proteins interact. The auto-activation capacity test is crucial to reduce false positive results. The examination was carried out with the DNA binding construct and activation domain constructs in β-galactosidase assays. Cloning of the constructs was done in the course of this thesis, while all Y2H analyses and identification of potential new binding partners were performed by the Prof. Wanker group at the MDC, Berlin.

The cloning processes were carried out by recombining the *Cenp-C* full length and subdomain sequences into Y2H bait and prey vectors. The cDNAs were cut out of the TOPO vectors (see Fig.8) by *Xho*I and *Not*I enzymes and combined with the *Sal*I and *Not*I fragments of the Y2H vectors pBTM117 and pGAD426, as described in Material & Methods. The recombinants were verified by digestion with several restriction enzymes.

Introduction of *Cenp-C* full length and subdomain constructs as bait into yeast MATa (that carries the three reporter genes *His3*, *URA3* and *lacZ)* and introduction of CENP-A, CENP-H, CENP-I and 2000 human cDNA fragment constructs as preys into yeast MATα revealed that *Cenp-C1-943* and *Cenp-C1-315* could not be examined by Y2H. Transformation of full length *Cenp-C* into yeast MATa resulted in cell death. CENP-C 1-943 might have failed to localize to the yeast nucleus; it is associated with chromosome scaffold proteins which have a high hydrophobicity (158). Proteins comprising a hydrophobic transmembrane domain often fail to reach the nucleus (181). Alternatively, CENP-C might be lethal for yeast. CENP-C 1-315 protein showed auto-activation (see Fig. 13A): this CENP-C subdomain was able to activate the transcription of the gene reporter by itself (indicating the presence of a transcription-activating function in CENP-C 1-315) and thus excluding this CENP-C subdomain from further Y2H analyses. Experiments were continued using CENP-C 315-635 and CENP-C 635-943 as bait. The prey proteins were found to be free from auto-activation activity.

The array mating was performed to connect bait and prey proteins. The preys were transformed into yeast L40ccα. Baits in L40cca were used individually for mating against the prey protein matrix. Diploid yeast containing bait and prey clones that formed on YPD plates were selected on YPD agar lacking tryptophan and leucine (SDII) and transferred onto YPD agar lacking tryptophan, leucine, histidine and uracil (SDIV medium) for two-hybrid selection. The combination between CENP-C 315-635 and CENP-C 635-943 with CENP-A, CENP-H, CENP-I and 2000 human proteins that activated the gene reporter in two independent co-transformation assays, were selected for further studies. The mating studies on SDIV plates between CENP-C 315-635 and CENP-C 635-943 with human CENP-A, CENP-H and CENP-I revealed negative results: no interactions were found by Y2H between those human centromere proteins. The screening of interaction partners for CENP-C 351-635 and CENP-C 635-943 using 2000 human proteins derived from a cDNA library, however, resulted in several interacting proteins (Table 1, Fig. 13B) that might be involved in kinetochore assembly: four interacted with CENP-C 315-635 and ten interacted with CENP-C 635-943 (of which two interacted with both subfragments).

All positive interacting proteins from the auxotrophic assay with the LEU2 reporter (see Fig. 13B) were screened in the colorimetric β-galactosidase assay with the *lacZ* reporter (see Fig. 13C). In this assay, the bait-prey combinations that positively interact will be able to activate the gene reporter (*lacZ*), hence a positive bait-prey interaction results in a blue colony. Those proteins, for which the β-galactosidase assay confirmed an interaction with the two CENP-C subdomains, were KIAA1377, UBR1, CRMP1, SETDB1 and QARS (see Table 1, Human protein interactor, purple).

Most of the proteins found by Y2H to interact with CENP-C were non-nuclear proteins (as judged from NCBI protein description); these are: PCP4, MRPL20, UBR1, MGC2574, Contig1893, EPB49, CRMP1, SPG7 and QARS (see Table 1, Description, white). Surprisingly, also the non-nuclear proteins UBR1, CRMP1 and QARS that do not display cell cycle activity (see Table 1), showed blue colonies in the β-galactosidase assay. Nevertheless, due to the molecular property as non-nuclear proteins, the UBR1, CRMP1 and QARS were not expected to contribute to the inner kinetochore function and hence excluded from the further studies. The nuclear proteins found here by the auxothrophic assay to interact with the CENP-C subdomains were KIAA1377, SETDB1 and PSMB10 (Table 1, Description, pink).

Two of the three nuclear proteins, suggested by Y2H to interact with CENP-C subfragments, were speculated to have interesting potential functions during mitosis and were thus analyzed further: PSMB10 and SETDB1.

The protein interaction network (178) illustrated that mitosis proteins and chromatin/chromosome structure proteins may interact physically with proteins that carry out methylation, acetylation, phosphorilation and sumolation modifications. One of such proteins, SETDB1, a nuclear protein methylating histone H3 at lysine 9 (177) was detected as a CENP-C subfragment interaction partner in both Y2H assays and was thus analyzed further.

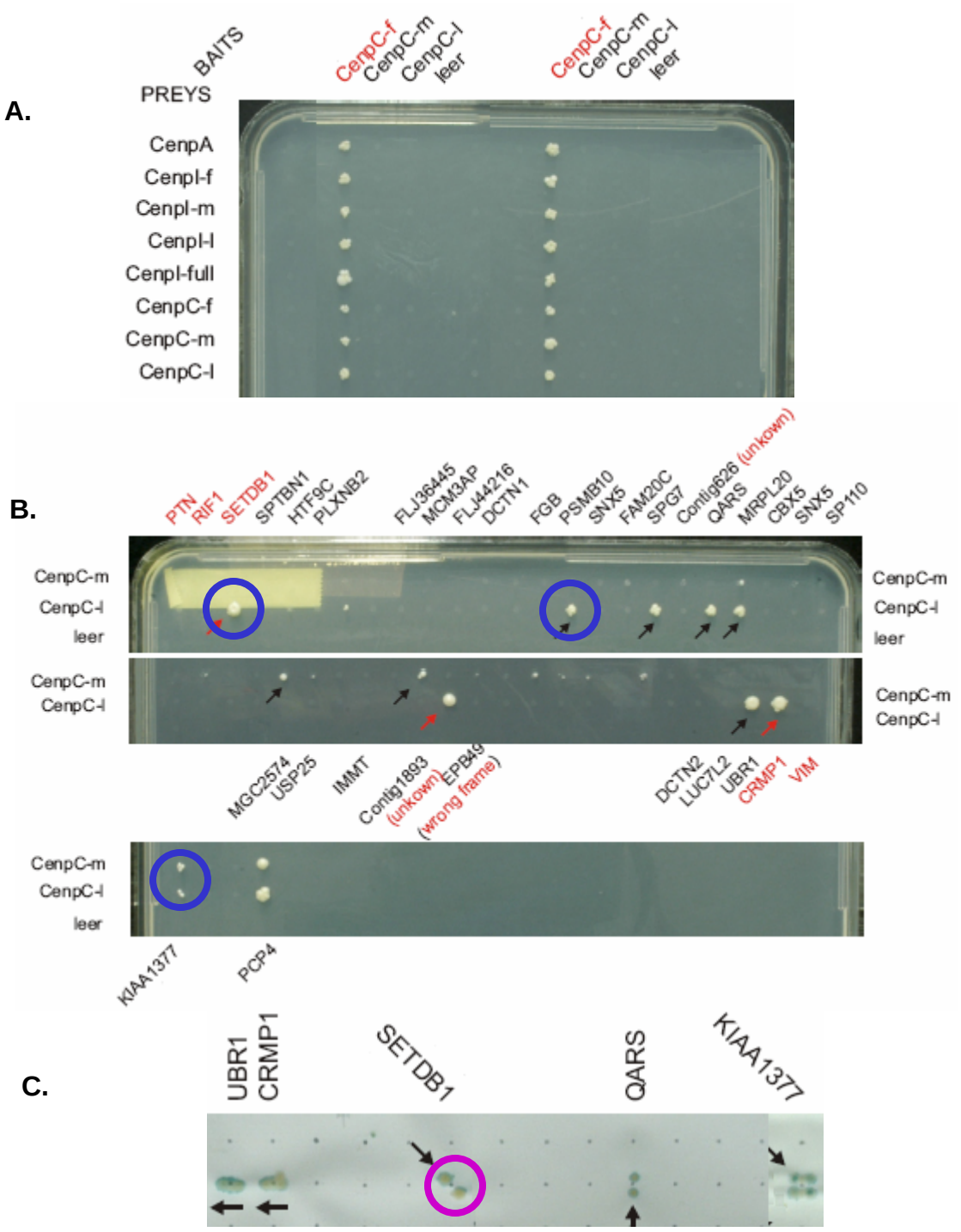

Fig. 13. Identification of CENP-C interaction partner. A) Yeast clones spotted onto SDII (-Trp-Leu) agar plates for autoactivation test. CENP-C 1-315 (red letter CenpC-f) showed autoactivation, B) Identification of matting bait by assaying diploid yeast onto SDIV (-Trp-Leu-His-Ura) medium agar plates. Blue ring; the candidate mediator protein. Wrong frame: protein in the wrong frame, resulting in a short peptide. (unknown): unknown function protein. C) Confirmation of second interaction mating in β-galactosidase assay. Purple ring: the positive interactor

CENP-C	Human protein interactor	Description
CENP-C 315-635	MGC2574	human renal ephitelial protein, unknown function (191)
	Contig1893	gi | 23304102 | emb | AL773541.6 | , human DNA sequence from clone XXbac-11J22 on chromosome 6, unknown function (228)
	KIAA1377	human chromosomal protein involved in cell signaling, cell structure, nucleic acid management and protein management (137)
	PCP4	Purkinje cell protein in human brain, unknown function (78)
CENP-C 635-943	PCP4	Purkinje cell protein in human brain, unknown function (78)
	KIAA1377	human chromosomal protein involved in cell signaling, cell structure, nucleic acid management and protein management (137)
	EPB49	erythrocyte membrane protein, unknown function (56)
	UBR1	human ubiquitin protein ligase (97)
	CRMP1	human collapsing response mediator protein, a novel invasion-suppression protein expressed in nervous system (69)
	SETDB1	human SET domain bifurcated protein, a novel KAP-1-associated histone H3 in chromatin that contributes to HP1-mediated silencing of euchromatic genes by KRAB zinc-finger proteins (177)
	PSMB10	a mammalian proteasome β subunit, unknown function (39)
	SPG7	human mitochondrial protein that has role in membrane trafficking, intracellular motility, organelle biogenesis, protein folding and proteolysis (161)
	QARS	human glutamyl-tRNA synthetase, a protein that is catalizing the aminoacylation of tRNA and predicted as the first protein to appear in evolution (99)
	MRPL20	human mitochondrial ribosomal protein, unknown function (202)

Table 1. List of human proteins interacting with CENP-C

According to Yeast two-hybrid analysis screening result.

Human protein interactor, purple: proteins with β-galactosidase assay confirmed interaction

Description, pink: nuclear proteins

Sources of description: NCBI data base

PSMB10 found in the chromosome 16q22.1 (103), is a 26S proteasome family member (39). The 26S proteasome is involved in protein degradation and rapid breakdown of ubiquitinated proteins and thus has a role in sister chromatid separation during the cell cycle process (92, 68, 219). During mitosis, securin which inactives separase, is polyubiquitinated by the Anaphase Promoting Complex/Cyclosome (APC/C) and thus becames the target of the proteasome 26S (68). These potential roles of PSMB10 in mitosis led us select this protein for further studies although its interaction with a CENP-C subfragment was not confirmed in the second assay (see Fig. 13 C). As mentioned above, Y2H results are not strictly conclusive.

The KIAA1377 protein showed blue colonies (Fig. 13 C) in the confirmation assay indicating a positive interaction with CENP-C. KIAA1377 is found at chromosome 11q22.1, is involved in cell signaling and protein regulation. Furthermore, this protein is categorized as being able to interact selectively with any protein complex that may include non-protein molecules (137). A previous Y2H assay revealed many proteins interacting with KIAA1377 with no physiological relevance (false positive results) (188, U. Stelzel, personal communication). Moreover, according to the interaction network (178), most likely cell signaling proteins are not directly involved in mitosis activity. These observations suggest that KIAA1377 might not interact functionally with CENP-C. Therefore, KIAA1377 was excluded from further studies.

Comprehensively, the nuclear proteins PSMB10 and SETDB1 were analyzed further.

3.2. Analysis of Y2H identified interacting proteins

The Y2H identified CENP-C subdomain interacting proteins SETDB1and PSMB10 were tagged with the green fluorescent protein (“GFP”) and expressed in HEp2 cells: The *SETDB1* (RZPD-IOH14445) and *PSMB10* (RZPDo834D015D) cDNAs were amplified by PCR and subcloned into the pDONR vector of the Gateway system. From the resulting entry vectors, the genes were cloned into the destination vector pEGFP of the Gateway system and its presence verified by restriction with several enzymes. The recombinant DNAs were transfected into HEp2 cells. The expressed proteins were analyzed with Western blot using an anti GFP antibody. The Western blot analysis detected 73 kDa GFP-SETDB1 and 56 kDa GFP-PSMB10 (Fig. 14).

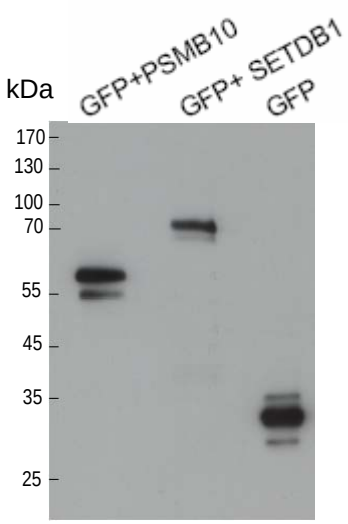

Fig. 14. The nuclear protein SETDB1 and PSMB10. The proteins were tagged with GFP. In the Western blot, anti GFP antibodies were applied.

The human nuclear protein SETDB1 is a 46 kDa KAP1-associated SET domain protein with histone H3-K9 specific methylase activity (177). The sequence analysis of 1194 bp SETDB1 by the PSORTII web server revealed that this gene encodes a nuclear localization signal ("NLS") type path 7 at amino acids 226 to 232 with the amino sequence PGKKYKVK.

The HEp2 cells were transfected with GFP-SETDB1. The size of the GFP-SETDB1 protein is relatively small; hence the transfection efficiency was high: approximately 50 % of cells on the slides were transfected. During incubation, the microscope observations demonstrated that cell growth was normal (Fig. 15, DIC images). Cells with very strong GFP-SETDB1 expression stained the nucleus and the cytoplasm; however, at moderate or low expression, SETDB1 stained only the nucleus (see Fig. 15). In addition to the homogenous nucleus staining, the microscope images showed small (and in some cells additionally also larger) SETDB1 accumulations in the majority of the cell nuclei (white arrows in Fig. 15A and 15B). The cellular localization was analyzed with immunofluorescence. The nuclei were labeled with two different antibodies:

1. centromeres were marked with ACA serum, and
2. heterochromatin was labelled with a polyclonal anti heterochromatin antibody (EKE serum, recognizing HP1α, HP1β and HP1γ)

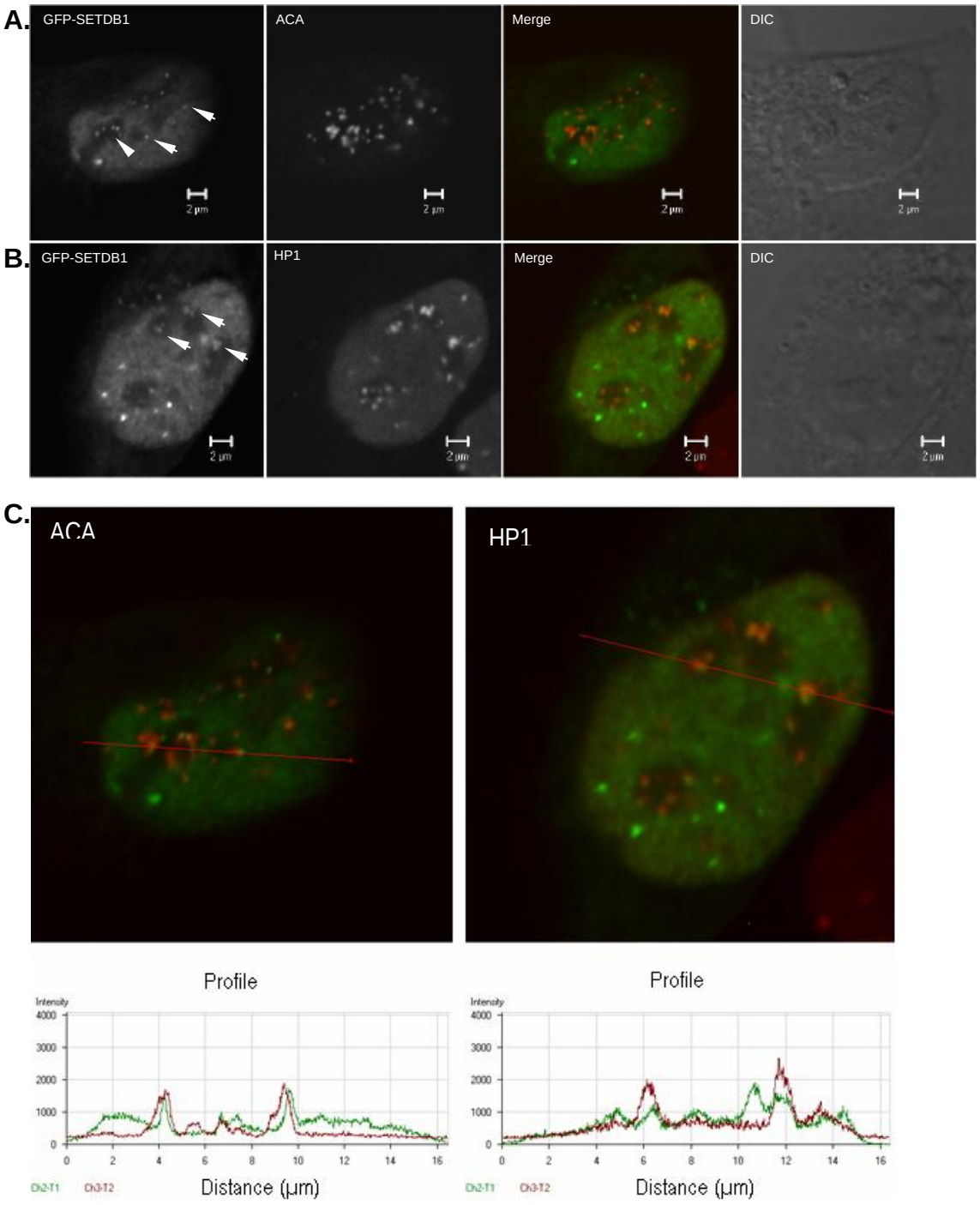

Fig 15. SETDB1 localized partially to centromeres and centromeric heterochromatin. Immunofluorescence analyses showed colocalization using A) ACA antibodies and B) polyclonal anti heterochromatin antibody (EKE serum). C) colocalization profile of SETDB1 with centromere and heterochromatin. Red curve: endogenous protein with antibody, green curve: GFP-fusion protein. White arrow: SETDB1 pool protein colocalization sites

Immunolabelings was carried out with a specific single antibody for each slide. These antibodies in the nuclei were then visualized by binding of Rhodamin labeled anti human antibodies. Partial colocalization was observed in all transfected cells on the cover slip, with varying intensity signals depending on the size of SETDB1 protein spots.

SETDB1 showed partial colocalization with centromeres and heterochromatin component HP1 (merge Fig. 15A, 15B; and indicated in the intensity plots of the colocalization profiles, Fig. 15C). The immunofluorescence analysis with ACA antibodies (a mixture against CENP-A, -B and –C) in fixed cells demonstrated that SETDB1 partially localized at centromeres (see Fig. 15A).

Histone H3 methylated at K9 by SETDB1 is a binding site for HP1 (49, 189). Therefore, SETDB1 colocalization with HP1 was investigated. The colocalization signal from cells that were labeled with EKE serum recognizing the three HP1 isoforms HP1α, HP1β and HP1γ indicated partial colocalization (see Fig. 15B). These data illustrated that SETDB1 resides partially at heterochromatin.

The data present a hint that SETDB1 might carry out its function also at human centromeres. However, these preliminary results need to be analyzed further in a thorough study beyond the time limits of this thesis.

Human PSMB10 is a 26S proteasome β subunit member with unknown function (39). The sequence analysis of 822 bp PSMB10 by the PSORTII web server revealed that this gene does not encode a NLS. Nevertheless, the 29 kDa PSMB10 can enter the nucleus may be due to the small size of this protein: a protein with less than 45 kDa can freely diffuse between the nuclear and cytoplasmic compartment, while proteins with a size larger than 45 kDa need a NLS for import into the nucleus (85, 138, 117).

The GFP-PSMB10 was transfected into HEp2 cells. The transfection efficiency was similar to that of SETDB1: about 50 % of the cell populations on the slides were transfected. During incubation, the microscope observations demonstrated that cell growth was normal (Fig. 16, DIC images). GFP-PSMB10 over expression stained the nucleus and cytoplasm; however, at moderate or low expression during interphase, PSMB10 only stained the nucleus (Fig. 16A). In addition to the homogenous nucleus staining, the microscope images demonstrated PSMB10 accumulations (green dot) in the majority of the cell nuclei (Fig. 16A). The proteasome proteins reside in all cell

compartments; the relative amount in each compartment depends on cell type, cell density and growth condition (219, 166). The cellular localization of PSMB10 was analyzed with immunofluorescence (see Fig. 16). The endogenous centromeres were labeled with ACA serum.

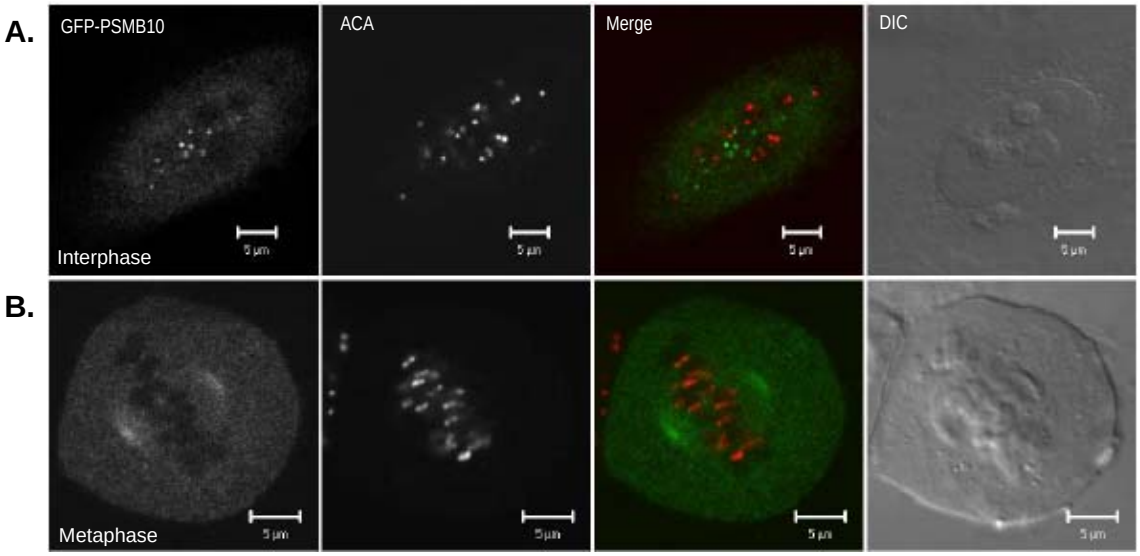

Fig 16. Localization analysis of PSMB10 to centromeres. Indirect immunofluorescences using ACA serum did not show colocalization. A) PSMB10 form pool proteins in interphase and B) PSMB10 stain the whole cell and accumulate at spindle poles during metaphase.

The immunofluorescence analysis with ACA antibodies (see Fig. 16) indicated that PSMB10 did not localize to the centromeres. Interestingly, PSMB10 accumulated in the spindle pole during metaphase (Fig. 16B).

The PSMB10 protein aggregation in the nucleus was analyzed further. The colocalization analysis between PSMB10 with nuclear body components was carried out using two different antibodies:

(1) human anti PML antibody and

(2) human anti Cajal body antibody.

Surprisingly, the immunofluorescence experiments demonstrated that PSMB10 colocalized with PML bodies and Cajal bodies (see Fig. 17 A, B and C), suggesting that PSMB10 might be involved in the particular functions of these nuclear bodies.

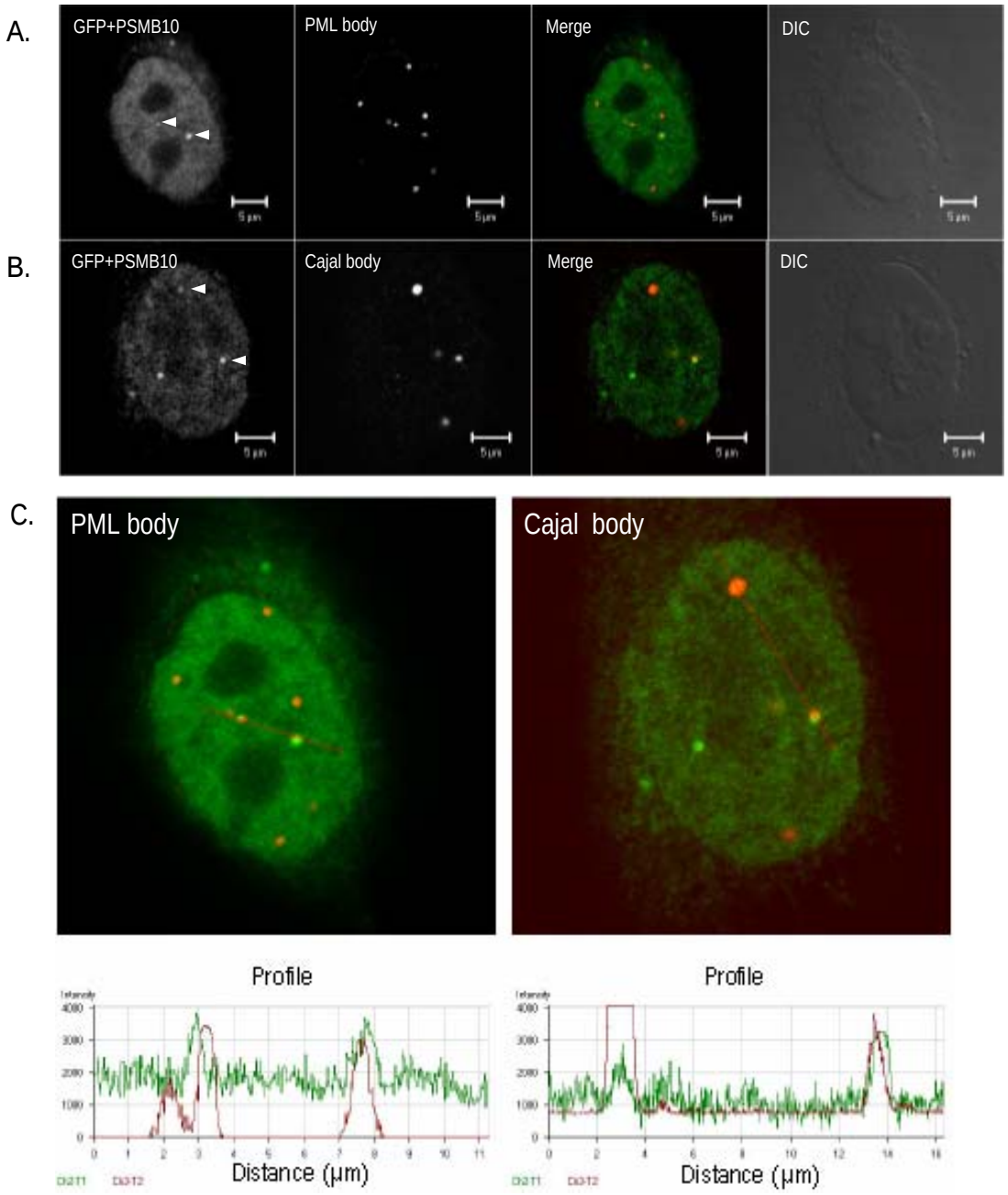

Fig 17. PSMB10 colocalized and associated partially with PML and Cajal bodies. A) Endogenous PML bodies were labeled with human anti-PML antibody and B) endogenous Cajal bodies were labeled with human anti-Cajal antibody. White arrow indicated PSMB10 pool protein colocalization sites. C) Colocalization profile. Green curve: GFP-fusion protein, red curve: endogenous protein labeled with antibody

The nuclear function of PML nuclear bodies is not known (19, 182). However, its colocalization with Cajal bodies (Fig 17 B and C) implicates a potential role in the assembly or modification of the transcription machinery. Such a role would be in agreement with previous reports (238, 123). Since PSMB10 did not localize to the centromeres (Fig. 16), PSMB10 might have no function at the kinetochore.

3.3. Localization analysis of CENP-C and hMis12

CENP-C is localized at the centromere (168). Previous analyses showed that CENP-C has a DNA binding domain and is able to bind α-satellite DNA, however sequence unspecifically (229, 213). Interestingly, despite CENP-C being essential for the kinetochore (90), the activity of CENP-C in the kinetochore assembly is not well defined due to the various domains encoded in this large protein (213). A molecular dissection study of CENP-C into subfragments suggested that CENP-C protein truncation affects its association with the kinetochore and indicates which subfragment is responsible for centromere binding (185). In general, the properties of the CENP-C subdomains are not fully determined. Thus, the localization of the three subdomains of CENP-C to the centromere was analyzed by immunofluorescence. The other kinetochore protein studied here, hMis12, resides at the centromere and is loaded by a separate pathway (65). However, whether hMis12 was bound to the kinetochore during all phases of the cell cycle and whether the CENP-C truncation constructs were still able to localize at the centromeres had not been fully worked out yet.

To address these questions, the CENP-C constructs and hMis12 were genetically tagged with green fluorescent protein (GFP) and transfected into HEp2 cells. Protein expressions were analyzed by Western blots. As illustrated in Figure 18, the Western blot analysis with anti GFP antibody detected weakly 130 kDa GFP-CENP-C 1-943, and strongly 63 kDa GFP-CENP-C 1-315, 64 kDa GFP-CENP-C 315-635, 62 kDa GFP-CENP-C 635-943 as well as 51 kDa GFP-hMis12.

Localization analysis of the GFP-fused proteins was carried out by indirect immunofluorescence. The endogenous centromeres of HEp2 cells were primary labeled with ACA serum antibodies followed by Rhodamin labeled anti human antibodies as

secondary antibodies emitting its own fluorescence to allow for the localization of the protein antibodies in the cells.

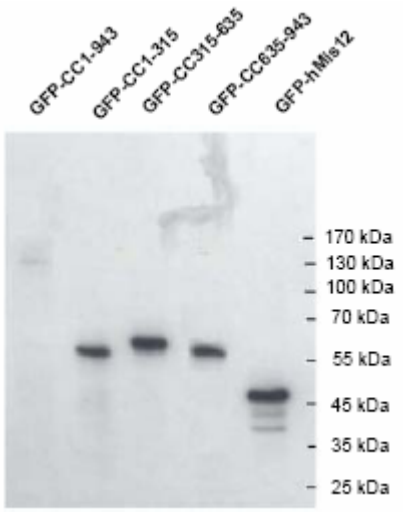

Fig. 18. Western blot detection of GFP-CENP-C and its subdomains as well as GFP-hMis12 fusion protein in HEp2 cells, detected with an anti GFP antibodv.

3.3.1. Localization analysis of CENP-C and CENP-C truncated proteins

The immunofluorescence analysis demonstrated that in HEp2 cells, as expected, GFP-CENP-C 1-943 completely colocalized with centromeres which were labeled with ACA serum (Fig. 19). There was no protein fraction detected staining the nucleoplasm. CENP-C completely colocalized with the centromere also during mitosis (see Fig. 19B). These data illustrate that CENP-C resides at the centromere throughout the cell cycle.

Next, the three CENP-C subfragments were analyzed with immunofluorescence. The *in vitro* and *in vivo* analysis of the N-terminus of CENP-C indicated that this region oligomerizes (194). However, the molecular properties of this region were not fully determined. The GFP-CENP-C 1-315 construct was transfected into HEp2 cells. The microscope observations during incubation demonstrated that the cells showed normal growth. The localization profiles of the recombinant proteins were analysed by immunolabeling the nuclei with ACA serum in order to mark the centromeres. In cells with low expression, GFP-CENP-C 1-315 localized at centromeres with a very low level of background in the nucleoplasm (Fig. 20B). During mitosis, the protein completely localized in the nucleoplasm (Fig. 20C) and the tagged protein did not localize at centromeres (approximately 90 % of transfected cells did not shown colocalization).

Cells with strong expression demonstrated that the protein stains the nucleus and the cytoplasm (see Fig. 20A). The colocalization profiles (Fig. 20D) demonstrated no colocalization in the overexpressed cells (see Fig. 20A) and in mitosis (see Fig. 20C). Thus, the CENP-C N-terminus shows weak centromere targeting function during interphase and no centromere localization during mitosis, supporting the previous instability data (102).

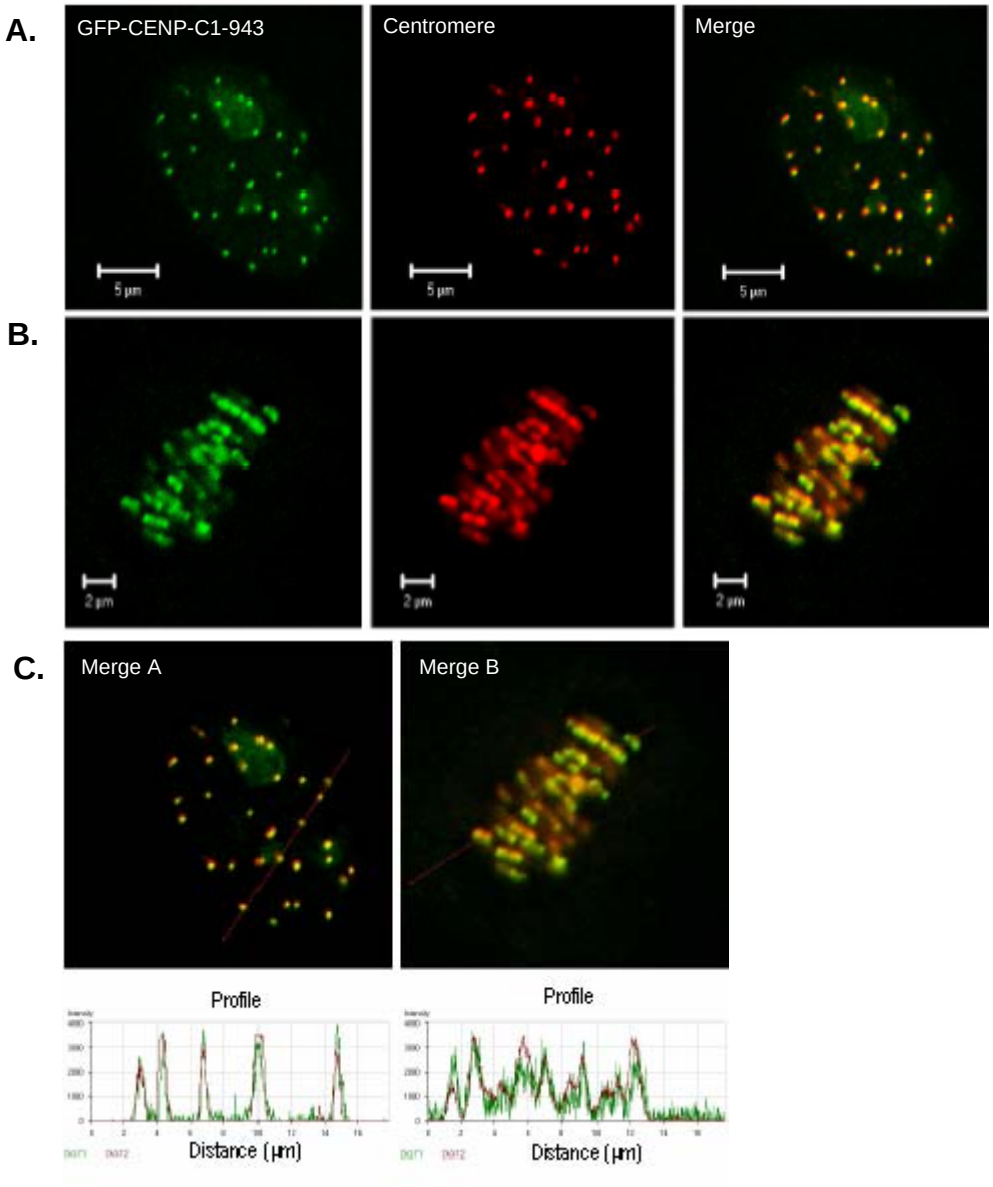

Fig. 19. Localization analysis of GFP-CENP-C 1-943. GFP-CENP-C is totally bound to centromeres during the whole cell cycle (merge image). A) Interphase, B). Mitotic cell, C) colocalization profiles

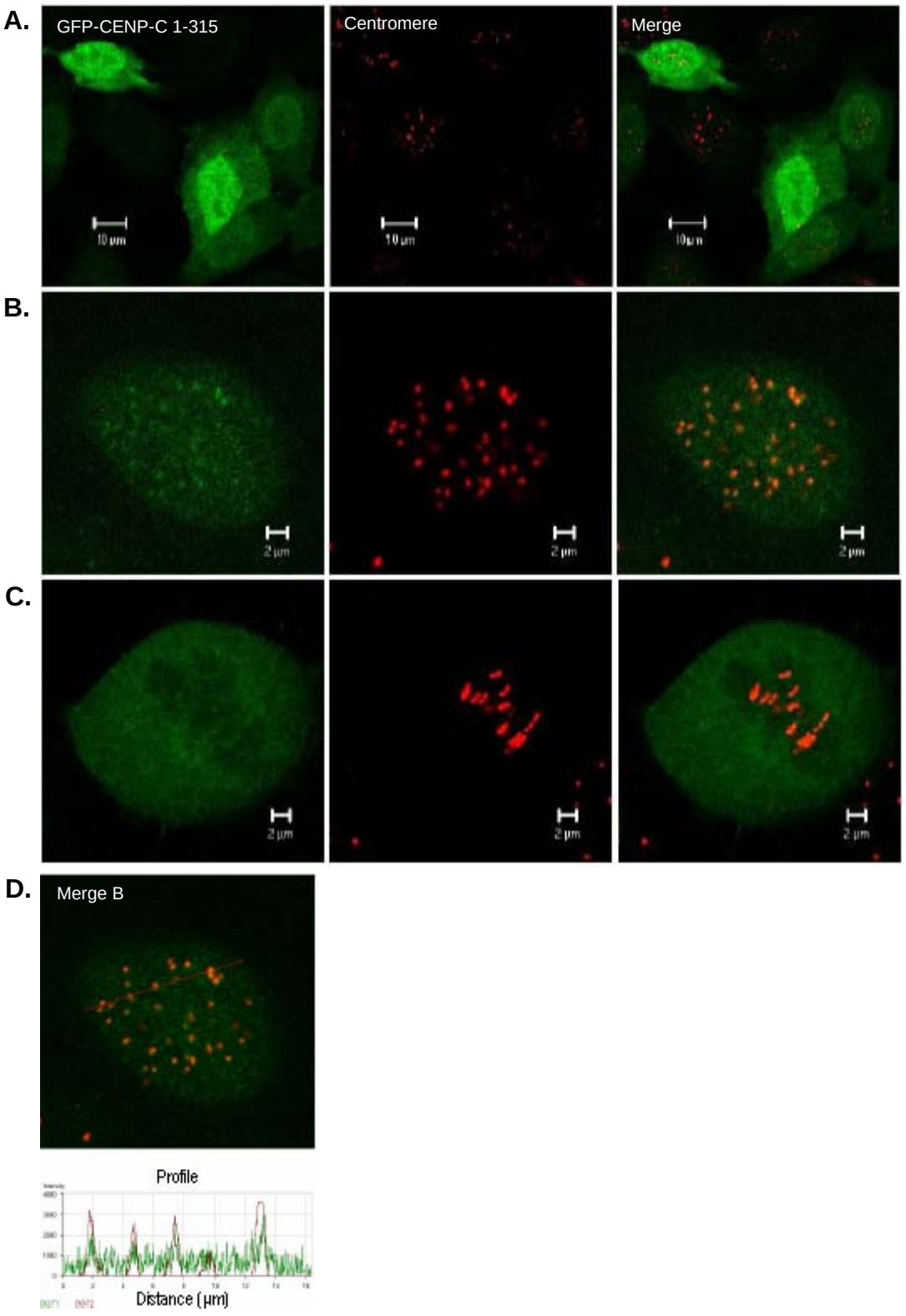

Fig. 20. Localization analysis of GFP-CENP-C 1-315. A.) the accumulation of CENP-C 1-315 in the nucleus and the cytoplasm. B) At low expression levels, CENP-C 1-315 localised well to centromeres. C) No colocalization in the mitotic cell. D). Colocalization profiles at low expression protein (see Fig. 20B)

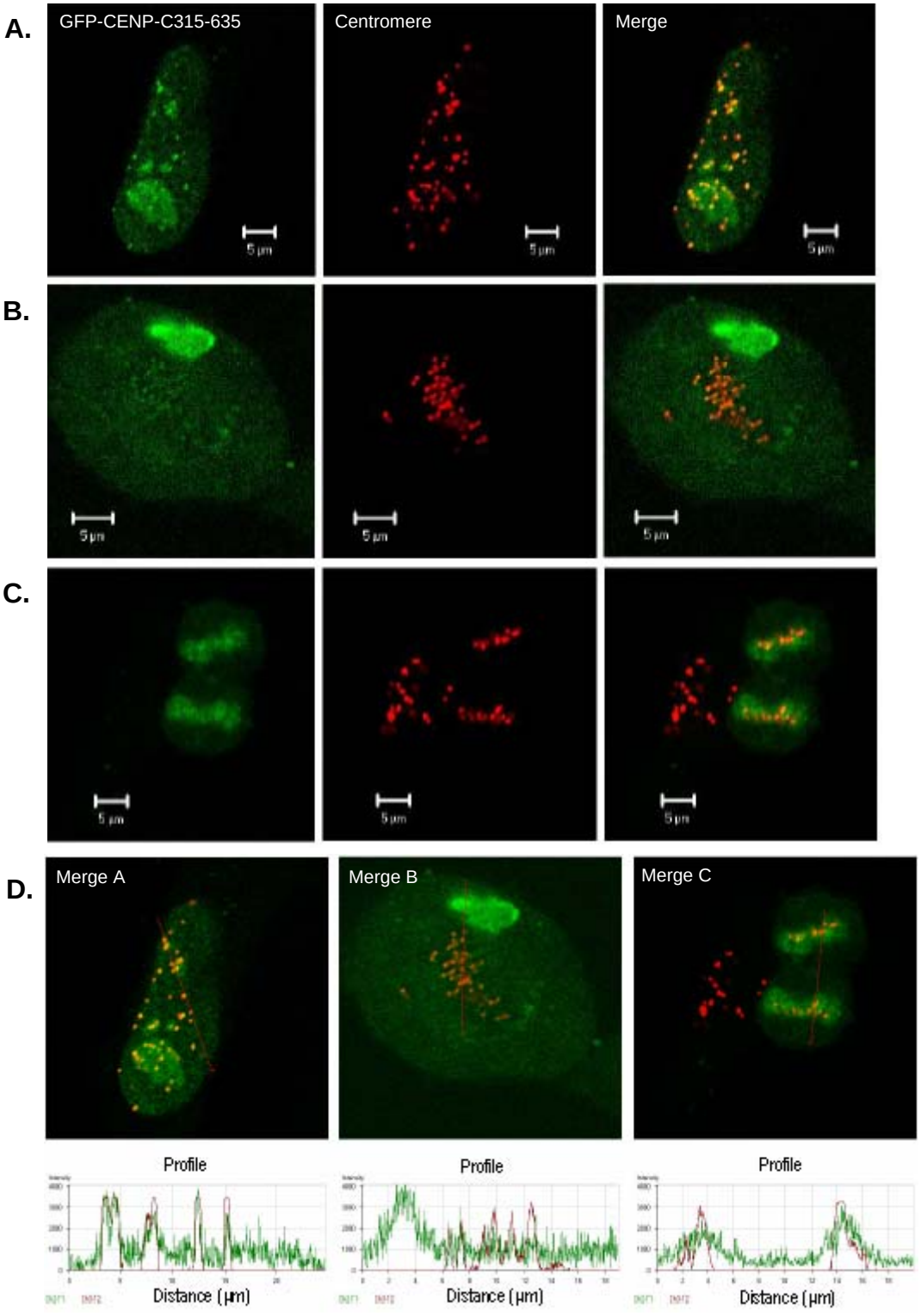

Fig. 21. Localization analysis of GFP-CENP-C 315-635. GFP-fused protein localized to centromeres and the nucleolus. Protein diffused staining nucleoplasm and cytoplasm. A) Interphase B) Prometaphase C) Telophase D) Colocalization profiles

The CENP-C central region contains a NLS, a DNA binding and a centromere localization domain (229, 185). In this study, GFP-CENP-C 315-635 was transfected into HEp2 cells. To analyze the localization profile, the endogenous centromere in nuclei was labeled with ACA serum antibodies. The experiment was carried out as described above. The GFP-CENP-C 315-635 colocalized with centromeres throughout the cell cycle. Moreover, a protein fraction stained the nucleoplasm showing that this truncated protein does not bind completely to the centromere. During prometaphase, this CENP-C fragment stained the nucleolus (where this CENP-C subdomain might bind to RNA), then the nucleolus disappeared and the tagged protein bound to the centromere (Fig. 21B, 21C).

A mutational analysis suggested that the CENP-C centromere localization domain resides in the central portion of CENP-C between amino acids 522 to 533 (185). To address this point, a 76 bp long DNA encoding the speculative centromere localization domain 522 to 533 aa with an upstream NLS was generated by DNA hybridization (Fig. 22B). The 12 aa truncated protein would be able to enter the nucleus by passive diffusion, however, in order to force all expressed protein to enter the nucleus, this short peptide was complemented with a NLS sequence. Additionally, a GFP tag was fused to this short peptide for easy localization in the cells. The GFP-NLS-CENP-C 522-533 targeting domain was expressed in HEp2 cells. Western blot analysis demonstrated the correct full length of the protein (Fig. 22C). Indirect immunofluorescence analysis showed that this protein was able to reside in the nucleus; it also stained the nucleolus (Fig 22D), however, it did not localize to the centromeres. Either, this short peptide alone does not have centromere localization properties by itself or, alternatively, the added amino acids (GFP, NLS) sufficiently mask or even destroy this function.

The C-terminus of CENP-C was shown to be able to bind α-satellite DNA and to localize to centromeres (213). In this study, GFP-CENP-C 635-943 was transfected into HEp2 cells and the localization profile analysis was carried out by immunofluorescence. In order to mark endogenous centromeres, the nuclei were labeled with ACA serum antibodies. The experiment was carried out as described above. GFP-CENP-C 635-943 localized to the centromeres, and in addition, diffused throughout the nucleoplasm. During mitosis however, this protein constantly bound to the centromeres (see Fig. 23B).

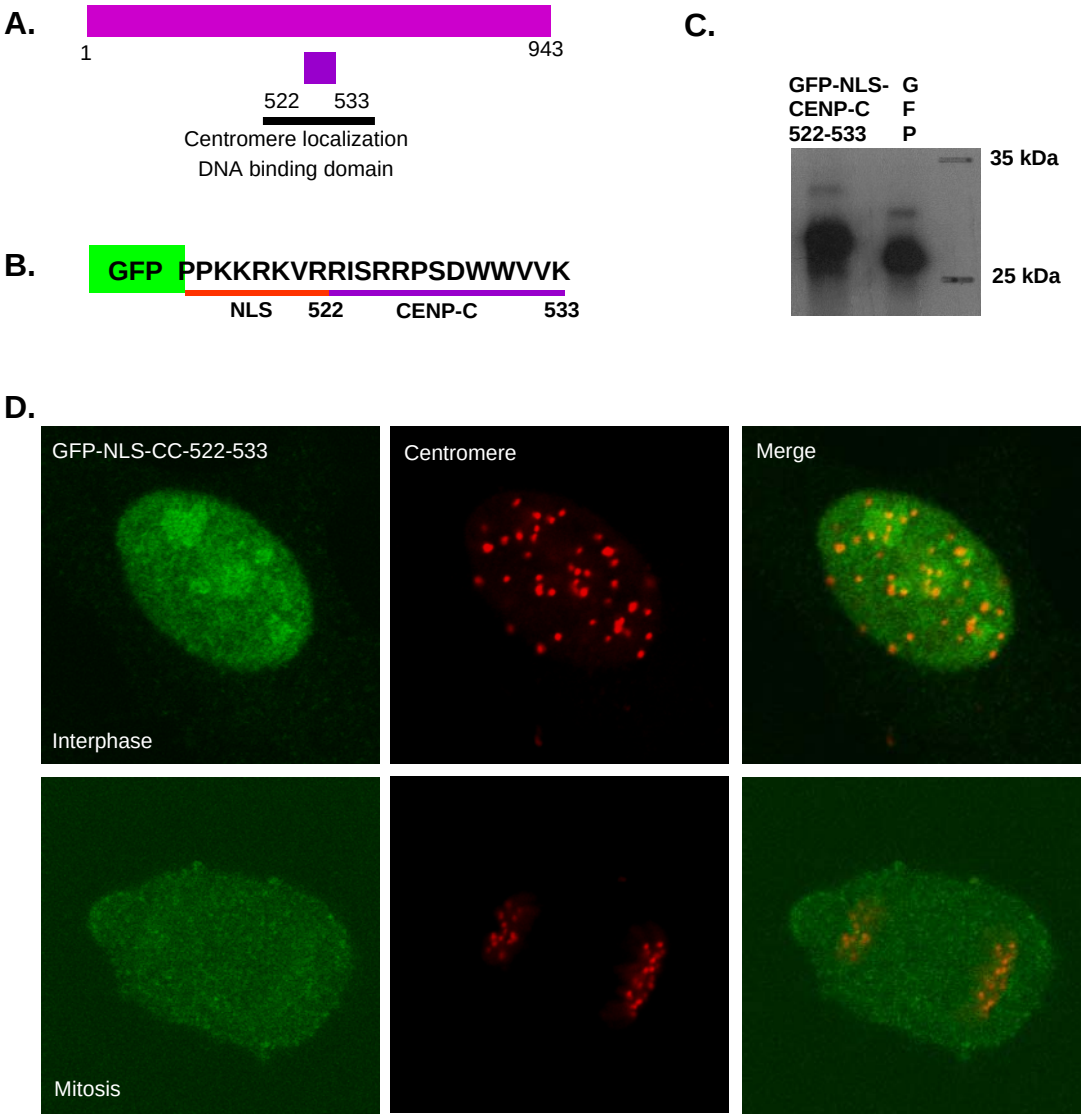

Fig. 22. GFP-NLS-CENP-C centromere localization domain analysis in HEp2 cells
A) sequence localisation, B) sequence construct GFP-NLS-CENP-C 522-533 C) Western blot analysis. D) Immunofluorescence analysis of NLS-GFP-CENP-C 522-533, protein did not colocalize with centromeres but binds the nucleolus. Upper panel: interphase, lower panel: mitosis.

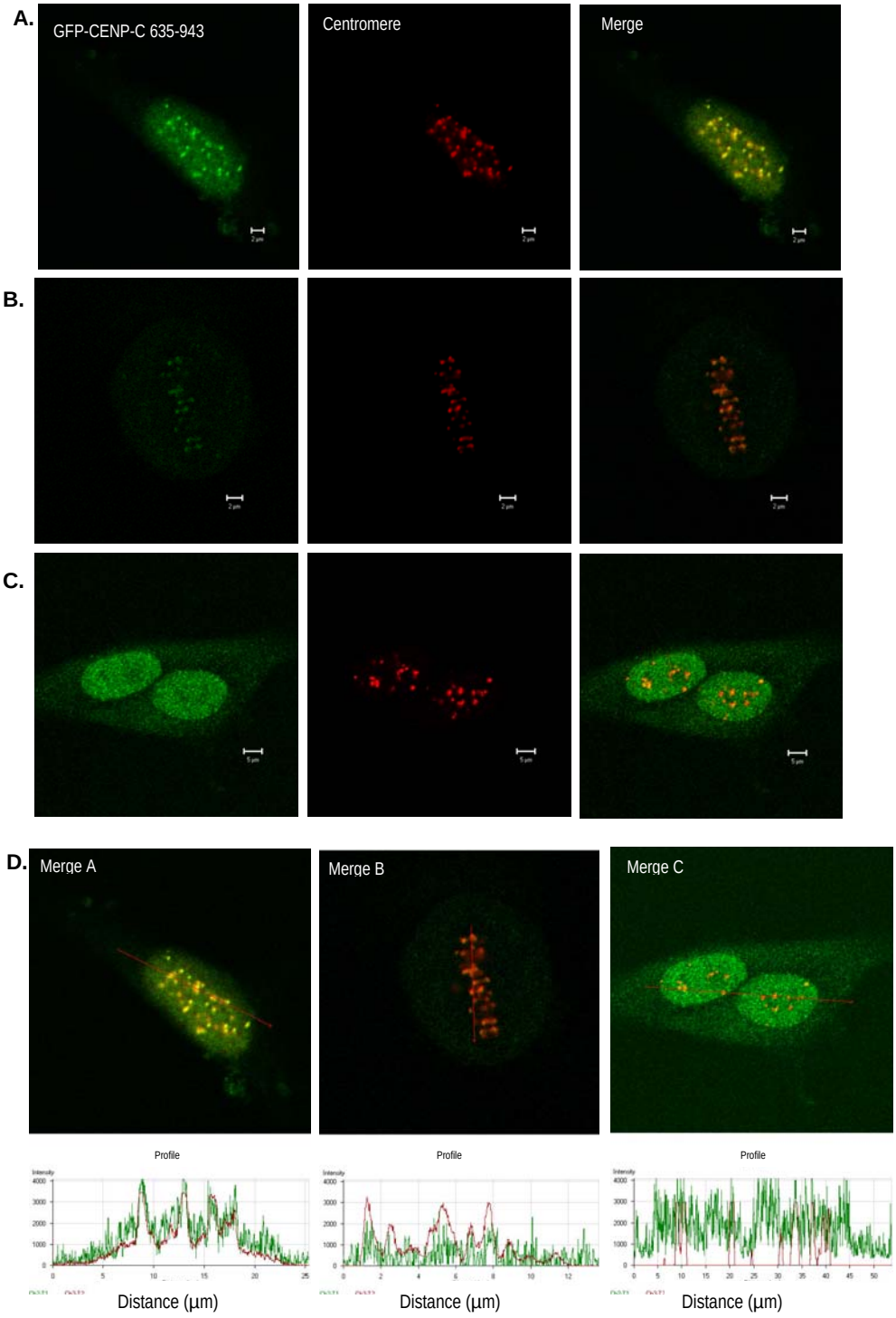

Fig. 23. Localization analysis of GFP-CENP-C 635-943. A) during interphase and B) during mitosis, CENP-C 635-943 colocalized with centromeres and diffusely stained the nucleoplasm. C) In some cells, the protein was unable to bind to centromeres, no colocalization was detected and the protein diffused to the cytoplasm as illustrated in colocalization profile D) Colocalization profiles

As illustrated in Fig. 23C and 23D, in less than 10 % transfected cells, GFP-CENP-C 635-943 showed diffuse localization and protein staining all over the nucleus and the cytoplasm with no pool protein colocalizing with centromeres. The sequence of CENP-C 635-943 was analyzed using the PSORTII web server in order to verify the presence of nuclear import and export signal sequences. The sequence analysis identified two NLS motifs, at 734 to 740 aa (PNVRRTK) and at 779 to 797 aa (KRKAKENIGKVNKKSNKK). In addition, a nuclear export signal (NES) was identified at 809 to 821 aa (LMVNLGIPLGDPL).

Taken together, the molecular dissection of CENP-C affected the binding properties. The CENP-C subfragments were still able to localize to the centromeres, however, at different levels.

3.3.2. Localization analysis of hMis12

hMis12 forms a complex with three further kinetochore proteins: hNnf1, hNsl1,hDsn1, and this complex is important for outer kinetochore protein binding (93). Sequence analysis identified a potential NES at 85 to 99 aa (LFLQLILRIPSNILL), however, no NLS sequence. In this study, GFP-hMis12 was transfected into HEp2 cells. To analyze the localization profile, the endogenous centromeres were labeled with ACA serum antibodies, and the experiment was carried out as described above. hMis12 colocalized with the centromeres throughout the cell cycle (Fig. 24). The fluorescence analysis displayed its presence in the nucleoplasm during interphase (Fig. 24A). Surprisingly, the protein was bound completely to the centromeres during mitosis (Fig. 24B). No protein fraction stained the cytoplasm. Taken together, the data suggest that hMis12 binds to the centromeres less tightly during interphase but very strongly during mitosis.

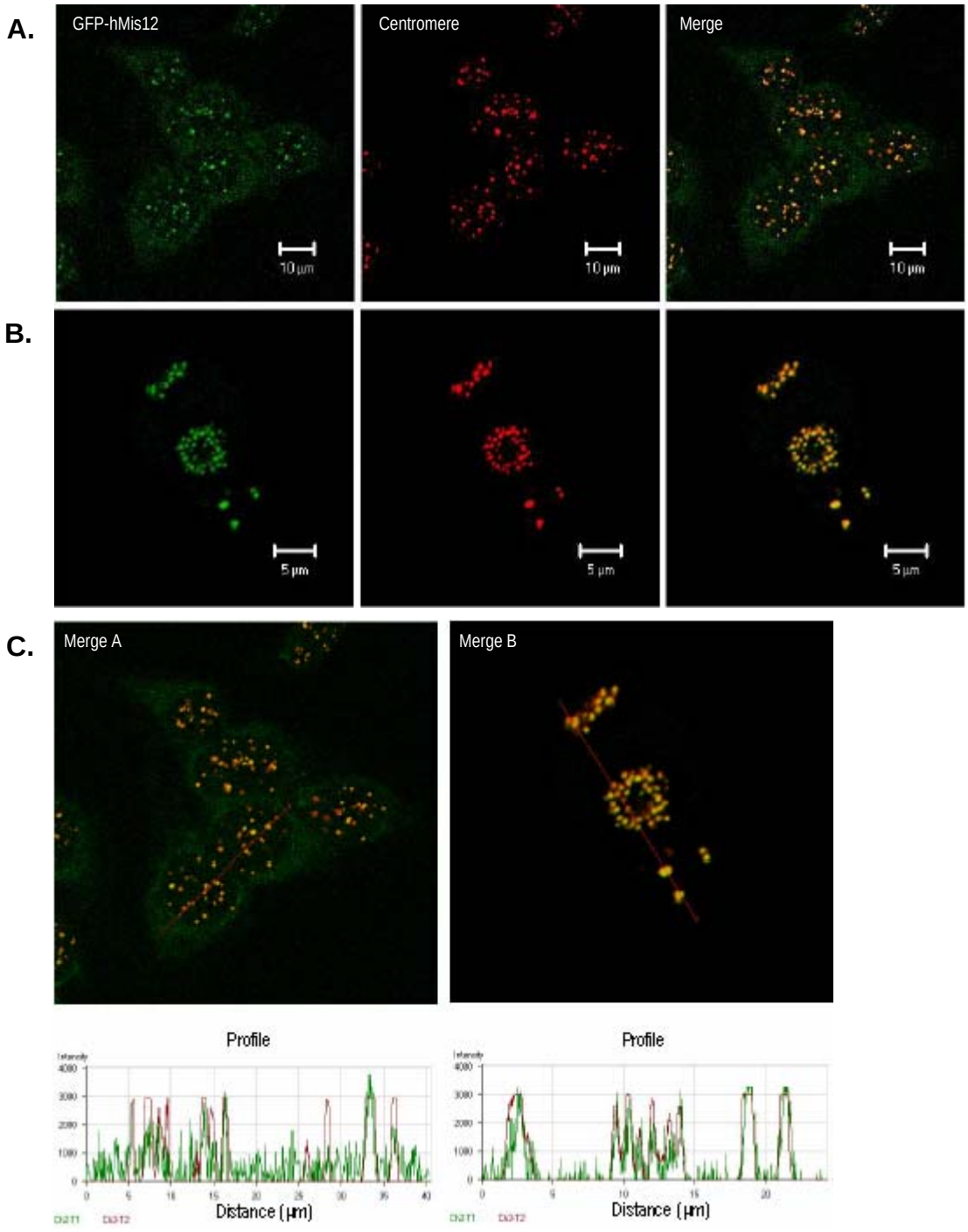

Fig. 24. Localization analysis of hMis12. A.) GFP-hMis12 localised to centromeres and appeared slightly diffuse in the nucleoplasm during interphase, B) It binds completely to the centromeres during mitosis. C) Colocalization profiles.

3.4. Dynamic behavior measurements of CENP-C and hMis12

3.4.1. FCS

In order to understand the dynamical behavior of these proteins in living cells, Fluorescence Correlation Spectroscopy (FCS) (211) and Fluorescence Recovery After Photobleaching (FRAP) (76, 153) were employed. Cell culture and transfection experiments for these analyses were performed in the course of this thesis. The microscopy measurements and data evaluations presented here were performed together with Stefanie Weidtkamp-Peters in our group.

FCS is able to analyze diffusion of molecules in the living cell (43). The dynamic behavior of GFP-fused proteins in HEp2 cells were measured in the nucleus during interphase. The fluorescence fluctuation rate represents the photon count rate averages that are detected by the avalanche photodiode detectors over short time intervals as a function of time. Periods of increase of photon frequency correspond to periods when fluorescent molecules are diffusing through the focal volume. The autocorrelation function (vertical marks: ACF (normalized *autocorrelation function*)) is computed from photon intervals and plotted versus time (τ/ms). It characterizes the time dependent decay of the fluorescence fluctuations to their equilibrium value. From this function, the diffusion coefficient (D) and the average number of fluorophore particles in the observation volume (N) can be determined. The amplitude of the autocorrelation function at $\tau=0$ is inversely proportional to the average number of molecules in the observation volume. The decay of the autocorrelation with time reflects fluorescence fluctuations with different time constants. Autocorrelation curves were documented and fitted to an anomalous diffusion model as described (174). Anomalous diffusion describes a hindered diffusion, in which the mean square displacement of a diffusing particle is proportional to some power of time less than one (172). It is reported that the anomalous diffusion model is suitable to measure the dynamics of proteins in the nucleus (221). Most biologically active proteins measured to date have diffusion coefficients in the order of 0.1 to 50.0 $\mu m^2/s$ (167). The diffusion coefficients of GFP in the nucleus and cytoplasm were determined to 9.5 $\mu m^2/s$ and 30 $\mu m^2/s$, respectively (174).

The intracellular FCS measurement was carried out in a cell at equidistant positions along a straight line. For control, FCS scanned a non-transfected cell to account for the cellular autofluorescence background.

The HEp2 cells transfected with GFP-CENP-C 1-943 were measured under the same conditions as the control. To collect enough data, 30 individual transfected cells were chosen. The diffusion coefficient (D) was computed from these 30 measurements per nucleus, 10 data sets each were averaged. This averaged correlation curve was exported to the Microcal origin software for further analysis. The images of the cells before and after FCS measurement were recorded. No correlation and no free protein pool could be detected in the nucleoplasm by FCS so that no diffusion parameters could be determined. The fact that CENP-C 1-943 could not be detected in the nucleoplasm suggests that CENP-C is physically anchored to the kinetochore completely.

The FCS measurements of CENP-C subfragments were carried out by the same procedure as for CENP-C 1-943. The diffusion times of all CENP-C subfragments are truly indicating that these proteins are highly mobile (see Table 2). The mobility of CENP-C 315-635 in the nucleus was slower than CENP-C 1-315 and CENP-C 635-943. This indicates that the degree of obstruction of CENP-C 315-635 was larger than CENP-C 1-315 and CENP-C 635-943. The availability of the CENP-C subfragments in the nucleoplasm confirms the immunofluorescence results (see above): the CENP-C subfragments were observed to bind to the centromeres less stably than full length CENP-C.

The diffusion coefficients of proteins in solution depend on their molecular weight, on their binding to other molecules, and on the collision or obstruction by other structures (106). The molecular weight of GFP is 27 kDa while the molecular weight of GFP-CENP-C 1-315 and GFP-CENP-C 635-943 are 63 kDa and 62 kDa, respectively. The FCS measurement detected that the mobility of GFP-CENP-C 1-315 and GFP-CENP-C 635-943 were very similar with diffusion coefficients of 1.51 $\pm$ 0.10 and 1.54 $\pm$ 0.21 $\mu m^2/s$, respectively (see Table 2). Thus, although being only about twice as large, these proteins are approximately six times less mobile compared to control GFP in the nucleus. The particle numbers detected in the measurement volume were 9.51 $\pm$ 0.05 and 27.39 $\pm$ 0.27 for CENP-C 1-315 and CENP-C 635-943, respectively (see Table 2).

The anomaly factor (α) represents the interaction of the GFP-tagged proteins with the cellular environment within the nucleus and the cytoplasm (221, for a review see 70). The values of α of anomalous diffusion in the living cells are in the range between 0 to 1 (179). By fitting 10 different datasets from different nuclear cells for each GFP-fusion protein, the anomaly diffusions were detected with almost similar α values. The anomaly factor of GFP-CENP-C 1-315, GFP-CENP-C 315-635, GFP-CENP-C 635-943 and GFP-hMis12 are 0.61 $\pm$ 0.006, 0.61 $\pm$ 0.016, 0.62 $\pm$ 0.013 and 0.55 $\pm$ 0.014, respectively (see Table 2). These values were corroborated with diffusion coefficient (D) values that indicated the CENP-C fragments and hMis12 were mobile but still constrained in the nucleus compared to control GFP with an anomaly factor 0.75.

The FCS results are summarized in Table 2. The autocorrelation curves of CENP-C subfragments and hMis12 are presented in Figure 25.

GFP-Centromere	FCS Measurement Result		
	Diffusion coefficient (D) (µm2s-1)	Anomaly factor (α)	Particle number (N)
GFP-CENP-C 1-943	Not mobile	-	-
GFP-CENP-C 1-315	1.51 $\pm$ 010	0.61 $\pm$ 0.006	9.51 $\pm$ 0.05
GFP-CENP-C 315-635	1.08 $\pm$ 0.05	0.61 $\pm$ 0.016	8.39 $\pm$ 0.08
GFP-CENP-C 635-943	1.54 $\pm$ 0.21	0.62 $\pm$ 0.013	27.39 $\pm$ 0.27
GFP-hMis12	0.70 $\pm$ 0.45	0.55 $\pm$ 0.014	9.03 $\pm$ 0.12

Tabel 2. FCS measurement results of CENP-C and hMis12. The measurements were conducted in interphase cells.

Fig. 25. FCS autocorrelation. Black: autocorrelation data; red: fitted curve according to the anomalous diffusion model; green insert: residual plot of the fit. A) GFP-CENP-C 1-315, B) GFP-CENP-C 315-635, C) GFP-CENP-C 635-943, D) GFP-hMis12. R: dynamic radius, N: particle number detected, TAUan: (τ_{an}) anomaly diffusion time, alpha (α): anomaly factor, FT: function of triplet, tautrip (τ_{trip}): triplet state time, DC: transport coefficient, SP: structural parameter.

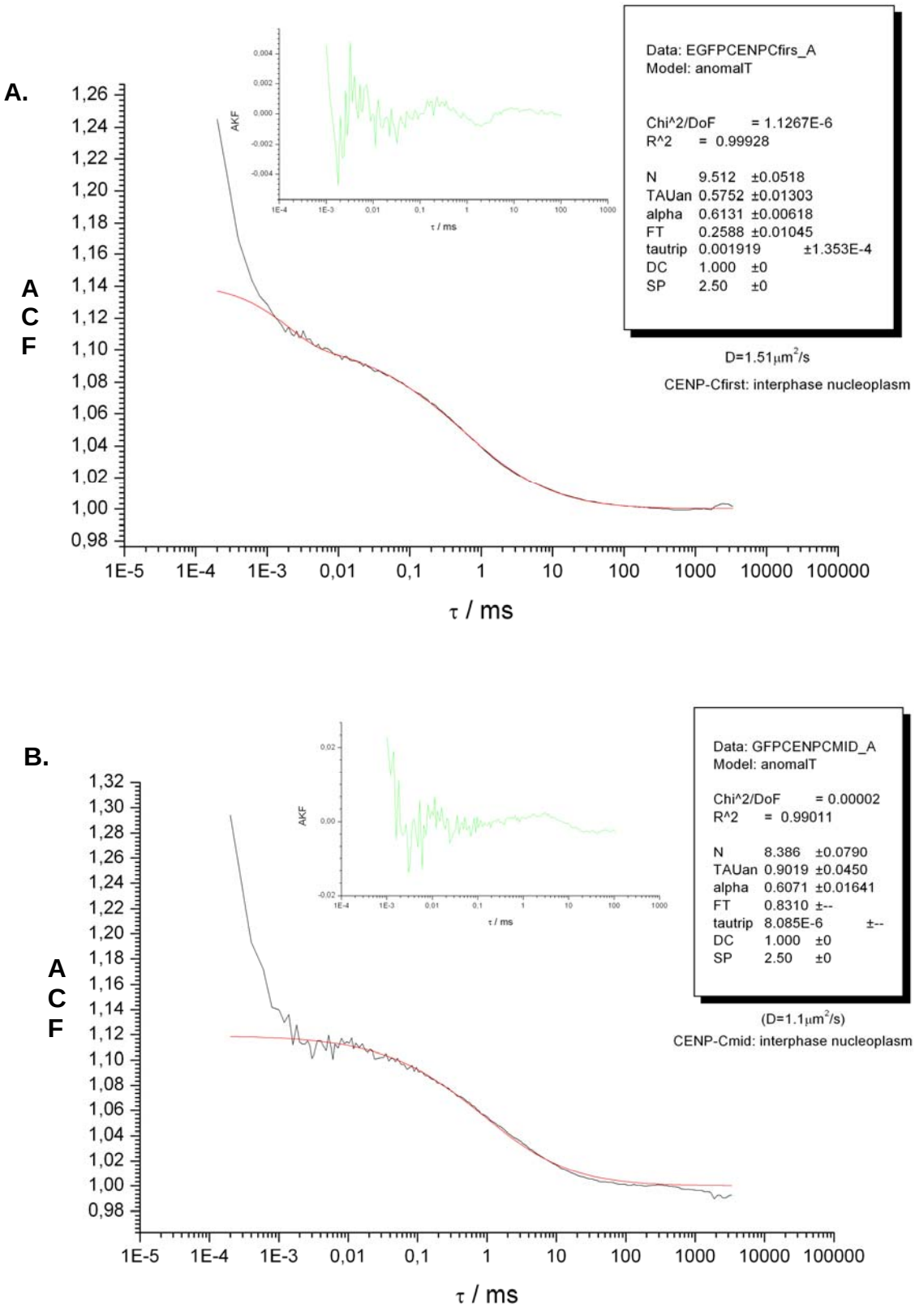

Fig. 25 to be continued to the next page

C.

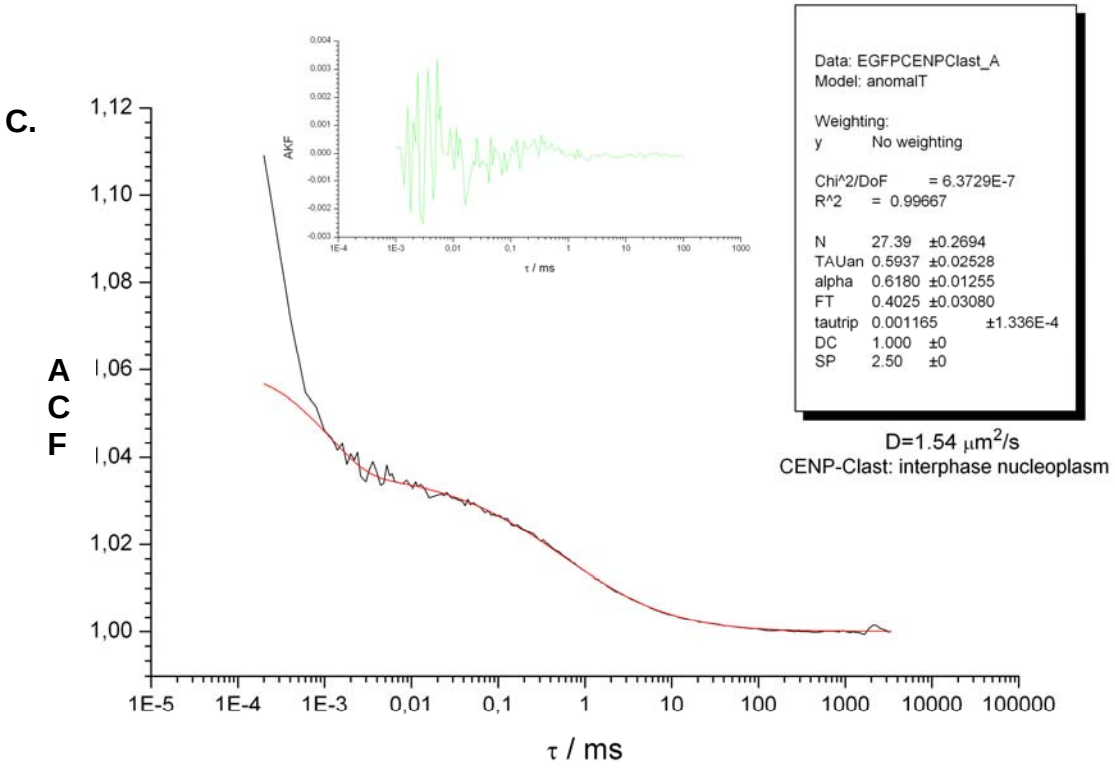

D=1.54 μm²/s
CENP-Clast: interphase nucleoplasm

D.

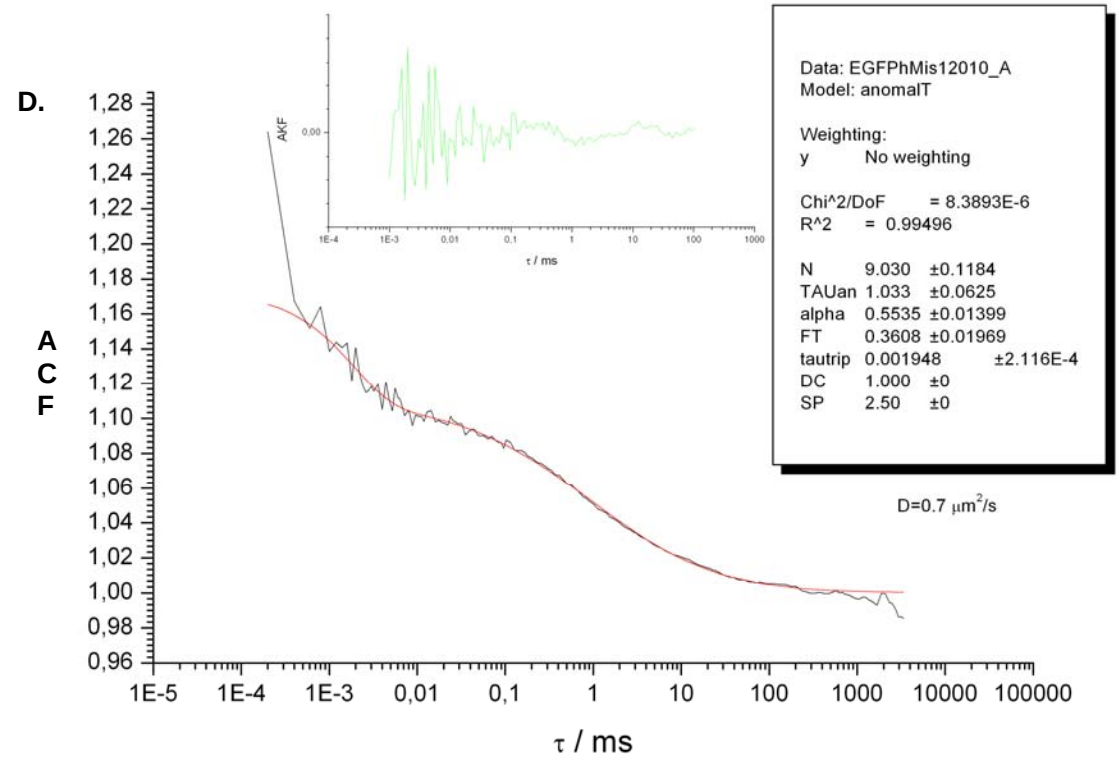

D=0.7 μm²/s

The fluorescence localization results demonstrated that CENP-C 315-635 contains a centromere localization domain. Interestingly, the central portion of CENP-C moved slightly slower with a diffusion coefficient of 1.08 ± 0.05 $\mu m^2/s$. The mobility of the central CENP-C subdomain might be restrained by a stable structure or colliding with nuclear components in the nucleus, potentially with DNA since it harbors the unspecific DNA binding region of CENP-C (229). This would explain why the central fragment is less mobile compared to the CENP-C N- and C-terminal regions. Taken together, the CENP-C subfragments are dynamic in the nucleus, in strong contrast to the CENP-C full length protein. Nevertheless, the truncated CENP-C proteins seem to transiently interact with the nuclear components which obstruct their diffusion.

The dynamic measurements of hMis12 were carried out with the same approach as for CENP-C. During mitosis, hMis12 proteins diffusing in the nucleoplasm could not be detected. During interphase, the FCS measurements revealed a diffusion coefficient for hMis12 of 0.70 $\mu m^2/s$ with a particle number in the focal volume of 9.03 ± 0.12 and an anomaly factor of 0.55 ± 0.014 (see Table 2). Despite the molecular weight of GFP-hMis12 being less than that of the CENP-C subdomains, the FCS data demonstrated that hMis12 was less mobile. These data correspond to the previous result showing that hMis12 interacts with several nuclear proteins (141). Thus, hMis12 diffuses with a rate similar to its binding partner HP1γ (174). This might be explained by an interaction of the two proteins. Conclusively, during interphase, hMis12 is not a stable kinetochore component; it is released from the foundation kinetochore complex as a rather mobile protein.

In a second step, the dynamic properties of CENP-C and hMis12 in living cells were further studied by FRAP experiments.

3.4.2. Fluorescent recovery after photo-bleaching (FRAP)

In the FRAP experiments, a small distinct region (region of interest, ROI) in a human HEp2 cell expressing a GFP-tagged protein is briefly bleached with high laser intensity, and the movement of unbleached fluorescent molecules from unbleached areas of the cell into the bleached region is followed with low-intensity laser light (114, 116). The velocity of bleaching recovery is a measure for the rate of molecule diffusion of the

tagged protein. When all molecules are immobile, the bleached region will remain bleached and no fluorescence recovery will be observed. A FRAP mobility coefficient is calculated from the fluorescence intensity increase in the bleached region plotted as a function of time. This coefficient, $t_{1/2}$, is the time required for the fluorescence intensity in the ROI to recover to 50 % of the pre-bleached fluorescence intensity. A mobile fraction is determined by computing the ratio of the (within the observation time) final to the initial fluorescence intensity in the bleached region, corrected for the amount of fluorescence removed during photo-bleaching.

The GFP fusion proteins containing CENP-C 1-943, the CENP-C subdomains and hMis12 in living HEp2 cells were irreversibly bleached by high-powered laser pulses in ROI areas of the nucleus under control conditions. Subsequently, fluorescence recovery in the bleached spots was recorded over time by sequential imaging scans in the microscope. This recovery is a consequence of GFP-fusion proteins moving from unbleached areas into the bleached area exchanging the bleached protein. The FRAP kinetics were computed with the Excel program. The FRAP measurement results were compiled and are presented in Table 3 and Figure 26 and 27.

The FRAP results showed that CENP-C is an immobile protein (within the observation time): the bleached spot showed no recovery within 100 s (see Fig. 26A and B) and the recovery curve showed no fluorescence recovery in the bleached region (see Fig. 26E). The experiment was continued with long-term FRAP: now, the time recovery after photo-bleaching was measured over 3.5 hours. In interphase, CENP-C 1-943 showed slight diffusion with a recovery time ($t_{1/2}$) of more than 3 hours with a 20 % mobile fraction (see Table 3). Interestingly, measurements in mitotic cells demonstrated no fluorescence recovery in this time range. The mobile fraction might represent over-expressed CENP-C that was unable to bind to centromeres. Conclusively, these data corroborated the immunofluorescence analysis and FCS results that CENP-C is a stable component of the kinetochore and is associated with the complex steadily throughout the cell cycle. CENP-C might be slowly but continuously assembled into the kinetochore during interphase.

GFP-Centromere	FRAP Measurement Result	
	Fluorescence Recovery Halftime (t1/2)	Mobile Fraction (%)
GFP-CENP-C 1-943 interphase	> 3 hrs	20
GFP-CENP-C 1-943 mitosis	No recovery	<5
GFP-CENP-C 1-315	4.0 s	90
GFP-CENP-C 315-635	4.8 s	75
GFP-CENP-C 635-943	4.0 s	90
GFP-hMis12 interphase	4.8 s	90
GFP-hMis12 mitosis	No recovery	15

Tabel 3. FRAP results for CENP-C and its subdomains and hMis12. The mobile fraction of the full length proteins were conducted in interphase and mitosis. The CENP-C truncated protein mobile fractions were measured during interphase. The error of the FRAP measurements was between 5 to 10 %.

The CENP-C subfragments were shown to diffuse rapidly. The bleaching recovery of GFP-CENP-C 1-315 and GFP-CENP-C 635-943 were 4.0 sec in both cases with a mobile fraction of 90 % (Tabel 3, Fig. 27B and 27D). GFP-CENP-C 315-635 was slightly slower with a recovery of 4.8 sec and a mobile fraction of 75 % (see Table 3, Fig. 27A and 27C). These data support the FCS results which revealed that CENP-C 315-635 has a reduced mobility. All three subfragments were not capable of stably binding to the kinetochore. Stable binding of CENP-C to the kinetochore, as observed here, thus is a result not of the properties of the subfragments by themselves but may be of the dimerization and oligomerization properties of the whole CENP-C protein.

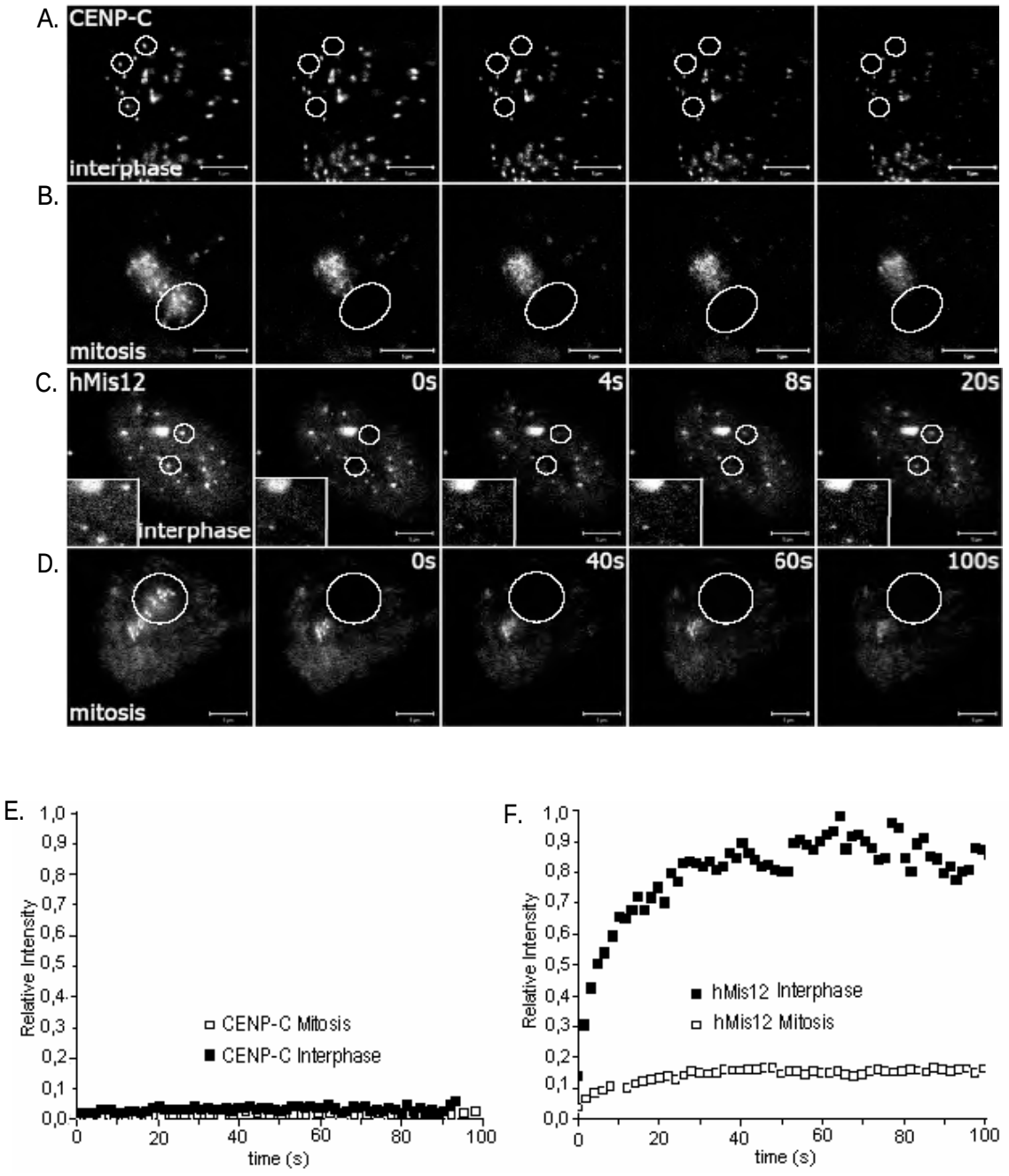

Fig. 26. Dynamic behavior of CENP-C and hMis12 in the living cell. The indicated region was bleached with high laser power to approximately half of the brightness and recovery of the fluorescence signal in the bleached area was monitored over time (post bleached image = 0 s). A) GFP-CENP-C 1-943 interphase, B) GFP-CENP-C 1-943 mitotic cell, C) GFP-hMis12 interphase, D) hMis12 mitotic cells, E) FRAP curves of GFP-CENP-C 1-943, F) FRAP curves of GFP-hMis12. Relative (fluorescence) intensity (I), time (s): bleaching recovery time. The FRAP error measurements were between 5 to 10 %.

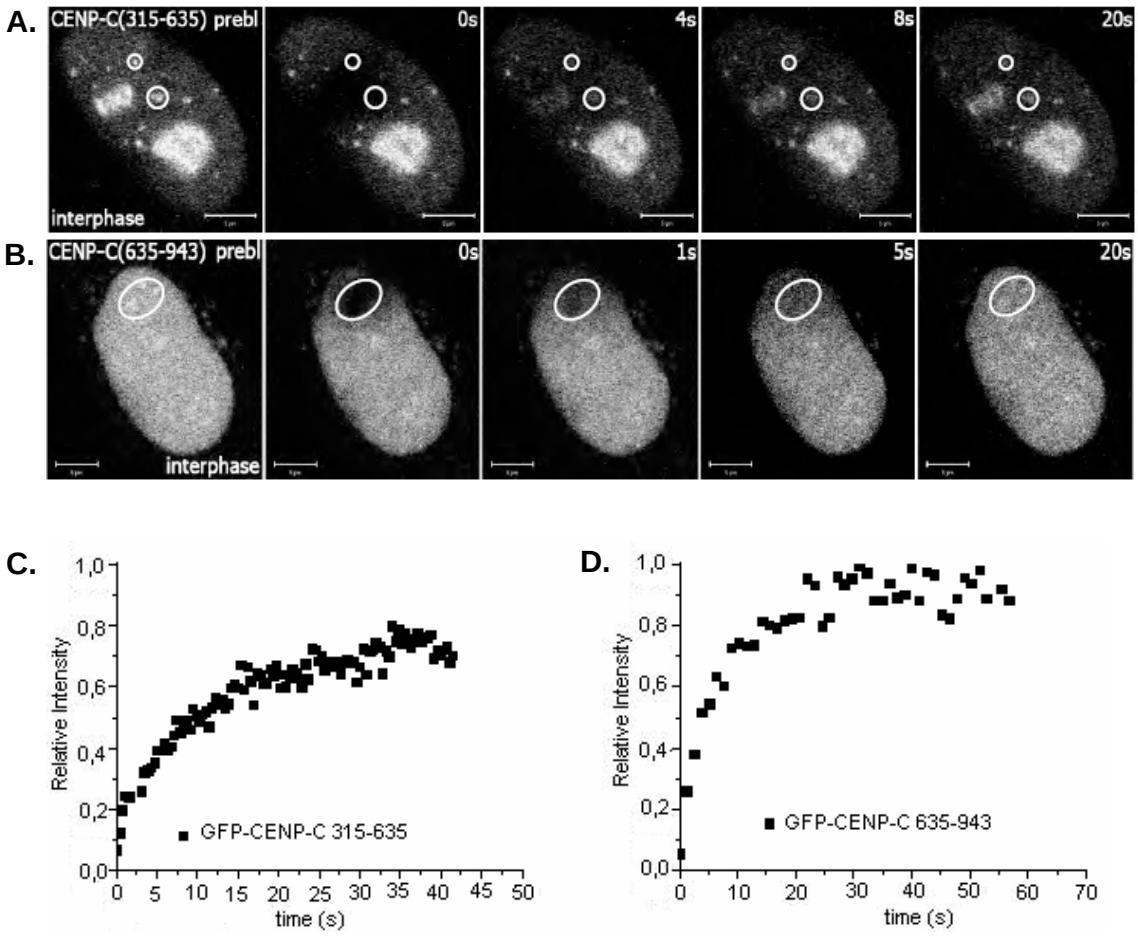

Fig. 27. Dynamic behavior of CENP-C 315-635 and CENP-C 635-943. The indicated region was bleached with high laser power to approximately half of the brightness and recovery of the fluorescence signal in the bleached area was monitored over time (post bleached image = 0 s). A) GFP-CENP-C 315-635 B) GFP-CENP-C 635 -943 C) FRAP curves of GFP-CENP-C315-635, F) FRAP curves of GFP-CENP-C635-943. Relative (fluorescence) intensity (I), time (s): bleaching recovery time. The FRAP error measurements were between 5 to 10 %.

Our dynamic observations during interphase revealed that hMis12 is a rapidly exchanging component of the inner kinetochore. However, immunofluorescence experiments indicated that there was no free protein in the cell during mitosis. FRAP measurements demonstrated that the photobleaching recovery in interphase was very fast with $t_{1/2}$ = 4.8 sec (Fig. 26C and 26F) with a mobile fraction of 90 % (Table 3). In contrast, during mitosis, hMis12 showed only a very small recovery with a similar $t_{1/2}$ as during interphase (Fig. 26D and 26F) but with a mobile fraction of only 15 % (Table 3).

The mobile fraction detected during mitosis might be the rest of the free protein fraction in interphase that was unable to bind to the kinetochore when the cell entered mitosis. Evidently, these data corroborated the localization analysis and FCS results that hMis12 is a stable kinetochore component during mitosis with weak binding during interphase. Furthermore, its own loading pathway that makes hMis12 become independent from the other foundation centromere proteins (65) likely supports the hypothesis that hMis12 is not restrained in the chromosome scaffold and is able to move freely during interphase. This suggests an inducible structural role of hMis12 on the outer kinetochore assembly during mitosis.

In summary, localization studies of CENP-C and hMis12 demonstrated that CENP-C is a structural protein that binds completely to the kinetochore. The molecular dissection resulted in different binding properties of the CENP-C subfragments. In the case of hMis12, colocalization with the centromere was observed, however complete kinetochore binding was only observed during mitosis. The dynamic data supported the localization studies. The data presented suggest that CENP-C is anchored to the kinetochore throughout the cell cycle, while hMis12 docking to the kinetochore is cell cycle dependent.

4. DISCUSSION

Several identified foundation inner kinetochore proteins in humans are believed to be crucial factors for building the kinetochore (5). Recent reports (146, 54) identified 11 additional proteins that are directly (the "NAC" proteins) or more distally (the "CAD" proteins) linked to CENP-A. NAC consist of CENP-M, CENP-N, CENP-T, CENP-U, CENP-C and CENP-H while CAD consists of CENP-K, CENP-L, CENP-O, CENP-P, CENP-Q, CENP-R and CENP-S. This thesis deals with two of the inner kinetochore proteins, CENP-C and hMis12.

Various indications from previous studies provided evidence that CENP-C function in mitosis is dependent on other proteins (213, 40, 144). Centromere targeting of CENP-C requires CENP-H and CENP-I (59, 140) but direct interaction is solely demonstrated with CENP-B (203). CENP-C associates with α-satellite DNA and binds DNA *in vivo*, directly or indirectly (160). Antibody injection inhibiting CENP-C function resulted in trilaminar stucture disruption and defects in chromosome segregation (57, 90). This study found that CENP-C is totally immobile at the centromeres (see Fig. 19, Fig. 26, Table 2 and 3). The molecular dissection of CENP-C into three subdomains showed reduction of binding: all of the CENP-C subdomains were mobile in the cell nucleus (Table 3, Fig. 25 and 27).

hMis12 has a kinetochore loading pathway independent from CENP-A and forms a complex structure with several nuclear proteins (65, 141). hMis12 depleted cells showed a delayed mitosis with misaligned chromosomes and disorientations (141). The data presented in this study demonstrate that hMis12 is mobile during interphase and immobile in the mitotic phase. This dynamic behavior (see Fig. 25 and 26) is likely explained by the role of hMis12 in the outer kinetochore assembly during mitosis. In hMis12 depleted cells, Hec1 targeting is decreased (29) suggesting an interaction of hMis12 with the Hec1 complex. Thus, hMis12 might be a bridge between the inner and outer kinetochore. Therefore it remains interesting to investigate which role of hMis12 plays in both, the inner and outer kinetochore, and how it contributes to the assembly of kinetochore.

4.1. CENP-C and hMis12 failed to show the direct interaction with identified foundation kinetochore proteins

This study applied (i) a biochemical and (ii) a cellular *in vivo* approach to investigate potential interactions between kinetochore proteins. These strategies were expected to demonstrate the interaction of CENP-C and hMis12 either with identified binding partners or with proteins from the collection in cDNA libraries. The previous interaction studies successfully demonstrated physical interactions between CENP-C with the CENP-A/CENP-B/DNA complex and CENP-B (6, 203), human nuclear protein UBF/NOR-90 (158), human nuclear body hDaxx (159) and ND10 (50). Physical interactions between hMis12 with other human kinetochore proteins were successfully demonstrated. The identified human proteins that were reported to interact with hMis12 are Hec1/Kntc2, Zwint1, HP1α, HP1γ, KIAA1570, c200rf172, DC8, pMF1 complex (141), Hec1 (29) and the hDsn1, hNnf1, hNsl1 complex (93).

The efforts of this thesis to detect interactions of CENP-C and hMis12 with human CENP-A, CENP-B and CENP-C proteins by *in vitro* assays failed. From the technical point of view, several reasons can explain this negative result: (i) the quality of one of the two binding partners was poor due to incorrect protein folding. In the Coomassie gel, the GST-CENP-C 315-635 and GST-hMis12 appeared as three and two bands, respectively (see Fig. 10B). (ii) The extraction and elution process of the proteins from the human cells may have influenced or destroyed the native protein conformation. Theoretically, purified human CENP-A, CENP-B and CENP-C from cell lines will be ideal as binding partners to demonstrate the interaction of CENP-C and hMis12 tagged proteins with human inner kinetochore proteins *in vitro*. Practically, to find the appropriate purification protocols for human centromere proteins is a difficult task. In nature, human CENP-A, CENP-B and CENP-C are associated with a chromosome scaffold fraction that is very insoluble. The kinetic studies on CENPs solubilization demonstrated that MNase digestion first releases the CENP-A chromatin complex into the soluble fraction, later CENP-B and CENP-C (234). CENP-A interacts with DNA and finally forms a complex with CENP-B and CENP-C (6). The data suggest that the protein solubilization procedures might affect the structure of the proteins through disruption of the protein-

protein interactions in the scaffold and release of the protein from the complex. Consequently, this method affected the protein ability to bind the ligand (21, 53, 87). Nevertheless, in one case, interaction studies using GST-CENP-C had been successful: Salt gradient-purified human UBF1 and NOR-90 interact with GST-CENP-C 635-943 (158). For future studies, in order to continue these *in vitro* experiments, the extraction methods have to be improved.

A successful effort to detect the direct interaction between CENP-C with other foundation inner centromere proteins was reported using a Yeast two-hybrid analysis which examined the interaction between CENP-C and CENP-B (203). The other successful analysis using this method reported the interaction between CENP-C with hDaxx, a nuclear protein that has a role in apoptosis and localizes transiently at interphase centromeres (159). In this study, the Y2H method was used to examine the interaction between CENP-C and CENP-A, CENP-H, and CENP-I. No interaction was detected. This negative result suggests the existence of mediator interactions between CENP-C, CENP-A, CENP-H and CENP-I since these proteins form a stable inner kinetochore complex (see Discussion 4.4. and 4.6).

Chromatin immunoprecipitation (ChiP) assays detected that CENP-C is able to bind α-satellite DNA (160). However, the identification of a specific DNA target sequence for CENP-C failed (229). A previous study using a ChiP assay indicated the associations between CENP-C and the CENP-B/CENP-A nucleosome complexes (6). Mutation of CENP-A resulted in a complete failure in chromosome segregation (77). No report was able to demonstrate the direct interaction between CENP-C and CENP-A.

The findings of this study gave an insight into the experimental problems detecting the interaction of CENP-C and hMis12 with other foundation inner kinetochore proteins by *in vitro* techniques. Three components of the inner kinetochore (CENP-H, CENP-I and CENP-A) are required for CENP-C recruitment but suggested that the interactions between those proteins might be mediated by other yet unknown factors (60). Moreover, a previous study revealed that hMis12 physically interacts and makes a complex with Zwint1 and Hec1 (65, 29).

An alternative method to detect protein-protein interactions is fluorescence resonance energy transfer (FRET) (115). This method is able to detect the proximity of fluorescence

labeled molecules separated by distances from 10 to 100 Å. FRET occurs when the donor is quenched due to the presence of an acceptor (91, 150). A preliminary acceptor bleaching FRET study of CFP-CENP-C 1-943 and YFP-CENP-A in this thesis showed a weak FRET signal of the donor CFP-CENP-C (data not shown). CFP bleached very fast and turned out to be unstable (205, see also 165). In our group, the CFP tag was replaced by Cerulean, a monomeric and improved version of ECFP which is stable and 2.5 times brighter than ECFP (165). FRET experiments using the Cerulean tag (147) identified the neighborhood between CENP-C and CENP-B in the kinetochore complex. This FRET data showed that the CENP-C N-termini associate in the complex. Furthermore, the FRET indicated that the CENP-C N-terminus is close to the CENP-B C-terminus. This result is in agreement with Y2H data that revealed a physical interaction between CENP-C and CENP-B (203).

4.2. False positive and false negative yeast two hybrid results

The Yeast two-hybrid (Y2H) assay exploits the ability of two proteins to bring a transcription activation domain into close proximity to a DNA-binding site that regulates the expression of an adjacent reporter gene (52). Thus Y2H is not applicable for proteins that are able to initiate transcription in yeast by themselves ("auto activation"). In this study, auto activation activity was observed for CENP-C 1-315 (see Fig. 13A). Hence, this assay could not detect any interaction partner of the CENP-C N-terminal subdomain.
Several classes of proteins caused failures of the Y2H analysis (181). These proteins are able to repress or terminate cell growth because the proteins are toxic to yeast, lack the posttranslational modification, are unstable, fold improperly, fail to localize in the yeast nucleus, degrade other essential yeast proteins or might be counter-selected during yeast growth (124, 218). In this study, yeast transformed with CENP-C 1-943 was unable to grow. The same phenomenon was reported for CENP-C 313-620 (185). Human proteins do not induce their toxicity to yeast: for example, the huntingtin protein is a toxic human protein but can be expressed in yeast (U. Stelzel, personal communication). Therefore, the expression failure of CENP-C 1-943 in yeast could be due to its size. Since large full length human proteins often fail to fold correctly and fail to enter the yeast nucleus, the

cDNA library for Y2H analyzes usually contains only partial sequences because subdomains of proteins may interact better than full length proteins (184). Moreover, a correct protein conformation is important for a positive interaction in this analysis, incorrect protein folding might result in a limited activity or in the inaccessibility of the binding sites (38).

To provide a sensitive detection of protein interactions *in vivo* and internal controls for interaction validation, multiple reporter genes with promoters to eliminate the false positive result has been engineered. This study is using *HIS3* and *LEU2* genes to allow a positive selection for prototrophic growth and *lacZ* gene that permits a colorimetric colony screen. Nevertheless, false positive results were detected. The mating assay between the CENP-C central domain and the CENP-C C-terminus in SDIV medium found 12 interacting human proteins from the human cDNA library (see Table 1 and Fig. 13B). As a next step, the 12 proteins were subjected to the β galactosidase assay resulting in 5 positive interaction partners (showing blue colonies): UBR1, CRMP1, SETDB1, QARS and KIAA1377 (see Fig. 13C). Based on the blast analysis using the NCBI web site, three of these proteins; UBR1, CRMP1 and QARS are non-nuclear proteins. Their interaction with CENP-C in Y2H assay might be false positive results, thus these proteins were secluded from further analysis in this thesis. Frequently, the false positive results are caused by bait proteins that act as transcriptional activators. Bait or prey proteins often show a tendency for non-specific interactions (181). The other limitation of Y2H, the false negative results, might be caused by the inability of a protein to localize in the nucleus. If the prey protein is not expressed or bait or prey proteins are improperly posttranslationally modified, the interaction will be obstructed (181). Furthermore, the correlation of mRNA expression is not necessary for a protein interaction because the degradation rates of proteins are mostly different, hence the proteins that have weak expression correlation may still become *bona fide* interactors as long as these proteins adjoin in sufficient proximity within a cell (214, 86, 10).

In this thesis, the nuclear protein PSMB10, a member of the 26S proteasome family, was identified by Y2H to interact with CENP-C. Since mitotic function includes polyubiquitination of securin (68) and thus probably proteasomal degradation, it would be of a particular interest to find out whether an inner kinetochore protein like CENP-C

recruits a proteasome protein to the kinetochore. For this reason, PSMB10 was analyzed further although the interaction with CENP-C was not confirmed in a second Y2H assay. As mentioned above, Y2H results are not conclusive, thus might be false positive or false negative.

This study demonstrated that PSMB10 accumulates in the spindle pole during metaphase (see Fig. 16B). These data allow to speculate that PSMB10 has a molecular function at the centrosome or in sister chromatid separation. The 26S proteasome is involved in protein degradation and is accelerating breakdown of ubiquitinated proteins (92, 17), thus it might play a role in sister chromatid separation during mitosis (68). Securin is polyubiquitinated by the Anaphase Promoting Complex/Cyclosome (APC/C) which is engage with the mitotic activator Cdc20. The polyubiquitinated securin becomes the target of the proteasome 26S. Finally, the separase releases Scc1 and the sister chromatid is segregated (68).

Corresponding to the Y2H result that PSMB10 might interact with CENP-C, we speculate that PSMB10 can be involved in these mitotic processes. Furthermore, PSMB10 colocalized with PML and Cajal bodies (see Fig.17). The molecular function of PML bodies remains elusive (19, 182). The Cajal bodies are involved in transcription and/or processing of mRNAs, snRNAs, histone mRNAs and rRNA in the nucleus (123, 238). The data obtained here present a hint that PSMB10 might be involved in these functions. Further experiments are required in order to elucidate this point.

This study also identified KIAA1377 as a protein potentially interacting with CENP-C. However, corresponding to its function as a signal transduction protein (137), KIAA1377 was secluded from further analysis.

4.3. SETDB1 interacts with CENP-C

SETDB1 was found to interact with the CENP-C C-terminus by the Y2H assay (see Fig. 13) and it localized to centromeres partially (see Fig. 15). SETDB1 is a member of the SUV39H1 family that methylates histone H3 at lysine 9 at pericentric heterochromatin (177, 151). An *in vitro* GST binding assay demonstrated that SETDB1 is capable to stimulate HP1 binding to histone H3 (177). Furthermore, HP1α, HP1β and HP1γ localize

to centromeric heterochromatin during interphase (71, 129). Interaction studies using a ChIP assay and affinity chromatography showed that SETDB1 interacts with the DNA methyltransferases DNMT3A and DNMT3B (108).

SETDB1 associates with the methyl-CpG binding protein (MBD1), thus MBD1 might recruit SETDB1 to the chromatin assembly factor (CAF-1) to methylate lysine-9 at newly stored histone H3 during S-phase (169). One can speculate that SETDB1 also might methylate CENP-C. SETDB1 does not bind to specific DNA sequences suggesting that it is recruited to its site of action by other proteins (108). Thus, SETDB1 might transiently bind to CENP-C and methylate neighboring proteins (like for example CENP-A or H3K9 if this is present at the centromeric site (54)). The interaction of SETDB1 with the DNA methyltransferases DNMT3A and DNMT3B (108) might potentially mediate these activities. Since CENP-C binds only to the active centromeres (31, 158), its interaction with SETDB1 might promote specific kinetochore methylation.

The hallmark of centromere function is replacing histone H3 with the histone H3 variant CENP-A in centromeric nucleosomes (98). However, it is currently unclear how CENP-A is targeted to centromeres and how centromeric chromatin directs kinetochore assembly. It might be that CENP-A and the centromeric DNA are epigenetically marked for centromere function and centromere identity: centromeric DNA modification might contribute to the kinetochore complex stability. CpG methylation within the CENP-B box DNA reduces the binding ability of CENP-B, thus it may regulate CENP-B binding to the CENP-B box (209,132).

DNMT3B, a SETDB1 binding partner, interacts physically with HP1α (105, 141). Human H3meK9, that is methylated by SETDB1, binds to HP1 which is directly associated with pericentric heterochromatin (49, 189, 237). This study presented the colocalization between SETDB1 with HP1 (see Fig. 5B and 15C). These data provide the perspective that the kinetochore assembly involves protein modifications (198, 66, 135) that influence the interaction between kinetochore proteins.

4.4. Molecular dissection of CENP-C demonstrates the binding ability and functional domain of truncated CENP-C

The FRAP analysis showed no CENP-C fluorescence recovery after photo-bleaching in the mitotic cell and in interphase (Tabel 3, Fig. 26). The FCS results confirmed the absence of any mobile fraction (Tabel 2). As a core member of inner centromere proteins, CENP-C totally colocalizes and stably binds to centromeres throughout the cell cycle (see Fig. 19). Thus the dynamic behavior demonstrates that CENP-C is a structural protein. Molecular dissection studies of CENP-C identified its functional domains (102, 229, 194, 185, 213). The N-terminus of CENP-C failed to localize to the centromeres (102). CENP-C has two domains that independently localize to centromeres and associate with α-satellite DNA (185, 213). This study observed that the central portion of CENP-C is able to bind to centromeres and RNA in the nucleolus (see Fig. 19 and 21), however, it is unable to bind steadily. The subdomain stained the nucleoplasm but not the cytoplasm (see Fig. 21). This central domain was observed to be less mobile then the N-terminal and the C-terminal domains. A previous study using mutational analysis indicated that the centromere targeting domain and DNA binding domain of CENP-C *in vivo* is located in the region from 522 to 534 aa (185). This study found that this region by itself (linked to an NLS and to GFP) is unable to localize to the centromeres (Fig. 22). Thus, the targeting domain of CENP-C might include the amino acids region 522 to 533 but likely it is longer.

The C-terminus of CENP-C was reported to be capable of binding DNA *in vivo* and *in vitro* although less efficiently than the central domain (229, 160). This study presented data that the C-terminal domain was able to localize to the centromere unsteadily (with no protein fraction detected in the nucleolus) (see Fig. 23). Strikingly, the measurements demonstrated that the CENP-C subdomains are highly mobile (Tabel 2 and 3). Moreover, the CENP-C N- and C-termini were described to oligomerize and dimerize, respectively (194). The particle number (N) detected in the observation volume by FCS for CENP-C 315-635 and CENP-C 635-943 were 9.51 $\pm$ 0.05 molecule/fl and 27.39 $\pm$ 0.27 molecule/fl, respectively. If the proteins in known concentration are all soluble, the oligomeric state can be estimated from the average number of particles. In practice, the

proteins can absorb to the well surface and form large aggregates reducing their observable concentration. Inversely, the evidence of a dimerization state can be identified from doubling of particle numbers detected in the local concentration volume (106).

The characterization of CENP-C subdomains elucidated their properties and leads to the conclusions that CENP-C full-length protein binds to the centromere. All CENP-C subdomains were unable to bind steadily to the centromere while full-length CENP-C binds tightly. Thus, this tight binding must have its origin in the interplay between centromere localization, multiple binding to CENP-B and DNA and/or dimerization or oligomerization functions. Such a stable binding as shown by CENP-C full-length protein was also found for the splicing factor component (SFC) (167, 44). In contrast, most other nuclear body proteins (like for example heterochromatin proteins; 174) are dynamic (186, 187).

4.5. hMis12 might bridge the inner and outer kinetochore

Three subunits of the hMis12 complex (141), hDsn1, hNnf1 and hNsl1, localize coincidently with CENP-A at the inner kinetochore and Hec1 (hNdc80) in the outer kinetochore (93, 94). hMis12 localized at the centromere throughout the cell cycle and is required for proper chromosome alignment and cell cycle progression (65). The FCS and FRAP measurements of this study showed that hMis12 diffuses into the nucleoplasm during interphase but steadily binds to the centromere during mitosis (see Fig. 24, Table 2, 3, Fig. 26). Those data are confirming the localization results. Thus, in interphase, hMis12 behaves as many nuclear proteins roaming within the nucleus, rapidly associated and dissociated with other nuclear proteins (96, 130, 131); the free mobile fraction diffuses through the nucleoplasm until it is captured by high affinity interactions at the inner kinetochore (167). During mitosis, hMis12 becomes a stable component of the mitotic inner kinetochore; thus the properties of hMis12 are cell cycle dependent. Probably, hMis12 is fixed to the kinetochore during mitosis due to the binding of further (outer) kinetochore proteins.

The other kinetochore proteins in the hMis12 complex are interdependent on kinetochore localization and stability, their inhibition caused aberrant bi-orientation of microtubules

to sister kinetochores (93). In the kinetochore, hMis12 is required for the assembly of hZwint1, a member of the outer kinetochore (141). The hMis12 complex association with the Hec1 (hNdc80) complex connects hMis12 to the outer kinetochore (29, 93). In hMis12 depleted cells, inner and outer kinetochore targeting was affected (93, 94). The data presented here suggest that hMis12 likely localizes at the surface of the inner kinetochore. During mitosis it might establish a bridge between the inner and outer kinetochore.

The other foundation kinetochore proteins CENP-A, CENP-B, CENP-H and CENP-I form a stable kinetochore complex. The FRAP and FCS measurements demonstrated that those proteins have large immobile subpopulations (224).

4.6. Consequences to the inner kinetochore complex architecture

The two kinetochore proteins analysed in this thesis, show very different behavior. CENP-C was found to bind to active centromeres in a very stable manner, no exchange at the inner kinetochore site was detected by FRAP analysis, and the very sensitive FCS technique could not detect any free CENP-C in the nucleoplasm. This indicates that full length CENP-C binds tightly to the kinetochore complex. In the nucleus, a protein of such behavior is rarely observed (131, 62, 76, 120, 152). The situation changed when CENP-C subfragments were studied: its three subfragments located to the inner kinetochore, however, they exchanged with the pool of free molecules in the nucleus fast and completely, without an immobile fraction. The CENP-C (522-533) fragment had been suggested to be a DNA binding domain (185) which was not confirmed by data obtained in this thesis. The tight binding of the CENP-C full-length protein is thus not due to a subdomain very strongly binding to the centromere or kinetochore, but instead due to further elements supporting the binding and fixing the protein once bound. I speculate that these additional elements are CENP-C di- and oligomerization. CENP-C contains di- and oligomerisation domains at its C- and N-terminus, respectively (194). The contribution of di-/oligomerization of CENP-C to its binding stability that is supported by energy transfer data in our group (147) showing head-to-head association of the CENP-C molecules in the complex in living human cells. Based on experimental

results obtained for these proteins for the first time, this thesis yielded a convincing explanation for the tight binding of full-length CENP-C to the kinetochore.

In contrast to CENP-C, hMis12 exchanged very fast at the kinetochore during interphase but became immobilised in mitosis. This suggests that hMis12 is located at the surface of the inner kinetochore complex or middle zone and might serve there as a binding platform for mitotic kinetochore proteins which fix hMis12 to the complex upon binding. This rarely observed behavior suggests that hMis12 is not an inner kinetochore protein.

The dynamic rates and diffusion coefficients of the kinetochore proteins analyzed here (see Table 2 and Table 3) differ among themselves and also to those of the other inner kinetochore proteins CENP-A, CENP-B, CENP-H and CENP-I (224). Thus, the inner kinetochore proteins do not form a precomplex in the nucleoplasm before centromere binding (in this case, they all would show the same dynamic rates) but bind to the centromere as single proteins.

The observations in this thesis contributed to an explanation for the formation of human kinetochores and neocentromeres: the human centromere is built from tandem repeats of α-satellite DNA of 171 bp length. This DNA repeat length might offer a particular spacing in the centromeric chromatin structure which allows the bound inner kinetochore proteins to dimerize (CENP-B, may be also CENP-H) and oligomerize (CENP-C); and this process is supposed to stabilize the complex. In case the α-satellite DNA, and thus the spacing, is not available, the next best spacing would be selected for kinetochore location, forming a neocentromere. Without DNA spacing, the structure could form via a nucleation process (196, 126) followed by stepwise growth.

Moreover, epigenetic properties might guide kinetochore assembly. In preliminary experiments this study found that SETDB1 might physically interact with CENP-C. SETDB1 methylates Histone H3 at lysine 9 (177). One can hypothesize that also CENP-A might be methylated by SETDB1 at its lysine in position 9.

From these studies we conclude that the inner kinetochore forms a very stable complex (see also 220) during the whole cell cycle which serves as the basis for the functional mitotic kinetochore during mitosis. A simplified model is displayed in Fig. 28.

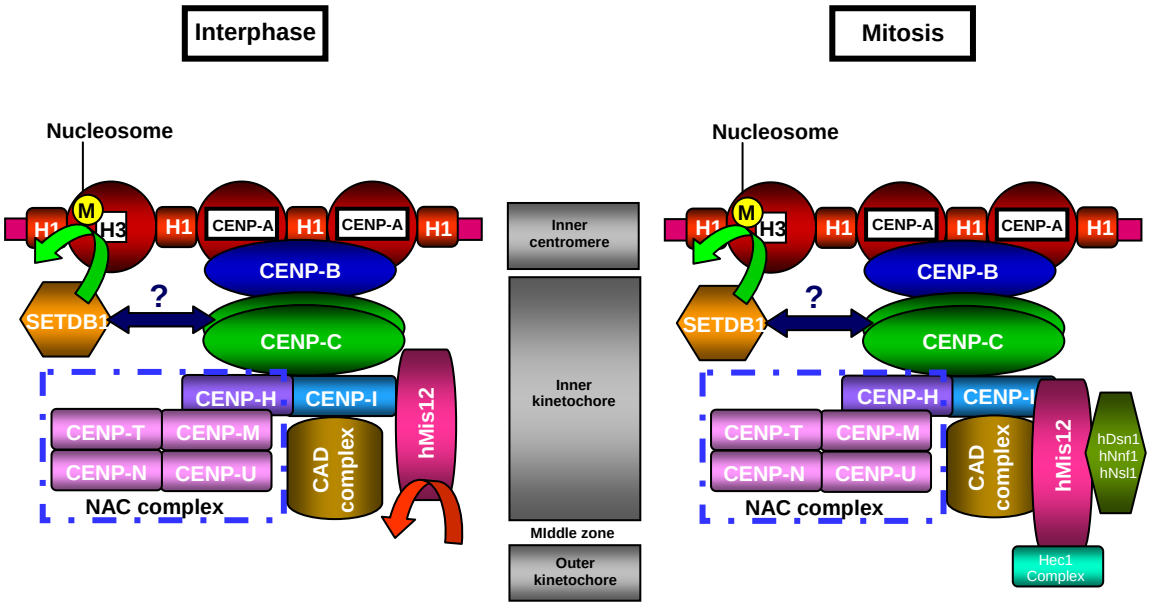

Fig. 28. Model of kinetochore assembly in vertebrate cells during interphase and mitosis. In each nucleosome CENP-A replaces Histone H3. Our group showed that Histone H1 binds to the linker DNA between nucleosomes (147). CENP-B and CENP-C that physically interact with one-another, are closely associated with CENP-A (6, 203, 147). SETDB1 that was shown by Schultz *et al.* to methylate Histone H3 at lysine 9 (177), interacts with CENP-C and might also methylate CENP-A. In interphase, hMis12 shuttles on and off the kinetochore (red arrow). During mitosis, hMis12 forms a stable complex with hDsn1, hNnf1 and hNsl1 (93). The complex binds to the kinetochore (for example to the Hec1 complex (141)). CENP-H and CENP-I interact with one another (111). The newly identified inner kinetochore NAC (dash box) and CAD complexes are part of the kinetochore (146, 54).

5. REFERENCES

1. Abrieu, A., Kahana, J.A., Wood, K.W., Cleveland, D.W. 2000. CENP-E as an essential component of the mitotic checkpoint *in vitro*. Cell, 102, 817-826.

2. Adams, R.R., Eckley, D.M, Vagnarelli, P., Wheatley, S.P., Gerloff, D.L., Mackay, A.M., Svingen, P.A., Kaufmann, S.H., Earnshaw, W.C. 2001. Human INCENP colocalizes with the aurora-B/AIRK2 kinase on chromosome and is overexpresed in tumor cells. Chromosoma, 110, 65 – 74.

3. Akhmanova, A., Hoogenraad, C.C., Drabek, K., Stepanova, T., Dortland, B., Verkerk, T., Vermeulen, V., Burgering, B.M., De Zeeuw, C.I., Grosveld, F., Galjart, N. 2001. CLASPs are CLIP-115 and -170 associating protein involve in the regional regulation of microtubule dynamics in motile fibroblast. Cell, 104, 923-935.

4. Albert, B., Bray, D., Johnson, A., Lewis, J., Raff, M., Roberts, K., Walter, P. 1997. Essential cell biology. Garland Publishing Inc, New York.

5. Amor, D.J., Kalitsis, P., Sumer, H., Choo, K.H.A. 2004. Building the centromere: from foundation proteins to 3D organization. Trends in Cell Biology, 14 (7), 359 – 368.

6. Ando, S., Yang, H., Nozaki, N., Okazaki, T., Yoda, K. 2002. CENP-A,-B, and –C chromatin complex that contain the I-type α-satellite array constitutes the prekinetochore in HeLa cells. Molecular and Cellular Biology, 22 (7), 2229 – 2241.

7. Andrews, P.D., Ovechkina, Y., Morrice, N., Wagenbach, M., Duncan, K., Worderman, L., Swedlow, J.R. 2004. Aurora B regulates MCAK at the mitotic centromere. Developmental Cell, 6, 253-268.

8. Bachewich, C., Thomas, D.Y., Whiteway, M. 2003. Depletion of a Polo Like Kinase in *Candida albicans* activate cyclase-dependent hypal-like growth. Molecular Biology of the Cell, 14, 2163-2180.

9. Baddeley, D. 2006. Kirchhoff Institute of Heidelberg University, unpublished data

10. Bader, J.S., Chaudhuri, A., Rothberg, J.M., Chant, J. 2004. Gaining confidence in high-throughput protein interaction network. Nature Biotechnology, 22 (1), 78-85.

11. Baneyx, F. 1999. Recombinant protein expression in *Escherichia coli*. Current Opinion Biotechnology, 10 (5), 411-421.

12. Bharadwaj, R., Yu, H. 2004. The spindle checkpoint, aneuploidy and cancer. Oncogene, 23, 2016 – 2027.

13. Bharadwaj, R., Qi, W., Yu, H. 2004. Identification of two novel component of the human NDC80 kinetochore complex. J. Biology Chemistry, 279, 13076-13085.

14. Black, B.E., Foltz, D.R., Chakravarty, S., Luger, K., Woods, V.L jr., Cleveland, D.W. 2004. Structural determinant for generating centromeric chromatin. Nature, 430 (6999), 578-582.

15. Blower, M.D., Karpen, G.H. 2001. The role of *Drosophila* CID in the kinetochore formation, cell cycle progression and heterochromatin interaction. Nature Cell Biology, 3, 730-739.

16. Blower, M.D., Sullivan, B.A., Karpen, G.H. 2002. Conserved organization of centromeric chromatin in flies and humans. Development Cell, 2, 319-330.

17. Bochtler, M., Ditzel, L., Groll, M., Hartmann, C., Huber, R. 1999. The proteasome. Annu. Rev. Biophys. Biomol. Struc., 28, 295-317.

18. Bomont, P., Maddox, P., Shah, J.V., Desai, A.B., Cleveland, D.W. 2005. Unstable microtubule capture at kinetochores depleted of the centromere-associated protein CENP-F. EMBO J., 24 (22), 3927-3939.

19. Borden, K.L.B. 2002. Pondering the Promyelocytic Leukemia Protein (PML) puzzle: possible functions for PML Nuclear Bodies. Molecular and Cellular Biology, 22 (15), 5259-5269.

20. Brown, M.T. 1995. Sequence similarities between the yeast chromosome segregation protein Mif2 and the mammalian centromere protein CENP-C. Gene, 160, 111-116.

21. Buchner, J. 1996. Supervising the fold: functional principles of molecular chaperones. FASEB J., 10, 10 – 19.

22. Büssow, K., Scheich, C., Sievert, V., Harttig, U., Schultz, J., Simon, B., Bork, P., Lehrach, H., Heinemann, U. 2005. Structural genomics of human proteins-target selection of a public catalogue of expression clones. Microbial Cell Factories, 4 (21), 1-13.

23. Carmena, M., Earnshaw, W.C. 2003. The cellular geography of Aurora kinases. Nature Reviews Molecular Cell Biology, 4, 842-854.

24. Carroll, C.W., Straight, A.F. 2006. Centromere formation: from epigenetic to self-assembly. Trends in Cell Biology, 16 (2), 70-78.

25. Celis, J.E. 1994. Cell biology: A laboratory handbook I,II,III. Academic Press, San Diego, USA.

26. Chan, G.K., Jablonski, S.A., Sudakin, V., Hittle, J.C., Yen, T.J. 1999. Human BUBR1 is a mitotic checkpoint kinase that monitor CENP-E functions at kinetochores and binds the cyclosome/APC. J. Cell Biology, 146 (5), 941-954.

27. Chan, G.K., Liu, S.T., Yen, T.J. 2005. Kinetochore structure and function. Trends in Cell Biology, 15 (11), 589-598.

28. Cheeseman, I.M., Desai, A. 2004. Feeling tense enough?, Nature, 428, 32 – 33.

29. Cheeseman, I.A., Niessen, S., Anderson, S., Hyndman. F., Yates III, J.R., Oegema, K., Desai, A. 2004. A conserved protein network controls assembly of the outer kinetochore and its stability to sustain tension. Genes & Development, 18, 2255-2268.

30. Chen, Y., Riley, D.J., Chen, P.L., Lee, H.W. 1997. HEC, a novel nuclear protein rich in leucine heptad repeats specifically involve in mitosis. Molecular and Cellular Biology, 17, 6049-6056.

31. Choo, K.H.A. 1996. The centromere. Oxford University Press, New York, USA.

32. Choo, K.H.A. 1997. Centromere DNA dynamics: Latent centromeres and neocentromere formation. Am. J. Human Genetic, 61, 1225-1233.

33. Ciferri, C., De Luca, J., Monzani, S., Ferrari, K.J., Ristic, D., Wyman, C., Stark, H., Kilmartin, J., Salmon, E.d., Musacchio, A. 2005. Architecture of the human Ndc80-Hec1 complex, a critical constituent of the outer kinetochore. J. Biological Chemistry, 280 (32), 29088-29095.

34. Cimini, D., Degrassi, F. 2005. Aneuploidy: a matter of bad connections. Trends in Cell Biology, 15 (8), 442 – 451.

35. Cooke, C.A., Bernat, R.L., Earnshaw, W.C. 1990. CENP-B: a major human centromere protein located beneath the kinetochore. J. Cell Biology, 110 (5), 1475-1488.

36. Cottarel, G., Shero, J.H., Hieter, P., Hegemann, J.H. 1989. A 125-base pair CEN6 DNA fragment is sufficient for complete meiotic and mitotic centromere functions in *Saccharomyces cerevisiae.* Molecular and Cellular Biology, 9, 3342-3349.

37. Craig, J.M., Earnshaw, W.C., Vagnarelli, P. 1999. Mammalian centromeres: DNA sequence, protein composition, and role in cell cycle progression. Experimental Cell Research, 246, 249-262.

38. Criekinge, W.V., Beyaert, R. 1999. Yeast two hybrid: state of the art. Biological Procedures Online, 2 (1), 1 – 38.

39. Cruz, M., Elenich, L.A., Smolarek, T.A., Menon, A.G., Monaco, J.J. 1997. DNA sequence, chromosomal localization and tissue expression of the mouse proteasome subunit *Lmp10* (*Psmb10*) gene. Genomics, 45, 618-622.

40. Deehan, R., Heald, R. 2004. Centromere glue provide spindle glue. Cell, 118, 529 – 534.

41. DeLuca, J.G., Dong, Y., Hergert, P., Strauss, J., Hickey, J.M., Salmon, E.D., McEwen, B.F. 2005. Hec1 and Nuf2 are core components of the kinetochore outer plate essential for organizing microtubule attachment sites. Molecular Biology of the Cell, 16, 519-531.

42. Dewar, H., Tanaka, K., Nasmyth, K., Tanaka. T.U. 2004. Tension between two kinetochores suffices for their bi-orientation on the mitotic spindle. Nature, 428, 93-97.

43. Dittrich, P., Malvezzi-Campeggi, F., Jahnz. M., Schwille, P. 2001. Accessing molecular dynamics in cell by fluorescence correlation spectroscopy. Biology Chemistry, 384, 491-494.

44. Dundr, M., Misteli, T. 2001. Functional architecture in the cell nucleus. Biochemistry J., 356, 297 – 310.

45. Dyson, M.R., Shadbolt, S.P., Vincent, K.J., Perera, R.L. McCafferty, J. 2004. Production of soluble mammalian proteins in *Escherichia coli*: identification of protein features that correlate with successful expression. BMC Biotechnology, 4 (32), 1-18.

46. Earnshaw, W.C., Ratrie, H., Stretten, G. 1989. Visualization of centromere proteins CENP-B and CENP-C on stable dicentric chromosome in cytological spreads. Chromosoma (Berlin), 98, 1 – 12.

47. Earnshaw, W.C., McKay A.M. 1994. The role of non histone proteins in the chromosomal event of mitosis. FASEB J. 8, 947 – 956.

48. Einarson, M.B., Orlinick, J.R. 2002. Identification of protein-protein interaction with Gluthatione-S-transferase fusion proteins. *In* Protein-Protein Interaction, ed. Golemis, E. Cold Spring Harbor Lab. Press, 37 – 57.

49. Elgin, S.C.R., Grewal, S.I.S. 2003. Heterochromatin: Silence is golden. Current Biology, 13 (23), R895-R898.

50. Everett, R.D., Earnshaw, W.C., Pluta, A.F., Sternsdorf, T., Ainsztein, A.M., Carmena, M., Ruchaud, S., Hsu, W.L., Orr, O. 1999. A dynamic connection between centromeres and ND10 proteins. J. Cell Science, 112, 3443 – 3454.

51. Fields, S., Song, O.K. 1989. A novel genetic system to detect protein-protein interaction. Nature, 340, 245 – 246.

52. Fields, S., Sternglantz, R. 1994. The two-hybrid system: an assay for protein-protein interactions. TIG, 10 (8), 286-292.

53. Fink, A. L. 1999. Chaperon-mediated protein folding. Physiological Reviews, 79 (2), 425-449.

54. Foltz, D.R., Jansen, L.E., Black, E.E., Bailey, O.A., Yates, J.R., Cleveland, D.W. 2006. The human CENP-A centromeric nucleosome-associated complex. Nature Cell Biology, 8 (5), 458-469.

55. Formosa, T., Burke, R.L., Alberts, B.M. 1983. Affinity purification of bacteriophage T4 proteins essential for DNA replication and genetic recombination. Proc. Natl. Acad. Sci. USA, 80, 2442 – 2446.

56. Frank, B.S., Vandar, D., Chrishti, A.H., McKnight, C.J. 2004. The NMR structure of dematin headpiece reveal a dynamic loop that is conformationally altered upon phosphorylation at a distal site. J. Biological Chemistry, 279 (9), 7909-7916.

57. Fukagawa, T., Brown, W.R. 1997. Efficient conditional mutation of the vertebrate CENP-C gene. Human Molecular Genetic, 6, 2301-2308.

58. Fukagawa, T., Regnier, V., Ikemura, T. 2001. Creation and characterization of temperature-sensitive CENP-C mutants in vertebrate cells. Nucleic Acids Research, 29 (18), 3796 – 3803.

59. Fukagawa, T., Mikami, Y., Nishihashi, A., Regnier, V., Haraguchi, T., Hiraoka, Y., Sugata, N., Todokoro, K., Brown, W., Ikemura, T. 2001. CENP-H, a constitutive centromere component, is required for centromere targeting of CENP-C in vertebrate cells. The EMBO J., 20 (16), 4603 – 4617.

60. Fukagawa, T. 2004. Centromere DNA, proteins and kinetochore assembly in vertebrate cells. Chromosome Research, 12, 557-567.

61. Fukagawa, T., Nogami, M., Yoshikawa, M., Ikeno, M. Okazaki, T., Takami, Y., Nakayama, T., Oshimura, M. 2004. Dicer is essential for formation of the heterochromatin structure in vertebrate cells. Nature Cell Biology, 6, 784-791.

62. Gasser, S.M. 2002. Visualizing chromatin dynamics in interphase nuclei. Science, 296, 1412-1416.

63. Gassmann, R., Carvalho, A., Henzing, A.J., Ruchaud, S., Hudson, D.F., Honda, R., Nigg, E.A., Gerloff, D.I., Earnshaw, W.C. 2004. Borealin: a novel chromosomal passenger required for stability of the bipolar mitotic spindle. J. Cell Biology, 166, 179-191.

64. Goshima, G., Saitoh, S., Yanagida, M. 1999. Proper metaphase spindle length is determined by centromere proteins Mis12 and Mis6 required for faithful chromosome segregation. Genes & Development, 13, 1664 – 1677.

65. Goshima, G., Kiyomitsu, T., Yoda, K., Yanagida, M. 2003. Human centromere chromatin protein hMis12, essential for equal segregation, is independent of CENP-A loading pathway. J. Cell Biology, 160 (1), 25 – 39.

66. Grewal, S.I. Moazed, D. 2003. Heterochromatin and epigenetic control of gene expression. Science, 301, 798-802.

67. Grimes, B., Cooke, H. 1998. Engineering mammalian chromosome. Human Molecular Genetic Review, 7 (10), 1635 – 1640.

68. Haering, C.H., Nasmyth, K. 2003. Building and breaking bridges between sister chromatids. BioEssay, 25, 1178 – 1191.

69. Hamajima, N., Matsuda, K., Sakata, S., Tamaki, N., Sasaki, M., Nonaka, M. 1996. A novel gene family defined by human dihydropyrimidinase and three related proteins with differential tissue distribution. Gene, 180 (1-2), 157-163.

70. Haustein, E., Schwille, P. 2003. Ultrasensitive investigations of biological systems by Fluorescence Correlation Spectroscopy. Methods, 29, 153-166.

71. Hayakawa, T., Haraguchi, T., Masumoto, H., Hiraoka, Y. 2003. Cell cycle behaviour of Human HP1 subtypes; distinct molecular domains on HP1 are required for their centromeric localization during interphase and metaphase. J. Cell Science, 116 (16), 3327-3338.

72. He, D., Zeng, C., Woods, K., Zhong, L., Turner, D., Bush, R.K., Brinkley, B.R., Busch, H. 1998. CENP-G: A new centromeric protein that associated with alpha-I satellite DNA subfamily. Chromosoma (Berlin), 107, 189-197.

73. Henikoff, S., Malik, H.S. 2002. Selfish drivers. Nature, 417, 227.

74. Holt, S.V., Vergnolle, M.A., Hussein, D., Wozniak, M.J., Allan, V.J., Taylor, S.S. 2005. Silencing CENP-F weakens centromeric cohesion, prevents chromosome alignment and activates the spindle checkpoint. J. Cell Science, 118, pt 20, 4889-4900.

75. Horri, T., Yamaguchi, T., Hiraoka, Y., Kimura, H., Fukagawa, T. 2003. Dynamic behaviour of Nuf2-Hec1 complex that localizes to the centromere and is essential for mitotic progression in vertebrate cells. J. Cell Science, 116, 3347-3362.

76. Houtsmuller, A.B., Vermeulen, W. 2001. Macromolecular dynamics in living cell nuclei revealed by fluorescence redistribution after photobleaching. Histochemistry and Cell Biology, 115, 13-21.

77. Howman, E.V., Fowler, K.J., Newson, A.J., Redward, S., MacDonald, A.C., Kalitsis, P., Choo, K.H.A. 2000. Early disruption of centromeric chromatin organization in centromere protein A (Cenpa) null mice. Proc. Natl. Acad. Sci. USA, 97 (3), 1148 – 1153.

78. Hubert, R. S., Korenberg, J. R. 1997. PCP4 maps between D21S345 and P31P10SP6 on chromosome 21q22.2-q22.3. Cytogenetics and Cell Genetics, 78, 44-45.

79. Hudson, D.F., Foeler, K.J., Earle, E., Saffery,R., Kalitsis, P., Trowell, H., Hill, J., Wreford, N.G., de Kretser, D. M., Cancilla, M. R., Howmann, E., Hii, L., Cutts, S.M., Irvine, D.V., Choo, K.H. 1998. Centromere protein B null mice are mitotically and meiotically normal but have lower body and testis weights, J. Cell Biology, 141, 309-319.

80. Ikeno, M., Masumoto, H., Okazaki, T. 1994. Distribution of CENP-B boxes reflected in CREST centromere antigenic sites on long range alpha satellite DNA arrays of human chromosome 21. Human Molecular Genetics, 3, 1245-1257.

81. Ikeno, M., Grimes, B., Okazaki, T., Nakano, M., Saitoh, K., Hoshino, H., McGill, N.I., Cooke, H., Masumoto, H. 1998. Construction of YAC-based mammalian artificial chromosomes. Nature Biotechnology, 16, 431-439.

82. Ito, T., Chiba, T., Ozawa, R., Yoshida, M., Hattori, M., Sakaki, Y. 2001. A comprehensive two-two hybrid analysis to explore the yeast protein interactome. Proc. Natl. Acad. Sci. USA, 98 (8), 4569-4574.

83. Izuta, H., Ikeno, M., Suzuki, N., Tomonaga, T., Nozaki, N., Obuse, C., Kisu, Y., Goshima, N., Nomura, F., Nomura, N., Yoda, K. 2006. Comprehensive analysis of the ICEN (Interphase centromere complex) component enriched in the CENP-A chromatin of human cells. Genes Cells, 11, 6, 673-684.

84. Jablonski, S.A., Chan, G.K., Cooke, C.A., Earnshaw, W.C., Yen, T.J. 1998. The hBUB1 and hBUBR1 kinases sequentially assemble onto kinetochores during prophase with hBUBR1 concentrating at the kinetochore plates in mitosis. Chromosoma, 107 (6-7), 386-396.

85. Jans, D.A., Hassan, G. 1998. Nuclear targeting by growth factors, cytokines and their receptors: a role in signaling?, BioEssay, 20, 400-411.

86. Jansen, R., Greenbaum, D., Gerstein, M. 2002. Relating whole-genome expression data with protein-protein interactions. Genome Research, 12, 37-46.

87. Jones, S., Thornton, J.M. 1996. Principles of protein-protein interaction. Proc. Natl. Acad. Sci. USA, 93, 13-20.

88. Kapoor, M., de Oca Luna, R.M., Liu, G., Lozano, G., Cummings, C., Mancini, M., Ouspenski, I., Brinkley, B.R., May, G.S. 1998. The *cenpB* gene is not essential in mice. Chromosoma, 107, 570-576.

89. Karpen, G.H., Allshire, R.C. 1997. The case for epigenetic effects on centromere identity and function. Trends in Genetics, 13, 489-496.

90. Kalitsis, P., Fowler, K.J., Earle, E., Hill, J., Choo, K.H.A. 1998. Targeted disruption of mouse centromere protein C gene leads to mitotic disarray and early embryo death. Proc. Natl. Acad. Sci. USA, 95, 1136 – 1141.

91. Kenworthy, A.K. 2001. Imaging protein-protein interaction using fluorescence resonance energy transfer microscopy. Methods, 24, 289-296.

92. Khan, S., Zimmerman, A., Basler, M., Groettrup, M., Hengel, H. 2004. A cytomegalovirus inhibitor of gamma interferon signaling controls immunoproteasome induction. J. Virology, 78 (4), 1831-1842.

93. Kline, S.L., Cheesemann, I.M., Hori, T., Fukagawa, T., Desai, A. 2006. The human Mis12 complex is required for kinetochore assembly and proper chromosome segregation. J. Cell Biology, 173 (1), 9-17.

94. Kline-Smith, S.L., Sandall, S., Desai, A. 2005. Kinetochore spindle microtubule interactions during mitosis. Current Opinion in Cell Biology, 17, 35-46.

95. Knehr, M, Poppe, M, Schroeter, D., Eickelbaum, W., Finze, E.M., Kiesewetter, U.L., Enulescu, M., Arand, M., Paweletz, N. 1996. Cellular expression of human centromere protein C demonstrates a cyclic behavior with highest abundance in the G1 phase. Proc. Natl. Acad. Sci. USA, 93, 10234 – 10239.

96. Kruhlak, M.J., Lever, M.A., Fischle, W. 2000. Reduced mobility of the alternate splicing factor (ASF) through the nucleoplasm and steady state speckle compartments. J. Cell Biology, 150, 41-51.

97. Kwon, Y.T., Reiss, Y., Fried, V.A., Hershko, A., Yoon, J.K., Gonda, D.K., Sangan, P., Copeland, N.G., Jenkins, N.A., Varshavsky, A. 1998. The mouse and human genes encoding the recognition component of the end-rule pathway. Proc. Natl. Acad. Sci. USA, 95 (14), 7898-7903.

98. Lam, A.L., Boivin, C.D., Bonney, C.F., Rudd, M.K., Sullivan, B.A. 2006. Human centromeric chromatin is a dynamic chromosomal domain that can spread over noncentromeric DNA. Proc. Natl. Acad. Sci. USA, 103 (11), 4186-4181.

99. Lamour, V., Quevillon, S., Diriong, S., N`Guyen, V.C., Lipinski, M., Mirande, M. 1994. Evolution of the G1x-tRNA synthetase family: the glutamyl enzyme as a case of horizontal gene transfer. Proc. Natl. Acad. Sci. USA, 91 (18), 8670-8674.

100. Lampson, M.A., Renduchitala, K., Khodjakov, A., Kapoor, T.M. 2004. Correcting improper chromosome-spindle attachments during cell division. Nature Cell Biology, 6 (6), 232-237.

101. Lampson, M.A., Kapoor, T.M. 2005. The human mitotic checkpoint protein BubR1 regulates chromosome-spindle attachment. Nature Cell Biology, 7 (1), 93 – 98.

102. Lanini, L., McKeon, F. 1995. Domain required for CENP-C assembly at the kinetochore. Molecular Biology of the Cell, 6, 1049 – 1059.

103. Larsen, F., Solheim, J., Kristensen, T., Kolsto, A., Pridz, H. 1993. A tight cluster of five unrelated human on chromosome 16q22.1. Human Molecular Genetic, 2, 1589-1595.

104. Legrain, P., Wojcik, J., Gaunthier, J. 2001. Protein-protein interaction maps: a lead towards cellular functions. Trends Genetics, 17 (6), 346-352.

105. Lehnertz, B., Ueda, Y., Derijck, A.A., Braunchweig, U., Peterz-Burgos, L., Kubichek, S., Chen, T., Li, E., Jenuwein, T., Peters, A.H. 2003. Suv39-mediated histone H3 lysine 9 methylation directs DNA methylation to major satellite repeats at pericentric heterochromatin. Current Biology, 13, 1192-1200.

106. Levin, M.K., Carson, J.H. 2004. Fluorescence correlation spectroscopy and quantitative cell biology. Differentiation, 72, 1-10.

107. Li, W., Lan, Z., Wu, H., Wu, S., Meadow, J., Chen, J., Zhu, V., Dai, W. 1999. BUBR1 phosphorylation is regulated during mitotic checkpoint activation. Cell Growth Differentiation, 10 (11), 769-775.

108. Li, H., Rauch, T., Chen, Z.X., Szabo, P.E., Riggs, A.D., Pfeifer, G.P. 2006. The histone methyltransferase SETDB1 and the DNA methyltransferase DNMT3A interact directly and localize to promoters silenced in cancer cells. J. Biological Science, 281 (28), 19489-19500.

109. Liao, H., Winkfein, R.J., Mack, G., Rattner, J.B., Yen, T.J. 1995. CENP-F is a protein of the nuclear matrix that assembles kinetochore at late G2 and is rapidly degraded after mitosis. J. Cell Biology, 130 (3), 507-518.

110. Liu, D., Zhang, N., Du, J., Cai, X., Zhu, M., Jin, C., Dou, Z., Feng, C., Yang, Y., Liu, L., Takeyasu, K., Xie, W., Yao, X. 2006. Interaction of Skp1 with CENP-E at the midbody is essential for cytokinesis. Biochem Biophys Res Commun., 345 (1), 394-402.

111. Liu, S.T., Rattner, J.B., Jablonski, S.A., Yen, T. 2006. Mapping the assembly pathway that specify formation of the trilaminar kinetochore plates in human cells. J. Cell Biology, 175 (1), 41-53.

112. Liu, S.T., Hittle, J.C., Jablonski, S.A., Campbell, M.S., Yoda, K., Yen, T.J. 2003. Human CENP-I specifies localization of CENP-F, MAD1 and MAD2 to kinetochores and is essential for mitosis. Nature Cell Biology, 5 (4), 341-345.

113. Liu, S.T., Chan, G.K.T., Hittle, J.C., Fujii, G., Lees, E., Yen, T.J. 2003. Human MPS1 kinase is required for mitotic arrest induced by the loss of CENP-E from kinetochores. Molecular Biology of the Cell, 14, 1638-1651.

114. Lippincott-Schwartz, J., Snapp, E., Kenwothy, A. 2001. Studying protein dynamics in living cells. Nature Reviews, 2, 444 – 456.

115. Lippincott-Schwartz, J., Patterson, G.H. 2003. Development and use of fluorescent protein markers in living cells. Science, 300, 87-91.

116. Lippincott-Schwartz, J., Altan-Bonnet N., Patterson, G.H. 2003. Photobleaching and photoactivation: following protein dynamic in living cell. Nature Review Imaging in Cell Biology, S7-S14.

117. Macara, I.G. 2001. Transport into and out of the nucleus. Microbiology and Molecular Biology Review, 65 (4), 570-594.

118. Maiato, H., DeLuca, J., Salmon, E.D., Earnshaw, W.C. 2004. The dynamic kinetochore-microtubule interface. J. Cell Science, 117 (23), 5461 – 5477.

119. Mao, Y., Desai, A., Cleveland, D.W. 2005. Microtubule capture by CENP-E silences BubR1-dependent mitotic checkpoint signaling. J. Cell Biology, 170 (6), 873-880.

120. Marshal, W.F. 2002. Order and disorder in the nucleus. Current Biology, 12, R185-R192.

121. Masumoto, H., Masukata, H., Muro, Y., Nosaki, N., Okazaki, T. 1989. A human centromere antigen (CENP-B) interacts with a short specific sequence in alphoid DNA, a human centromeric satellite. J. Cell Biology, 109, 1963-1973.

122. Masumoto, H., Nakano, M., Ohzeki, J. 2004. The role of CENP-B and α satellite DNA: de novo assembly and epigenetic maintenance of human centromere. Chromosome Research, 12, 543-556.

123. Matera, A.G. 1999. Nuclear bodies: multifaceted subdomains of the interchromatin space. Trends in Cell Biology, 9, 302-309.

124. McAlister-Henn, L., Gibson, N., Panisko, E. 1999. Applications of the yeast two-hybrid system. Methods, 19, 330-337.

125. McAnish, A.D., Draviam, V.M., Toso, A., Sorger, P.K. 2006. Human kinetochore proteins Nnf1R and Mcm21R are required for accurate chromosome segregation. EMBO J., 25 (17), 4033-4049.

126. Meluh, P.B., Koshland, D. 1995. Evidence that the MIF2 gene of *Sacharomyces cerevisiae* encodes a centromere protein with homology to the mammalian centromere protein CENP-C. Molecular Biology Cell, 6, 793-807.

127. Meraldi, P., McAnish, A.D., Rheinbay, E., Sorger, P.K. 2006. Phylogenetic and structural analysis of centromeric DNA and kinetochore proteins. Genome Biology, 7 (3), R23

128. Mikami, Y., Hori, T., Kimura, H., Fukagawa, T. 2005. The functional region of CENP-H interacts with the Nuf2 complex that localizes to centromere during mitosis. Molecular Cell Biology, 25 (5), 1958-1970.

129. Minc, E., Allory, Y., Worman, H.J., Courvalin J.C., Buendia, B. 1999. Localization and phosphorylation of HP1 proteins during the cell cycle in mammalian cells. Chromosoma, 108, 220-234.

130. Misteli, T. 2001. Protein dynamic: implication for nuclear architecture and gene expression. Science, 291, 843 – 847.

131. Misteli, T. 2005. Concepts in nuclear architecture. BioEssay, 27 (5), 477 – 487.

132. Mitchell, A.R., Jepesen, P., Nicol, L., Morrison, H., Kipling, D. 1996. Epigenetic control of mammalian centromere protein binding: does DNA methylation have a role?. J. Cell Science, 109, 2199-2206.

133. Moroi, Y., Peebles, C., Fritzler, M.J., Steigerwald, J., Tan, E.M. 1980. Autoantibody to the centromere (kinetochore) in scleroderma sera. Proc. Natl. Acad. Sci. USA, 17, 1627 –1631.

134. Musacchio, A., Hardwick, K.G. 2002. The spindle Checkpoint: structural insight into dynamic signaling. Nature Reviews Molecular Cell Biology, 3, 731 – 741.

135. Muromoto, R., Sugiyama, K., Takachi, A., Imoto, S., Sato, N., Yamamoto, T., Oritani, K., Shimoda, K., Matsuda, T. 2004. Physical and functional interaction between Daxx and DNA methyltransferase 1-associated protein, DMAP1. J. Immunology, 172, 2985-2993.

136. Nagai, K., Thogersen, H.C. 1984. Generation of β-globin by sequence-specific proteolysis of a hybrid protein produced in *Escherichia coli*. Nature, 309, 810-812.

137. Nagase, T., Kikuno, R., Ishikawa, K, Hirosawa, M., Ohara, O. 2000. Prediction of the coding sequences of unidentified human genes. XVI. The complete sequences of 150 new cDNA clones from brain which code for large protein *in vitro*. DNA Research, 7, 65-73.

138. Nair, R., Carter, P., Rost, B. 2003. NLSdb: Data base of nuclear localization signals. Nucleic Acid Research, 31 (1), 397-399.

139. Nakagawa, H., Lee, J.K., Hurwitz, J., Allshire, R.C., Nakayama, J., Grewal, S.I.S., Tanaka, K., Murakami, Y. 2002. Fission yeast CENP-B homologs nucleate centromeric heterochromatin by promoting heterochromatin-specific histone tail modifications. Genes & Development, 16, 1766-1778.

140. Nishihasi, A., Haraguchi, T., Hiraoka, Y., Ikemura, T., Regnier, V., Dodson, H., Earnshaw, W.C., Fukagawa, T. 2002. CENP-I is essential for centromere function in vertebrate cells. Developmental Cell, 2, 463 – 476.

141. Obuse, C., Iwasaki, O., Kiyomitsu, T., Goshima, G., Toyoda, Y., Yanagida, M. 2004. A conserved Mis12 centromere complex is linked to heterochromatic HP1 and outer kinetochore protein Zwint-1. Nature Cell Biology, 6 (11), 1135 – 1141.

142. Obuse, C., Yang, H., Nozaki, N., Goto, S., Okazaki, T., Yoda, K. 2004. Proteomic analysis of the centromere complex from HeLa interphase cells: UV-damaged DNA binding protein 1 (DDB-1) is a component of the CEN-complex, while BMI-1 is transiently co-localized with the centromeric region in interphase. Genes to Cells, 9, 105-120.

143. Ogura, Y, Shibata, F, Sato, H., Murata, M., 2004. Characterization of CENP-C homolog in *Arabidopsis thaliana*. Genes Genet. Sys., 79, 139-144.

144. Ohi, R., Coughlin, M.L., Lane, W.S., Mitchison, T.J. 2003. An inner centromere protein that stimulates the microtubule depolimerizing activity of a KinI Kinesin. Developmental Cell, 5, 309-321.

145. Ohzeki, J., Nakano, M., Okada, T., Masumoto, H. 2002. CENP-B box is required for *de novo* centromere chromatin assembly on human alphoid DNA. J. Cell Biology, 159 (5), 765-775.

146. Okada, M., Cheeseman, I.M., Hori, T., Okawa, K., McLeod, I.X., Yates, J.R., Desai, A., Fukagawa, T. 2006. The CENP-H-I complex is required for efficient incorporation of newly synthesized CENP-A into centromeres. Nature Cell Biology, 8 (5), 446-457.

147. Orthaus, S. 2006. Thesis: Towards the architecture of the human inner kinetochore. Friedrich-Schiller Universität-Jena

148. Page, S.L., Earnshaw, W.C., Choo, K.H.A., Shaffer, L.G. 1995. Further evidence that CENP-C is a necessary component of active centromeres: Studies of a dic(X;15) with simultaneous immunofluorescence and FISH. Human Molecular Genetics, 4, 289 – 294.

149. Palmer, D.K., O'Day, K., Trong, H.L., Charbonneau, H., Margolis, R.L. 1991. Purification of the centromeric-specific protein CENP-A and demonstration that it is a distinctive histone. Proc. Natl. Acad. Sci. USA, 88, 3734-3738.

150. Patterson, G.H., Piston, D.W., Barisas, B.G. 2000. Föster distances between green fluorescence protein pairs. Analytical Biochemistry, 284, 438-440.

151. Peters, A.H., Kubichek, S., Mechtler, K., O'Sullivan, R.J., Derijck. A.A., Perez-Burgos, L., Kohlmaier, A., Opravil, S., Tachibana, M., Shinkai, Y., Martens, J.H., Jenuwein, T. 2003. Partitioning and plasticity of repressive histone methylation states in mammalian chromatin. Molecular Cell, 12 (6), 1577-1589.

152. Phair, R.D., Misteli, T. 2000. High mobility of proteins in the mammalian cell nucleus. Nature, 404, 604-609.

153. Phair, R.D., Misteli, T. 2001. Kinetic modeling approaches to *in vivo* imaging. Nature Review Molecular Cell Biology, 2, 898-907.

154. Phizicky, E.M., Fields, S. 1995. Protein-protein interactions: Methods for detection and analysis. Microbiological Reviews, 59 (1), 94 – 123.

155. Pidoux, A.L., Allshire, R.C. 2000. Centromere: getting a grip of chromosomes. Current Opinion Cell Biology, 12, 308-319.

156. Pluta, A.F., Cooke, C.A., Earnshaw, W.C. 1990. Structure of the human centromere at metaphase. Trends in Biochemical Sciences, 15, 181-185.

157. Pluta, A.F., Mackay, A.M., Ainsztein, A.M., Goldberg, I.G., Earnshaw, W.C. 1995. The centromere: Hub of chromosomal activities. Science, 270, 1591 – 1594.

158. Pluta, A.F., Earnshaw, W.C. 1996. Specific interaction between human kinetochore protein CENP-C and a nucleolar transcriptional regulator. J. Biological Chemistry, 271 (31), 18767 – 18774.

159. Pluta, A.F. Earnshaw, W.C., Goldberg, I.G. 1998. Interphase-specific association of intrinsic centromere protein CENP-C with HDaxx, a death domain-binding protein implicated in Fas-mediated cell death. J. Cell Science, 111, 2029-2041.

160. Politi, V., Perini, G., Trazzi, S., Pliss, A., Raska, I., Earnshaw, W.C., Valle, G.D. 2002. CENP-C binds alpha-satellite DNA in vivo at specific centromere domains. J. Cell Science, 115, 2317 – 2327.

161. Pullman, W.E., Bodmer, W.F. 1992. Cloning and Characterization of a gene that regulates cell adhesion. Nature, 356, 529-532; erratum in 1993, Nature, 361, 564.

162. Rattner, J.B., Bazett-Jones, D.P. 1989. Kinetochore structure: electron spectroscopic imaging of the kinetochore. J. Cell Biology, 108, 1209 – 1219.

163. Rattner, J.B., Rao, A., Fritzler, M.J., Valencia, D.W., Yen, T.J. 1993. CENP-F is a ca. 400 kDa kinetochore protein that exhibits a cell cycle dependent localization. Cell Motility and The Cytoskeleton, 26, 214-226.

164. Regnier, V., Vagnarelli, P., Fukagawa, T., Zerjal, T., Burns, E., Trouche, D., Earnshaw, W., Brown, W. 2005. CENP-A is required for accurate chromosome segregation and sustained kinetochore association of BubR1. Molecular and Cellular Biology, 25 (10), 3967-3981.

165. Rizzo, M.A., Springer, G.H., Granada, B., Piston, D.E. 2004. An improved cyan fluorescent protein variant useful for FRET. Nature Biotechnology, 22, 445-449.

166. Rivett, A.J., Palmer, A., Knecht, E. 1992. Electron microscopic localization of the multicatalytic proteinase complex in rat liver and in cultured cell. J. Histochemistry and Cytochemistry, 40, 1165-1172.

167. Roix, J., Misteli, T. 2002. Genomes, proteomes and dynamic network in the cell nucleus. Histochemistry and Cell Biology, 118 (2), 106-116.

168. Saitoh, H., Tomkiel, J., Cooke, C.A., Ratrie, H., Maurer, M., Rothfield, N.F., Earnshaw, W.C. 1992. CENP-C, an autoantigent in scleroderma, is a component of the human inner kinetochore plate. Cell, 70, 115 – 125.

169. Sarraf, S.A., Stancheva, I. 2004. Methyl-CpG binding protein MBD1 couples Histone H3 Methylation at Lysine 9 by SETDB1 to DNA replication and chromatin assembly. Molecular Cell, 15, 595-605.

170. Sambrook, J., Fritsch, E.F., Maniatis, T. 1989. Molecular cloning, a laboratory manual I, II, III. Cold Spring Harbour Laboratory Press, New York, USA.

171. Sato, H., Shibata, F., Murata, M. 2005. Characterization of a Mis12 homologue in *Arabidopsis thaliana*. Chromosome Research, 13 (8), 827-834.

172. Saxton, M.J. 2001. Anomalous diffusion in Fluorescence photobleaching recovery: a Monte Carlo study. Biophysical J., 81, 2226-2240.

173. Scholey, J.M., Brust-Mascher, I., Mogilner A. 2003. Cell division. Nature, 422, 746 – 752.

174. Schmiedeberg, L., Weisshart, K., Diekmann, S., Hoerste, G.M., Hemmerich, P. 2004. High- and low-mobility populations of HP1 in heterochromatin and mammalian cells. Molecular Biology of the Cell, 15, 2819-2833.

175. Schueler, M.G., Higgins, A.W., Rudd M.K., Gustashaw, K., Willard, H.F. 2001. Genomic and genetic definition of a functional human centromere. Science, 294, 109-115.

176. Schueler, M.G., Sullivan, B.A. 2006. Structural and functional dynamics of human centromeric chromatin. Annu. Rev. Genom. Human Genet. 7, 301-313.

177. Schultz, D.C., Ayyanathan, K., Negorev, D., Maul, G.G., Rauscher III, F.J. 2002. SETDB1: a novel KAP-1-associated histone H3, lysine 9-specific methyltransferase that contributes to HP1-mediated silencing of euchromatic genes by KRAB zinc-finger proteins. Genes & Develeopment, 16, 919-932.

178. Schwikowski, B., Uetz, P., Fields, S. 2000. A network of protein-protein interactions in yeast. Nature Biotechnology, 18, 1257-1261.

179. Schwille, P., Korlach, J., Webb, W.W. 1999. Fluorescence Correlation Spectroscopy with single-molecule sensitive on cell and model membranes. Cytometry, 36, 176-182.

180. Sen, S. 2000. Aneuploidy and cancer. Current Opinion Oncology, 12, 82-88.

181. Serebriiskii, I.G., Golemis, E., Uetz, P. 2005. The yeast two-hybrid system for detecting interacting proteins. Walker, J.M., (ed). The Proteomics Handbook, Humana Press, Totowa, New Jersey, USA.

182. Shen, T.H., Lin, K.H., Scaglioni, P.P., Yung, T.M., Pandolfi, P.P. 2006. the mechanisms of PML-Nuclear body formation. Molecular Cell, 24 (3), 331-339.

183. Shelby, R.D., Vafa, O., Sullivan, K.F. 1997. Assembly of CENP-A into centromeric chromatin requires a cooperative array of nucleosomal DNA contact sites. J. Cell Biology, 136, 501-513.

184. Sobhanifar, S. 2003. Yeast two hybrid assay: a fishing tale. BioTeach Journal, 1, 81 – 87.

185. Song, K., Gronemeyer, B., Lu, W., Eugster, E., Tomkiel, J.E. 2002. Mutational analysis of the central centromere targeting domain of human centromere protein C (CENP-C). Experimental Cell Research, 275, 81 – 91.

186. Spector, D.L. 2001. Nuclear domains. J. Cell Science, 114 (16), 2891-2893.

187. Spector, D.L. 2003. The dynamic of chromosome organization and gene regulation. Annu. Rev. Biochem. 72, 573-608.

188. Stelzl, U., Worm, U., Lalowski, M., Haenig, C., Brembeck, F.H., Goehler, H., Stroedicke, M., Zenkner, M., Schoenherr, A., Koeppen, S., Timm, J., Mintzlaff, S., Abraham, C., Bock, N., Kietzmann, S., Goedde, A., Toksöz, E., Droege, A., Krobitsch, S., Korn, B., Birchmeier, W., Lehrach, H., Wanker, E.E. 2005. A human protein-protein interaction network: a resource for annotating the proteome. Cell, 122 (6), 957-968.

189. Stewart, M.D., Li, J., Wong, J. 2005. Relationship between histone H3 lysine 9 methylation, transcription, repression and heterochromatin protein 1 recruitment. Molecular and Cellular Biology, 25 (7), 2525-2538.

190. Stucke, V.M., Baumann, C., Nigg, E.A. 2004. Kinetochore localization and microtubule interaction of the human spindle checkpoint kinase Mps1. Chromosoma, 113, 1-15.

191. Sugano, S., Suzuki, Y., Ota, T., Obayashi, M., Nishi, T., Isogai, T., Shibahara, T., Tanaka, T., Nakamura, Y. 2000. NCBI database: MGC2574 gene submission.

192. Sugata, N., Munekata, E., Todokoro, K. 1999. Characterization of a novel kinetochore protein, CENP-H. J. Biology Chemistry, 274 (39), 27343-27346.

193. Sugata, N., Li, S., Earnshaw, W.C., Yen, T.J., Yoda, K., Masumoto, H., Munekata, E., Warburton, P.E., Todokoro, K. 2000. Human CENP-H multimers

colocalize with CENP-A and CENP-C at active centromere-kinetochore complexes. Human Molecular Genetics, 9 (19), 2919 – 2926.

194. Sugimoto, K., Kuriyama, K., Shibata, A., Himeno, M. 1997. Characterization of internal DNA-binding and C-terminal dimerization domains of human centromere/kinetochore autoantigen CENP-C in vitro: role of DNA-binding and self-associating activities in kinetochore organization. Chromosome Research, 5, 132 – 141.

195. Sugimoto, K., Fukuda, R., Himeno, M. 2000. Centromere/kinetochore localization of human centromere protein A (CENP-A) exogenously expressed as a fusion to green fluorescent protein. Cell Structure Function, 25, 253-261.

196. Sulivan, B., Karpen, G. 2001. Centromere identity in *Drosophila* is not determined in vivo by replicating timing. J. Cell Biology, 154 (4), 683-690.

197. Sullivan, B.A., Blower, M.D., Karpen, G.H. 2001. Determining centromere: cyclical stories and forking paths. Nature Review, 2, 584 – 589.

198. Sullivan, B.A., Karpen, G.H. 2004. Centromeric chromatin exhibits a histone modification pattern that is distinct from both euchromatin and heterochromatin. Nature Structural and Molecular Biology, 11 (11), 1076-1083.

199. Sullivan, K.F., Hechenberger, M., Masri, K. 1994. Human CENP-A contains a Histone H3 related histone fold domain that is required for targeting to the centromere. J. Cell Biology, 127, 581-592.

200. Sullivan, K.F. 2001. A solid foundation: functional specialization of centromeric chromatin. Current Opinion Genetic Development, 11, 182-188.

201. Sun, X., Le, H.D., Wahlstrom, J.M., Karpen, G. 2003. Sequence analysis of a functional *Drosophila* centromere. Genome Research, 13, 182-194.

202. Suzuki, T., Terasaki, M., Takemoto-Hori, C., Hanada, T., Ueda, T., Wada, A., Watanabe, K. 2001. Structural compensation for the deficit of rRNA with proteins in the mammalian mitochondrial ribosome. Systematic analysis of proteins component of the large ribosomal subunit from mammalian mitochondria. J. Biological Chemistry, 276 (24), 21724-21736.

203. Suzuki, N., Nagano, M., Nozaki, N., Egashira, S., Okazaki, T., Masumoto, H. 2004. CENP-B interacts with CENP-C domains containing Mif2 regions responsible for centromere localization. J. Biological Chemistry, 279 (7), 5934 – 5946.

204. Takahashi, H, Yamada, H., Yanagida, M. 1994. Fission yeast minichromosome loss mutants mis cause lethal aneuploidy and replication abnormality. Molecular Biology of the Cell, 5, 1145-1158.

205. Tramier, M., Zahid, M., Mevel, J.C., Masse, M.J., Coppey-Moisan, M. 2006. Sensitivity of CFP/YFP and GFP/mCherry pairs to donor photobleaching on FRET determination by fluorescence lifetime imaging microscopy in living cells. Microsc. Res. Tech., 69 (11), 933-939.

206. Talbert, P.B., Bryson, T.D., Henikoff, S. 2004. Adaptive evolution of centromere proteins in plants and animals. J. Biology, 3 (18), 1-17.

207. Tanaka, T.U. 2002. Bi-orienting chromosomes on the mitotic spindle. Current Opinion in Cell Biology, 14, 365 – 371.

208. Tanaka, Y., Tachiwana, H., Yoda, K., Masumoto, H., Okazaki, T., Kurumizaka, H., Yokohama, S. 2005. Human centromere protein B induces translational positioning of nucleosomes on alpha-satellite DNA sequences. J. Biology Chemistry, 280 (50), 41609-41618.

209. Tanaka, Y., Kurumizaka, H., Yokohama, S. 2005. CpG methylation of CENP-B box reduces human CENP-B Binding. The FEBS Journal, 272, 282-289.

210. Taylor, S.S., Hussein, D., Wang, Y., Elderkin, S., Morrow, C.J. 2001. Kinetochore localization and phosphorylation of mitotic checkpoints Bub1 and BubR1 are differentially regulated by spindle events in human cells. J. Cell Science, 114 (Pt 24), 4385-4395.

211. Thompson, N.L., Lieto, A.M., Allen, N.W. 2002. Recent advances in fluorescence correlation spectroscopy. Current Opinion in Structural Biology, 12, 634 – 641.

212. Tomkiel, J., Cooke, C.A., Saitoh, H., Bernat, R.L., Earnshaw, W.C. 1994. CENP-C is required for maintaining proper kinetochore size and for a timely transition to anaphase. J. Cell Biology, 125 (3), 531 – 545.

213. Trazzi, S., Bernardoni, R., Diolaiti, D., Politi, V., Earnshaw, W.C., Perini, G., Valle, G.D. 2002. In vivo molecular dissection of human inner kinetochore protein CENP-C. J. Structural Biology, 140, 39 – 48.

214. Uetz, P., Ideker, T., Schwikowsky, B. 2002. Visualization and integration of protein-protein interaction. *In* Protein-protein interaction – A molecular cloning manual (ed. E. Golemis). Cold Spring Harbor, Cold Spring Harbor Laboratory Press.

215. Uetz, P., Giot, G., Mansfeld, T.A., Judson, R.S., Knight, J.R., Lockshon, D., naraya, V., Srinivasan, M., Pochart, P., Qureshi-Emili, A., Li, Y., Godwin, B.,

Conover, D., Kalbflesh, T., Vijayadamodar, G., Yang, M., Johnston, M., Fields, S., Rothberg, J.M. 2000. A comprehensive analysis of protein-protein interactions in *Saccharomyces cerevisiae*. Nature, 403, 623-627.

216. van Hooser, A.A., Mancini, M.A., Allis, C.D., Sullivan, K.F., Brinkley, B.R. 1999. The mammalian centromere: structure domains and attenuation of chromatin modeling. FASEB J., 13, S216 – S220.

217. van Hooser, A.A., Ouspenski, I.I., Gregson, H.C., Starr, D.A., Yen, T.J., Goldberg, M.L., Yokomori, K., Earnshaw, W.C., Sullivan, K.F., Brinkley, B.R. 2001. Specification of kinetochore-forming chromatin by the histone H3 variant CENP-A. J. Cell Science, 114 (19), 3529-3542.

218. von Mering, C., Krause, R., Snel, B., Cornell, M., Oliver, S.G., Fields, S., Bork, P. 2002. Comparative assessment of large-scale data sets of protein-protein interaction. Nature, 417, 399-403.

219. von Mikecz, A. 2006. The nuclear ubiquitin-proteasome system. J. Cell Science, 119 (10), 1977- 1984.

220. Vos, L.J., Famulski, J.K., Chan, G.K.T. 2006. How to build a centromere: from centromeric and pericentromeric chromatin to kinetochore assembly. Biochemistry and Cell Biology 84(4):619–639.

221. Wachsmuth, M., Waldeck, W., Langowski, J. 2000. Anomalous diffusion of fluorescent probes inside living cells nuclei investigated by spatially resolved fluorescence correlation spectroscopy. J. Molecular Biology, 298, 677-689.

222. Watanabe, Y., Kitajima, T.S. 2005. Shugoshin protects cohesin complexes at centromeres. Philos. Trans. R. Soc. Lond. B. Biol. Sci., 360, 515-521.

223. Weidtkamp-Peters. S., Hemmerich, P., Hoischen, C., Schmideberg, L., Erliandri, I., Diekmann, S. 2006. CENP-A, some CENP-B, CENP-C and CENP-I, but not hMis12 form a stable scaffold at the inner kinetochore in living human cells. J. Cell Biology, submitted

244. Weidtkamp-Peters. S. 2007. Thesis: Analysen zur Assemblierung von Centromeren und PML-Kernkörperchen in lebenden Zellen. Friedrich-Schiller Universität-Jena.

224. Wong, L.H., Choo, K.H.A. 2004. Evolutionary dynamic of transposable elements at the centromere. Trends in Genetics, 20 (12), 611-616.

225. Wieland, G., Orthaus, S., Ohndorf, S., Diekmann S., Hemmerich, P. 2004. Functional complementation of human centromere protein A (CENP-A) by Cse4p

from *Saccharomyces cerevisiae*. Molecular and Cellular Biology. 24 (15), 6620-6630.

226. Wordeman, L., Earnshaw, W.C., Bernat, R.L. 1996. Disruption of CENP antigen function perturbs dynein anchoring to the mitotic kinetochore. Chromosoma, 104, 551-560.

227. www.ensembl.org

228. Yang, C.H., Tomkiel, J., Saitoh, H., Johnson, D., Earnshaw, W.C. 1996. Identification of overlapping DNA-binding and centromere-targeting domains in the human kinetochore protein CENP-C. Molecular and Cellular Biology, 16 (7), 3576 – 3586.

229. Yang, X., Khosravi-Far, R., Chang, H.Y., Baltimore, D. 1997. Daxx, a novel Fas binding protein that activates JNK and apoptosis. Cell, 89, 1067-1076.

230. Yang, Z., Guo, J., Chen, Q., Ding, C., Du, J., Zhu, X. 2005. Silencing mitosin induces misaligned chromosomes, premature chromosome decondensation before anaphase onset, and mitotic cell death. Molecular and Cellular Biology, 25, 4062-4074.

231. Yao, X., Abrieu, A., Zheng, Y., Sullivan, K.F., Cleveland, D.W. 2000. CENP-E forms a link between attachment of spindle microtubules to kinetochores and the mitotic checkpoint. Nature Cell Biology, 2, 484 – 491.

232. Yen, T.J., Li, G., Schaar, B.T., Szilak, I., Cleveland, D.W. 1992. CENP-E is a putative kinetochore motor that accumulate just before mitosis. Nature, 359, 536-539.

233. Yoda, K., Ando, S. 2004. Immunological analysis and purification of centromere complex. Methods in Enzymology, 375, 270-277.

234. Yoda, K., Ando, S., Okuda, A., Kikhuchi. A., Okazaki, T. 1998. In vitro assembly of the CENP-B/α satellite DNA/core Histone complex: CENP-B causes nucleosome positioning. Genes to Cells, 3, 533 – 548.

235. Yoda, K., Kitagawa, K., Masumoto, H., Muro, Y., Okazaki, T. 1992. A human centromere protein, CENP-B, has a DNA binding domain containing four potential alpha helices at the NH2 terminus, which is separable from dimerizing activity. J. Cell Biology, 119 (6), 1413-1427.

236. Zhang, R., Liu, S.T., Chen, W., Bohmer, M., Pehrson, J., Yen, T.J., Adams, P.D. 2006. HP1 proteins are essential for a dynamic nuclear response that rescues the function of perturbed heterochromatin in primary human cells. Molecular and Cellular Biology, 27, 949-962.

237. Zimber, A., Nguyen, Q. D., Gespach, C. 2004. Nuclear bodies and compartment: functional roles and cellular signalling in health and disease. Cellular Signalling, 16, 1085-1104.

238. Zinkowski, R.P., Meyne, J., Brinkley, B.R. 1991. The centromere-kinetochore complex: a repeat subunit model. J. Cell Biology, 113 (5), 1091-1110.

APPENDIX 1: CENP-C gene (2832 bp)

```
atg gct gcg tcc ggt ctg gat cat ctc aaa aat ggc tac aga aga aga ttt tgt
 m   a   a   s   g   l   d   h   l   k   n   g   y   r   r   r   f   c

cga cct tcc agg gca cgt gac att aac aca gag caa ggc cag aat gtt ctg gaa
 r   p   s   r   a   r   d   i   n   t   e   q   g   q   n   v   l   e

atc tta caa gac tgt ttt gaa gaa aaa agt ctt gcc aat gat ttt agt aca aat
 i   l   q   d   c   f   e   e   k   s   l   a   n   d   f   s   t   n

tct aca aaa tca gtg cct aat tca aca cgc aaa ata aaa gac act tgt att cag
 s   t   k   s   v   p   n   s   t   r   k   i   k   d   t   c   i   q

tca cca agc aaa gag tgc cag aaa tca cat cca aag tca gtt cca gtt tct tca
 s   p   s   k   e   c   q   k   s   h   p   k   s   v   p   v   s   s

aag aag aaa gaa gcc tct cta cag ttt gtt gta gaa cca agt gaa gcc aca aac
 k   k   k   e   a   s   l   q   f   v   v   e   p   s   e   a   t   n

aga tca gtt cag gcc cat gaa gtt cat cag aaa att ctg gca act gat gtt agt
 r   s   v   q   a   h   e   v   h   q   k   i   l   a   t   d   v   s

tcc aaa aat aca cct gac tcg aaa aaa ata tca agt aga aac ata aat gat cat
 s   k   n   t   p   d   s   k   k   i   s   s   r   n   i   n   d   h

cac agt gaa gct gat gaa gaa ttt tac tta tcc gtt ggc tca cct tct gtt ctt
 h   s   e   a   d   e   e   f   y   l   s   v   g   s   p   s   v   l

ttg gat gca aaa aca tct gta tca caa aat gtt att cca tct agt gcc aaa aag
 l   d   a   k   t   s   v   s   q   n   v   i   p   s   s   a   k   k

aga gag act tac act ttt gaa aat tca gta aat atg ctg cct tca agt aca gag
 r   e   t   y   t   f   e   n   s   v   n   m   l   p   s   s   t   e

gtt tca gtt aaa acc aaa aaa agg tta aac ttt gat gat aaa gtt atg tta aag
 v   s   v   k   t   k   k   r   l   n   f   d   d   k   v   m   l   k

aaa ata gaa ata gat aat aaa gta tca gat gaa gag gat aaa aca tcg gaa gga
 k   i   e   i   d   n   k   v   s   d   e   e   d   k   t   s   e   g

caa gaa aga aaa cca tca gga tca tct cag aat aga ata cga gat tca gaa tat
 q   e   r   k   p   s   g   s   s   q   n   r   i   r   d   s   e   y

gaa att caa cga caa gct aaa aaa agt ttt tca aca ttg ttt tta gaa aca gta
 e   i   q   r   q   a   k   k   s   f   s   t   l   f   l   e   t   v

aaa cga aaa agt gaa tcc agt ccc att gtt agg cat gcg gca act gct cca cct
 k   r   k   s   e   s   s   p   i   v   r   h   a   a   t   a   p   p

cat tcg tgt cct ccc gat gat acg aag ttg ata gag gat gaa ttt ata att gat
 h   s   c   p   p   d   d   t   k   l   i   e   d   e   f   i   i   d

gag tcg gat caa agt ttt gcc agt aga tct tgg att aca ata cca aga aag gca
 e   s   d   q   s   f   a   s   r   s   w   i   t   i   p   r   k   a
ggg tct ctg aaa caa cgc aca ata tcc ccg gct gag agc act gca ctc ttt caa
 g   s   l   k   q   r   t   i   s   p   a   e   s   t   a   l   f   q

ggt aga aag tca aga gaa aag cat cat aat ata tta cct aag act ttg gca aat
 g   r   k   s   r   e   k   h   h   n   i   l   p   k   t   l   a   n

gac aaa cat tcc cat aaa cct cac cca gta gag aca tct cag ccc tct gat aaa
 d   k   h   s   h   k   p   h   p   v   e   t   s   q   p   s   d   k
```

```
aca gta ctg gat aca agt tat gct ttg ata gat gaa aca gta aat aat tat aga
 t   v   l   d   t   s   y   a   l   i   d   e   t   v   n   n   y   r

tct aca aaa tat gaa atg tat tcc aag aat gca gaa aaa cca tct aga agc aaa
 s   t   k   y   e   m   y   s   k   n   a   e   k   p   s   r   s   k

agg act ata aaa caa aaa cag aga aga aaa ttc atg gct aaa cca gct gaa gaa
 r   t   i   k   q   k   q   r   r   k   f   m   a   k   p   a   e   e

cag ctt gat gtg gga cag tct aaa gat gaa aac ata cat aca tca cat att acc
 q   l   d   v   g   q   s   k   d   e   n   i   h   t   s   h   i   t

caa gac gaa ttt caa aga aat tca gac aga aat atg gaa gag cat gaa gag atg
 q   d   e   f   q   r   n   s   d   r   n   m   e   e   h   e   e   m

gga aat gat tgt gtt tcc aaa aaa cag atg cca cct gtg gga agc aag aaa agt
 g   n   d   c   v   s   k   k   q   m   p   p   v   g   s   k   k   s

agc act aga aaa gat aag gaa gaa tct aaa aag aag cgc ttt tcc agt gag tcc
 s   t   r   k   d   k   e   e   s   k   k   k   r   f   s   s   e   s

aag aac aaa ctt gta cct gaa gaa gtg act tca act gtc acg aaa agt cga aga
 p   e   e   v   t   s   t   v   t   k   s   r   r   k   n   k   l   v

att tcc agg cgt cca tct gat tgg tgg gtg gta aaa tca gag gag agt cct gtt
 i   s   r   r   p   s   d   w   w   v   v   k   s   e   e   s   p   v

tat agc aat tct tca gta aga aat gaa tta cca atg cat cac aat agt agc cga
 y   s   n   s   s   v   r   n   e   l   p   m   h   h   n   s   s   r

aaa tct act aag aaa aca aat cag tca tct aag aat att agg aaa aaa act att
 k   s   t   k   k   t   n   q   s   s   k   n   i   r   k   k   t   i

cca ctt aaa agg cag aag aca gca act aaa ggc aac caa aga gta cag aag ttt
 p   l   k   r   q   k   t   a   t   k   g   n   q   r   v   q   k   f

tta aat gct gaa ggt tct gga ggt atc gtt ggt cat gat gaa att tcc aga tgt
 l   n   a   e   g   s   g   g   i   v   g   h   d   e   i   s   r   c

tca ctg agt gag cca ttg gaa agt gat gag gca gac ttg gct aag aag aaa aat
 s   l   s   e   p   l   e   s   d   e   a   d   l   a   k   k   k   n

ctt gat tgt tct aga tct aca aga agc tca aag aat gaa gat aac att atg act
 l   d   c   s   r   s   t   r   s   s   k   n   e   d   n   i   m   t

gca cag aat gtt ccc cta aag cct cag acc agt gga tat aca tgt aat ata cca
 a   q   n   v   p   l   k   p   q   t   s   g   y   t   c   n   i   p

aca gag tca aac ttg gat tct gga gag cat aag act tca gtt tta gag gaa agt
 t   e   s   n   l   d   s   g   e   h   k   t   s   v   l   e   e   s

gga cct tcc agg ctc aat aat aat tat tta atg tct gga aag aat gat gtg gat
 g   p   s   r   l   n   n   n   y   l   m   s   g   k   n   d   v   d

gat gag gaa gtt cat gga agt tca gat gac tca aaa caa tct aaa gtg ata cca
 d   e   e   v   h   g   s   s   d   d   s   k   q   s   k   v   i   p

aag aac aga atc cat cac aaa cta gta ttg ccc tcc aac aca cca aat gtt cgc
 k   n   r   i   h   h   k   l   v   l   p   s   n   t   p   n   v   r

agg acc aag aga aca cgt ttg aaa cct ttg gag tac tgg cga gga gag cga ata
 r   t   k   r   t   r   l   k   p   l   e   y   w   r   g   e   r   i
```

```
gat tat caa gga agg cca tca gga gga ttc gtg att agt gga gta cta tct cca
 d   y   q   g   r   p   s   g   g   f   v   i   s   g   v   l   s   p

gac aca ata tcg tct aaa agg aag gca aaa gaa aat att gga aaa gtc aac aaa
 d   t   i   s   s   k   r   k   a   k   e   n   i   g   k   v   n   k

aaa tct aat aag aaa agg atc tgt ctt gat aac gat gaa aga aag act aac tta
 k   s   n   k   k   r   i   c   l   d   n   d   e   r   k   t   n   l

atg gta aat cta ggt ata cct ctt gga gat cct ttg cag cca acg agg gta aag
 m   v   n   l   g   i   p   l   g   d   p   l   q   p   t   r   v   k

gac cca gaa aca aga gag att att ctc atg gat ctt gta agg cca caa gat aca
 d   p   e   t   r   e   i   i   l   m   d   l   v   r   p   q   d   t

tat caa ttt ttt gtt aag cat ggt gag ttg aag gta tac aag aca ttg gat aca
 y   q   f   f   v   k   h   g   e   l   k   v   y   k   t   l   d   t

ccc ttt ttt tct act ggg aaa ttg ata tta gga cca caa gaa gaa aag gga aag
 p   f   f   s   t   g   k   l   i   l   g   p   q   e   e   k   g   k

cag cat gtt ggc cag gat ata ttg gtt ttt tat gtt aac ttt ggt gac ctt ttg
 q   h   v   g   q   d   i   l   v   f   y   v   n   f   g   d   l   l

tgt act tta cat gaa aca cct tat ata tta agt act ggg gat tcg ttc tat gtt
 c   t   l   h   e   t   p   y   i   l   s   t   g   d   s   f   y   v

cct tca ggt aac tat tat aac atc aaa aat ctc cgg aat gag gaa agt gtt ctt
 p   s   g   n   y   y   n   i   k   n   l   r   n   e   e   s   v   l

ctt ttt act cag ata aaa aga tga
 l   f   t   q   i   k   r   -
```

APPENDIX 2: hMis12 gene (618 bp)

```
atg tct gtg gat cca atg acc tac gag gcc cag ttc ttt ggc ttc acg cca caa
 m   s   v   d   p   m   t   y   e   a   q   f   f   g   f   t   p   q

acg tgc atg ctt cgg atc tac att gca ttt caa gac tac cta ttt gaa gtg atg
 t   c   m   l   r   i   y   i   a   f   q   d   y   l   f   e   v   m

cag gcc gtt gaa cag gtt att ctg aag aag ctg gat ggc atc cca gac tgt gac
 q   a   v   e   q   v   i   l   k   k   l   d   g   i   p   d   c   d

att agc cca gtg cag att cgc aaa tgc aca gag aag ttt ctt tgc ttc atg aaa
 i   s   p   v   q   i   r   k   c   t   e   k   f   l   c   f   m   k

gga cat ttt gat aac ctt ttt agc aaa atg gag caa ctg ttt ttg cag ctg att
 g   h   f   d   n   l   f   s   k   m   e   q   l   f   l   q   l   i

tta cgt att ccc tca aac atc ttg ctt cct gaa gat aaa tgt aag gag aca cct
 l   r   i   p   s   n   i   l   l   p   e   d   k   c   k   e   t   p

tat agt gag gaa gat ttt cag cat ctc cag aaa gaa att gaa cag tta cag gag
 y   s   e   e   d   f   q   h   l   q   k   e   i   e   q   l   q   e

aag tac aag act gaa tta tgt act aag cag gcc ctt ctt gca gaa tta gaa gag
 k   y   k   t   e   l   c   t   k   q   a   l   l   a   e   l   e   e

caa aaa att gtt cag gcc aaa ctc aaa cag acg ttg act ttc ttt gat gag ctt
 q   k   i   v   q   a   k   l   k   q   t   l   t   f   f   d   e   l

cat aat gtt ggc aga gat cat ggg act agt gat ttt agg gag agt tta gta tcc
 h   n   v   g   r   d   h   g   t   s   d   f   r   e   s   l   v   s

ctg gtt cag aac tcc aga aaa cta cag aac att aga gac aat gtg gaa aag gaa
 l   v   q   n   s   r   k   l   q   n   i   r   d   n   v   e   k   e

tcg aaa cga ctg aaa ata tct taa
 s   k   r   l   k   i   s   -
```

APPENDIX 3: SETDB1 gene (1194 bp)

```
atg tct tcc ctt cct ggg tgc att ggt ttg gat gca gca aca gct aca gtg gag
 m   s   s   l   p   g   c   i   g   l   d   a   a   t   a   t   v   e

tct gaa gag att gca gag ctg caa cag gca gtg gtt gag gaa ctg ggt atc tct
 s   e   e   i   a   e   l   q   q   a   v   v   e   e   l   g   i   s

atg gag gaa ctt cgg cat ttc atc gat gag gaa ctg gag aag atg gat tgt gta
 m   e   e   l   r   h   f   i   d   e   e   l   e   k   m   d   c   v

cag caa cgc aag aag cag cta gca gag tta gag aca tgg gta ata cag aaa gaa
 q   q   r   k   k   q   l   a   e   l   e   t   w   v   i   q   k   e

tct gag gtg gct cac gtt gac caa ctc ttt gat gat gca tcc agg gca gtg act
 s   e   v   a   h   v   d   q   l   f   d   d   a   s   r   a   v   t

aat tgt gag tct ttg gtg aag gac ttc tac tcc aag ctg gga cta caa tac cgg
 n   c   e   s   l   v   k   d   f   y   s   k   l   g   l   q   y   r

gac agt agc tct gag gac gaa tct tcc cgg cct aca gaa ata att gag att cct
 d   s   s   s   e   d   e   s   s   r   p   t   e   i   i   e   i   p

gat gaa gat gat gat gtc ctc agt att gat tca ggt gat gct ggg agc aga act
 d   e   d   d   d   v   l   s   i   d   s   g   d   a   g   s   r   t

cca aaa gac cag aag ctc cgt gaa gct atg gct gcc tta aga aag tca gct caa
 p   k   d   q   k   l   r   e   a   m   a   a   l   r   k   s   a   q

gat gtt cag aag ttc atg gat gct gtc aac aag aag agc agt tcc cag gat ctg
 d   v   q   k   f   m   d   a   v   n   k   k   s   s   s   q   d   l

cat aaa gga acc ttg agt cag atg tct gga gaa cta agc aaa gat ggt gac ctg
 h   k   g   t   l   s   q   m   s   g   e   l   s   k   d   g   d   l

ata gtc agc atg cga att ctg ggc aag aag aga act aag act tgg cac aaa ggc
 i   v   s   m   r   i   l   g   k   k   r   t   k   t   w   h   k   g

acc ctt att gcc atc cag aca gtt ggg cca ggg aag aaa tac aag gtg aaa ttt
 t   l   i   a   i   q   t   v   g   p   g   k   k   y   k   v   k   f

gac aac aaa gga aag agt cta ctg tcg ggg aac cat att gcc tat gat tac cac
 d   n   k   g   k   s   l   l   s   g   n   h   i   a   y   d   y   h

cct cct gct gac aag ctg tat gtg ggc agt cgg gtg gtc gcc aaa tac aaa gat
 p   p   a   d   k   l   y   v   g   s   r   v   v   a   k   y   k   d

ggg aat cag gtc tgg ctc tat gct ggc att gta gct gag aca cca aac gtc aaa
 g   n   q   v   w   l   y   a   g   i   v   a   e   t   p   n   v   k

aac aag ctc agg ttt ctc att ttc ttt gat gat ggc tat gct tcc tat gtc aca
 n   k   l   r   f   l   i   f   f   d   d   g   y   a   s   y   v   t

cag tcg gaa ctg tat ccc att tgc cgg cca ctg aaa aag act tgg gag gac ata
 q   s   e   l   y   p   i   c   r   p   l   k   k   t   w   e   d   i
gaa gac atc tcc tgc cgt gac ttc ata gag gag tat gtc act gcc tac ccc aac
 e   d   i   s   c   r   d   f   i   e   e   y   v   t   a   y   p   n

cgc ccc atg gta ctg ctc aag agt ggc cag ctt atc aag act gag tgg gaa ggc
 r   p   m   v   l   l   k   s   g   q   l   i   k   t   e   w   e   g

acg tgg tgg aag tcc cga gtt gag gag gtg gat ggc agc cta gtc agg atc ctc
 t   w   w   k   s   r   v   e   e   v   d   g   s   l   v   r   i   l
```

```
ttc ctg gta ctg ttc ttc tct aca att ttg gag gca gag gtt ggt ggg ggg gga
 f   l   v   l   f   f   s   t   i   l   e   a   e   v   g   g   g   g

act taa
 t   -
```

APPENDIX 4: PSMB10 gene (822 bp)

```
atg ctg aag cca gcc ctg gag ccc cga ggg ggc ttc tcc ttc gag aaa tgc caa
 m   l   k   p   a   l   e   p   r   g   g   f   s   f   e   k   c   q

aga aat gca tca ttg gaa cgc gtc ctc ccg ggg ctc aag gtc cct cac gca cgc
 r   n   a   s   l   e   r   v   l   p   g   l   k   v   p   h   a   r

aag acc ggg acc acc atc gcg ggc ctg gtg ttc caa gac ggg gtc att ctg ggc
 k   t   g   t   t   i   a   g   l   v   f   q   d   g   v   i   l   g

gcc gat acg cga gcc act aac gat tcg gtc gtg gcg gac aag agc tgc gag aag
 a   d   t   r   a   t   n   d   s   v   v   a   d   k   s   c   e   k

atc cac ttc atc gcc ccc aaa atc tac tgc tgt ggg gct gga gta gcc gcg gac
 i   h   f   i   a   p   k   i   y   c   c   g   a   g   v   a   a   d

gcc gag atg acc aca cgg atg gtg gcg tcc aag atg gag cta cac gcg cta tct
 a   e   m   t   t   r   m   v   a   s   k   m   e   l   h   a   l   s

acg ggc cgc gag ccc cgc gtg gcc acg gtc act cgc atc ctg cgc cag acg ctc
 t   g   r   e   p   r   v   a   t   v   t   r   i   l   r   q   t   l

ttc agg tac cag ggc cac gtg ggt gca tcg ctg atc gtg ggc ggc gta gac ctg
 f   r   y   q   g   h   v   g   a   s   l   i   v   g   g   v   d   l

act gga ccg cag ctc tac ggt gtg cat ccc cat ggc tcc tac agc cgt ctg ccc
 t   g   p   q   l   y   g   v   h   p   h   g   s   y   s   r   l   p

ttc aca gcc ctg ggc tct ggt cag gac gcg gcc ctg gcg gtg cta gaa gac cgg
 f   t   a   l   g   s   g   q   d   a   a   l   a   v   l   e   d   r

ttc cag ccg aac atg acg ctg gag gct gct cag ggg ctg ctg gtg gaa gcc gtc
 f   q   p   n   m   t   l   e   a   a   q   g   l   l   v   e   a   v

acc gcc ggg atc ttg ggt gac ctg ggc tcc ggg ggc aat gtg gac gca tgt gtg
 t   a   g   i   l   g   d   l   g   s   g   g   n   v   d   a   c   v

atc aca aag act ggc gcc aag ctg ctg cgg aca ctg agc tca ccc aca gag ccc
 i   t   k   t   g   a   k   l   l   r   t   l   s   s   p   t   e   p

gtg aag agg tct ggc cgc tac cac ttt gtg cct gga acc aca gct gtc ctg acc
 v   k   r   s   g   r   y   h   f   v   p   g   t   t   a   v   l   t

cag aca gtg aag cca cta acc ctg gag cta gtg gag gaa act gtg cag gct atg
 q   t   v   k   p   l   t   l   e   l   v   e   e   t   v   q   a   m

gag gtg gat taa
 e   v   d   -
```

ACKNOWLEDGEMENTS

I am grateful to Prof. Dr. Stephan Diekmann for his supervision, time devotion and keen interest in this thesis.

I pay my sincere thanks to the DAAD for the scholarship for my PhD program. I am very grateful to Prof. Dr. Frank Grosse (FLI, Jena), Prof. Dr. Jörg Langowsky (DKFZ, Heidelberg), Dr. Martheen B. Malole (IPB, Bogor) and Dr. W. Basuki (Biotech Centre, BPPT, Jakarta) for their support.

I acknowledge my gratitude to PD Dr. Peter Hemmerich and Dr. Christian Hoischen for their kind help and valuable advices. I thank Christane Hirsch for helping me in various kinds of administration since I was in Jakarta, I am grateful to Marianne Koch, Sabine Ohndorf and Sylke Pfeifer for their help and sharing experiences during my experimental work, and to Thomas Liem, Jürgen Thomasch and Catherine Meissner for helping me preparing PCR products. Many thanks also go to Stephanie Weidtkamp-Peters for her assistance during microscope work.

I thank Dr. A. Tongta (Nebraska University, USA), Gabriella Lee (FRIM, Malaysia) and Prof. Dr. Stephan Diekmann for their substantial support in the English presentation of this thesis. I thank Dr. Alessandro Romualdi and Nikolina Kalchishkova for translating the summary of this thesis into German, and Dr. Annette Reif for German grammar correction.

I give enormous thanks to Prof. Sullivan (NUI Galway, Ireland), Dr. Beth Sullivan (Duke University, USA), Dr. Ulrich Stelzl (MDC-Berlin), Dr. J.J. van den Heuvel (GBF, Braunschweig), Dr. Ralf Glasser (Univ. Jena), Dr. S.B. Hake (Adolf Butenant Institute, Univ. Munich), Dr. M.K. Levin (UCHC, Farmington, USA) and David Baddeley (Kirchhoff Institute, Univ. Heidelberg) for valuable discussions.

I will never forget all my best friends that I always can rely on, especially; Michela, Paulius, Syahidul, Amna, Amal, Maria, Axel, Jibin, Feng Guo, Bogdan and Kerstin.

I dedicate this thesis to my beloved late father. I thank my mother, brothers and sisters for substantial support.

PUBLICATION AND SCIENTIFIC POSTER

Publications:

1. CENP-A, some CENP-B CENP-C and CENP-I but not hMis12 form a stable scaffold at the inner kinetochore in living human cells
   On Submission to J. Cell Biology

2. Direct physical interaction between human Kinetochore protein CENP-C C-terminus and SETDB1, a H3K9 methylase activity
   Manuscript in preparation

Scientific Poster:

Dynamic behavior of human kinetochore proteins

Workshop on Cell Biology and Microscopy
Alt Leiningen, Baden Württemberg, Germany, 7 – 11 December 2005

Selbständigkeitserklärung

Ich erkläre, dass ich die vorliegende Arbeit selbständig und nur unter Verwendung der angegebenen Literatur und Hilfsmittel angefertigt habe.

Jena, den 11.11.2006 Indri Erliandri

CURRICULUM VITAE

Indri Erliandri

Fritz Lipmann Institute (FLI)

Beutenbergstrasse 11, 07745 Jena, Germany

EDUCATION:

2003-2006 : **Ph D. (April 2003 onwards)**
Department of Molecular Biology, Fritz Lipmann Institute,
Jena, Germany

Feb 2000- Jan 2001 : **Training (Biotechnology Advance Training)**
Department of Microbial System
German Biotechnology Centre (GBF)
Braunschweig, Germany

1995 – 1998 : **M.S.**
Department of Biotechnology, Bogor Institute of Agriculture,
Bogor, Indonesia

1988 – 1993 : **B.Sc**
Agro-Industrial Technology,
Indonesia Institute of Technology (ITI)
Jakarta, Indonesia

FELLOWSHIPS:

FELLOWSHIPS:

Feb 2000-Jan 2001 : **Carl Duisberg Gesellschaft e.V. (CDG) scholarship**

Industrial Biotechnology Advance training

Training Place :
Molecular Biology and Gene Expression lab. Biochemical Engineering Department of Gesellschaft für Biotechnologie Forschung (GBF) of Braunschweig – Germany

March 2003 – May 2006: **DAAD Scholarship**

PhD program

Research Place:
Department of Molecular Biology, Institute of Molecular Biology (IMB), Jena, Germany

PROFESSIONAL EXPERIENCE:

- **1992 -1995 : Microbiology and Biochemistry Teaching Lab Assistant**
  Indonesia Institute of Technology (ITI), Jakarta, Indonesia

- **1995-1996 : Research Assistant**
  Pharmaceutical Biotechnology Project
  BPPT (Indonesia)-Technimont SpA (Italy)
  Jakarta Indonesia

- **1996-2003 : Research Assistant (Employee)**
  Genetic Engineering and Microbiology Lab.
  The Centre of The Assessment and Application of Technology
  Jakarta, Indonesia

Jena, den 11 .11.2006

Indri Erliandri